

Durham E-Theses

Synthesis and modification of water-soluble hyperbranched poly(amidoamine)s

Gargiuli, Joseph Fernand

How to cite:

Gargiuli, Joseph Fernand (2002) *Synthesis and modification of water-soluble hyperbranched poly(amidoamine)s*, Durham theses, Durham University. Available at Durham E-Theses Online:
<http://etheses.dur.ac.uk/3871/>

Use policy

The full-text may be used and/or reproduced, and given to third parties in any format or medium, without prior permission or charge, for personal research or study, educational, or not-for-profit purposes provided that:

- a full bibliographic reference is made to the original source
- a [link](#) is made to the metadata record in Durham E-Theses
- the full-text is not changed in any way

The full-text must not be sold in any format or medium without the formal permission of the copyright holders.

Please consult the [full Durham E-Theses policy](#) for further details.

SYNTHESIS AND MODIFICATION OF WATER-SOLUBLE HYPERBRANCHED POLY(AMIDOAMINE)S

Joseph Fernand Gargiuli

The copyright of this thesis rests with the author.
No quotation from it should be published without
his prior written consent and information derived
from it should be acknowledged.

A thesis submitted for the degree of Doctor of Philosophy



14 APR 2003

UNIVERSITY OF DURHAM

2002

Synthesis and modification of water-soluble hyperbranched poly(amidoamine)s

Abstract

The multi-step syntheses of two water-soluble AB₂ monomers, N-acryloyl-1,2-diaminoethane hydrochloride and N-acryloyl-1,2-daminoethane, are reported. The melt polymerisation at 210°C for 4 hours of N-acryloyl-1,2-diaminoethane hydrochloride gave, by Michael additions of the terminal ammonium salts (B₂ groups) of a monomer molecule or growing oligomer with the unreacted vinyl double bond (A group) of another monomer molecule or growing oligomer, hyperbranched macromolecules. High degrees of conversion, determined using ¹H NMR spectroscopy, were obtained and a degree of branching, determined using ¹⁵N NMR spectroscopy, was found to be equal or close to 1. However, this method proved difficult to reproduce and the alternative aqueous solution polymerisation at 100°C for 10 days of this monomer was investigated. The use of ampoules closed with Teflon taps as reactors lead to polymers displaying random signs of free radical polymerisation and high degrees of conversion due to such side-reaction, whereas, the alternative use of sealed Carius tubes lead to lower DP materials displaying no significant signs of free radical side-reactions. The kinetic study of this polymerisation allowed the determination of the rate constant associated with the oligomer growth and the MALDI analysis of these polymers revealed an evolution with time of the oligomer molecular weight distribution with time in agreement with the theoretical prediction. This last study also revealed that at least 70% of the molecules were not cyclised. On the other hand, the aqueous solution polymerisation of the corresponding free base monomer, N-acryloyl-1,2-diaminoethane, at 100°C for 90 minutes lead to hyperbranched macromolecules with high DP values. The kinetic study did not allow a precise determination of the rate constant associated with the oligomer growth due to the high reactivity of the free terminal amino groups. The MALDI analysis of these polymer samples showed that the evolution with time of the oligomer molecular weight distribution did not follow the theoretical prediction and that these macromolecules were cyclised.

Memorandum

The work described in this thesis was carried out in the Interdisciplinary Research Centre in Polymer Science and Technology, at the University of Durham, between October 1999 and September 2002. This work has not been submitted for any other degree and is the original work of the author, except when acknowledged by reference. Aspects of this work have been presented by the author at the international conference, "Polymers in the Third Millennium", held in Montpellier in September 2001. The same poster was also presented at the IRC Industrial Club Meeting held in Durham in September 2001.

Statement of Copyright

The copyright of this thesis rests with the author. No quotation from it should be published without his prior written consent and information derived from it should be acknowledged.

Acknowledgments

I wish to thank my supervisor, Professor W. J. Feast, for giving me the chance to carry out such an interesting project under his supervision. He always supported when I needed help and gave me hope when the experimental results were not those expected or desired. I also want to generally express my gratitude to all the staff of Durham University and the Interdisciplinary Research Centre in Polymer Science and Technology. They always found time to help me with my research and always showed great patience and professionalism. Their good humour and that of my fellow PhD students helped me go through the depressing times often associated with a PhD research project. I particularly want to thank Dr Dave Parker for his patience with me and without whom my thesis could not have been completed.

Last, but certainly not least, are my parents that always believed in me and always sacrificed themselves to help me realise my full potential. I will always be their grateful son and I wish to dedicate my success to them.

Contents

	page
Abstract	ii
Memorandum	iii
Statement of Copyright	iii
Acknowledgments	iv
Chapter One: Dendritic macromolecules	
1.1. Introduction	2
1.2. Dendrimers	2
1.2.1. Divergent growth	4
1.2.2. Convergent growth	6
1.2.3. Properties	8
1.3. Hyperbranched polymers	10
1.3.1. Synthetic strategies	13
1.3.2. Properties	16
Chapter Two: Monomer synthesis	19
2.1. Introduction	20
2.2. Experimental	21
2.2.1. Step 1: <i>N-tert</i> -butoxycarbonyl-1,2-diaminoethane	21
2.2.2. Step 2: <i>N-tert</i> -butoxycarbonyl- <i>N'</i> -acryloyl-1,2-diaminoethane	22
2.2.3. Step 3: <i>N</i> -acryloyl-1,2-diaminoethane hydrochloride	24
2.2.4. Synthesis of <i>N</i> -acryloyl-1,2-diaminoethane	25
2.3. Discussion	26
2.3.1. First step	26
2.3.2. Second step	29
2.3.3. Third step	33

2.3.4. Synthesis of the free-base monomer	34
Chapter Three: Polymerisation	36
3.1. Introduction	37
3.2. Experimental	38
3.2.1. Melt polymerisation of N-acryloyl-1,2-diaminoethane hydrochloride	38
3.2.2. Aqueous solution polymerisation of N-acryloyl-1,2-diaminoethane hydrochloride	39
3.2.3. Aqueous solution polymerisation of N-acryloyl-1,2-diaminoethane	40
3.2.3.1. High concentration monomer solution	40
3.2.3.2. Low concentration monomer solution	41
3.3. Discussion	42
3.3.1. Melt polymerisation of N-acryloyl-1,2-diaminoethane hydrochloride	42
3.3.2. Aqueous solution polymerisation of N-acryloyl-1,2-diaminoethane hydrochloride	50
3.3.3. Aqueous solution polymerisation of N-acryloyl-1,2-diaminoethane	53
Chapter Four: Kinetic study	57
4.1. Introduction	58
4.2. Kinetic study of the aqueous solution polymerisation of N-acryloyl-1,2-diaminoethane hydrochloride	58
4.2.1. Case 1: High concentration of monomer in aqueous solutions, polymerisations performed in closed ampoules	59
4.2.2. Cases 2 and 3: Lower concentration of monomer in aqueous solutions, polymerisations performed in closed ampoules	64
4.2.3. Case 4: lower concentration of monomer in aqueous solution, polymerisation performed in sealed Carius tubes	69

4.3. Kinetics of the polymerisation of N-acryloyl-1,2-diaminoethane in aqueous solutions	71
4.3.1. Case 1': High concentration of N-acryloyl-1,2-diaminoethane in deionised water, polymerisation in sealed Carius tubes	71
4.3.2. Case 2': Lower concentration of N-acryloyl-1,2-diaminoethane in deionised water, polymerisation in sealed Carius tubes	74
Chapter Five: MALDI-TOF analysis	78
5.1. Introduction	79
5.2. Analysis of the samples synthesised by the aqueous solution polymerisation of N-acryloyl-1,2-diaminoethane hydrochloride	81
5.3. Analysis of the samples synthesised by the aqueous solution polymerisation of N-acryloyl-1,2-diaminoethane	93
Chapter Six: Conclusions and suggested future work	97
6.1. Conclusions	98
6.2. Suggested future work	99
References	100
Appendix	102
Appendices 1.1 to 1.14	103
Appendices 2.1 to 2.33	110

Chapter One

Dendritic macromolecules

1.1. Introduction

Dendritic macromolecules are a relatively new family of synthetic polymers. As their name indicates, dendritic means tree-like in Greek, these macromolecules exhibit highly branched three-dimensional structures that resemble the structure of trees. Two types of dendritic macromolecule are recognised today; namely, dendrimers and hyperbranched polymers.¹

1.2. Dendrimers

The term “dendrimer” was first introduced by Tomalia² to describe a family of regularly branched poly(amidoamine)s in which all bonds converge to a single point: the core (C), each repeat unit or interior building block contains a branch junction (B), and the final molecule features a very large number of identical chain ends or surface groups (S). The interior building blocks are arranged into layers or generations, giving a fractal-like architecture to the dendrimer.³ This peculiar architecture results in a highly symmetrical structure where the number of building blocks in each generation and the number of terminal groups are defined by a geometrical progression based on the functional multiplicity of both the core molecule and the building blocks. This is illustrated in *Figure 1.1* which shows a dendrimer with a core multiplicity of 4 and three layers of building blocks with a branch multiplicity of 2. This arrangement gives rise to 32 terminal groups (i.e. 4×2^3) and 28 building blocks arranged in four layers of 16, 8, and 4 repeat units, respectively.

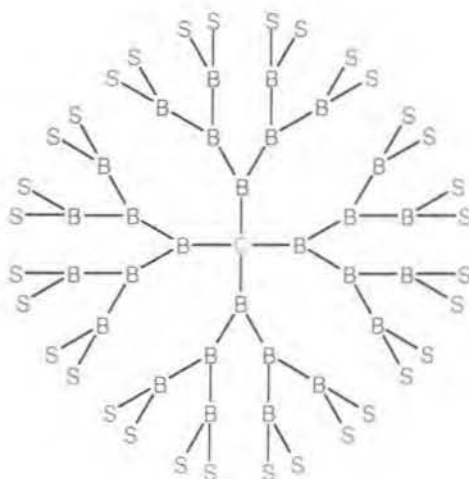


Figure 1.1. General structure of a dendrimer

The dendritic fragments, attached to the core, are usually called “dendrons”. This term can also describe dendritic structures that will become part of a larger macromolecule once they are attached to a core. For example, a dendron may react, via its focal point (F), with the reactive group (R) of a tetrafunctional core (C) to give a tetradendrion dendrimer, as shown in *Figure 1.2*.

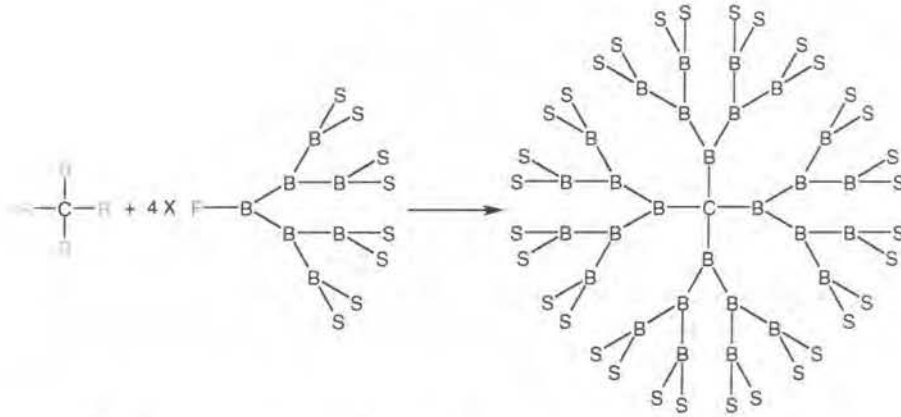


Figure 1.2. Synthesis of a dendrimer by addition of dendrons to core molecule

Once a certain size is reached, dendritic macromolecules tend to adopt a globular shape that resembles a sphere. They are quite different from conventional linear polymers, which usually display a random coil configuration. The dendrimer shape is similar to the globular shape of enzymes; however, the shape of dendrimers is the direct result of their branching pattern, as opposed to the folding or intramolecular interactions responsible for the shape of enzymes.

An interesting consequence of the globular structure of dendrimers is the concept of “dense packing” which was proposed by De Gennes and Hervet.⁴ The dendrimer surface congestion was expressed as a function of generation, according to the following equation:

$$A_Z = A_D / N_Z \text{ which is proportional to } r^2 / (N_c \cdot N_b^G)$$

Where: A_Z is the surface area per terminal group Z

A_D is the dendrimer surface area

N_Z is the number of surface groups Z per generation

r is the dendrimer radius

N_c is the core multiplicity

N_b is the branch cell juncture multiplicity

And G, the generation of the dendrimer

This relationship predicted that at higher generations G , the surface area per terminal group Z becomes increasingly small and once a specific generation number is reached, the available space for the next layer is insufficient for all the new monomer units to fit in. Therefore, regular growth is prevented and the surface is said to be “dense packed”. The generation then reached was termed: “the Starburst dense-packed generation”. Further growth beyond this dense packed state was predicted to lead to irregular growth and defects in the structure and shape of the dendrimer. In this picture of dendrimers, an ideal cascade growth without branch defect is only possible for generations preceding the dense packed state. However, this early prediction has been challenged and the general view is now that, for conformationally mobile systems, there can be backfolding of the outer layers into the less dense regions of the dendrimer.⁵

The synthesis of dendrimers can be achieved in two different ways, divergent growth or convergent growth, and they are discussed in the next sections.

1.2.1. Divergent growth

Tomalia successfully used the divergent growth in order to synthesise his starburst[®] PAMAM dendrimers.² This synthesis strategy involves the stepwise growth of the dendrimer, by radial addition of successive layers of branched units, starting from a polyfunctional core to the periphery. This synthesis strategy requires reactions that proceed in very high yield (100%) with no side products.⁶ The monomer units must give symmetrical branching to avoid asymmetric shape or unequal reactivity in the multifunctional branching unit.⁷ These problems were observed in Dankewalter’s work on poly(lysine) branched polymers.⁸ His goal was to synthesise dendritic architectures using lysine as the building block, but the asymmetrical shape of lysine and the non-equivalent reactivities of the two amino groups led to irregular globular structures possessing unsymmetrical and unequally branched segments.⁹

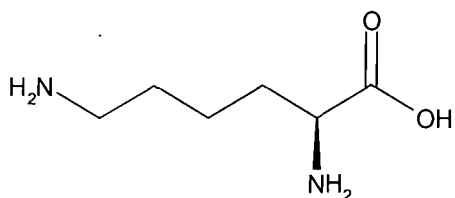


Figure 1.3. Structure of Lysine

Workers in the field have adopted many of the protection / deprotection sequences used in peptide and natural product chemistry.^{8, 10} Often, reactions are driven to 100% conversion, but this brings further problems and efficient separation and recovery procedures are required in order to obtain the dendrimer in a pure state at each step.

In Tomalia's poly(amidoamine) (PAMAM) dendrimers, ammonia was used as a trifunctional core. The process is shown in *Figure 1.4*, the first step involved a Michael addition of ammonia to an excess of methyl acrylate to generate a triester. This addition occurs very quickly at room temperature and in high yield. In the second step, the triester from step 1 was reacted with a large excess of ethylenediamine at room temperature giving rise, after isolation and purification, to generation 0. Repeating the sequence of steps 1 and 2 lead to a hexamine (generation 1). Repetition of this sequence of reactions and purifications produced the higher generation materials.

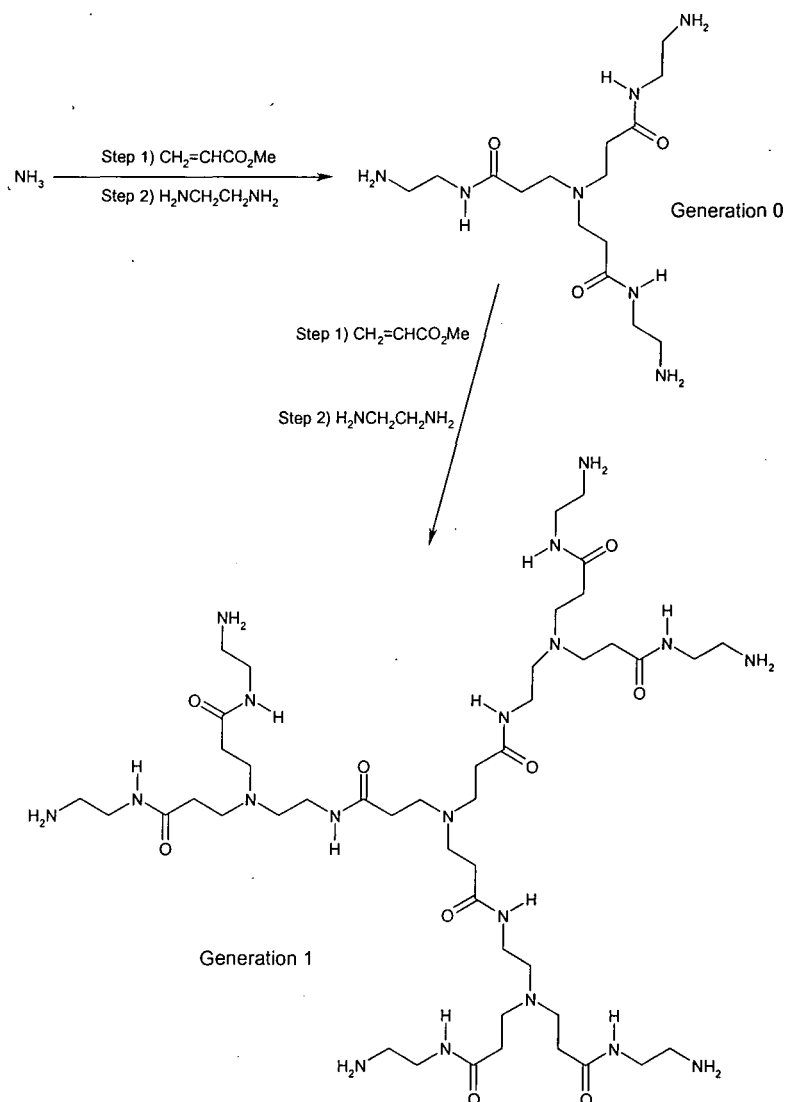


Figure 1.4. Divergent synthesis of Tomalia's generation 1 PAMAM dendrimer

The major drawback of this method is the requirement, as higher generations are reached, for an increasing number of activation and coupling reactions driven to complete conversion if perfect growth is to be achieved. As the size of the dendrimer increases, the risk of “bad” sequences or incomplete reactions also increases. As a consequence of the small difference in size and polarity between the perfect dendrimer and the dendrimers containing defects, their separation becomes almost impossible. The fact that large dendrimers made by the divergent route do contain species with structural defects was demonstrated by the application of soft-ionisation mass spectrometry;¹¹ namely electrospray mass spectrometry.

1.2.2. Convergent growth

The convergent method, inspired from a classical organic disconnection approach, starts growth of the globular dendrimer at what will become its chain-ends and proceeds toward what will become its focal point. Those dendrons are coupled to a multifunctional core to produce a dendrimer. This method allows greater flexibility in the synthesis of dendrimers than the divergent route. The convergent growth allows the accurate placement of more than one type of end group at the periphery of the dendrimer. The dendritic structures obtained by this method exhibit surfaces that can be differentiated as sectors, quadrants or hemispheres of different functionalities.^{12, 13} This route offers the possibility to build complex globular macromolecules with tailored properties and new supramolecular assemblies.¹⁴

Fréchet used the convergent growth in his synthesis of poly(arylalkylether) dendrimers.¹⁵ Each dendron was synthesised by convergent growth starting from the reaction between benzyl bromide (chain end) and 3,5-dihydroxybenzyl alcohol (AB₂ monomer). The unreacted aliphatic alcohol was activated by conversion to an alkyl bromide, which in its turn was reacted with the phenolic groups of 3,5-dihydroxybenzyl alcohol. This sequence of reaction-activation-reaction was repeated to build up the dendron, see *Figure 1.5*. Three of those dendrons were reacted with a trifunctional phenolic core to produce dendrimers of different generations, for example generation 4, with a molecular weight of 10,127 Daltons. This was the first report of the synthesis of unique macromolecules in this size range.

Unlike the divergent growth, the convergent growth only requires one activation reaction of the functional focal point of the dendron and the coupling step only involves two reactive sites of the monomer. As a consequence, the probability of side reactions is highly decreased and purification of the final product becomes easier. Furthermore, the big difference in size and polarity between the dendrimer and the side products or unreacted starting material allows relatively easy separation and purification. The limitation of the convergent growth approach is a possible steric inhibition at the focal point of the dendron at very high generations, which may limit the size of the final dendrimer that can be synthesised.

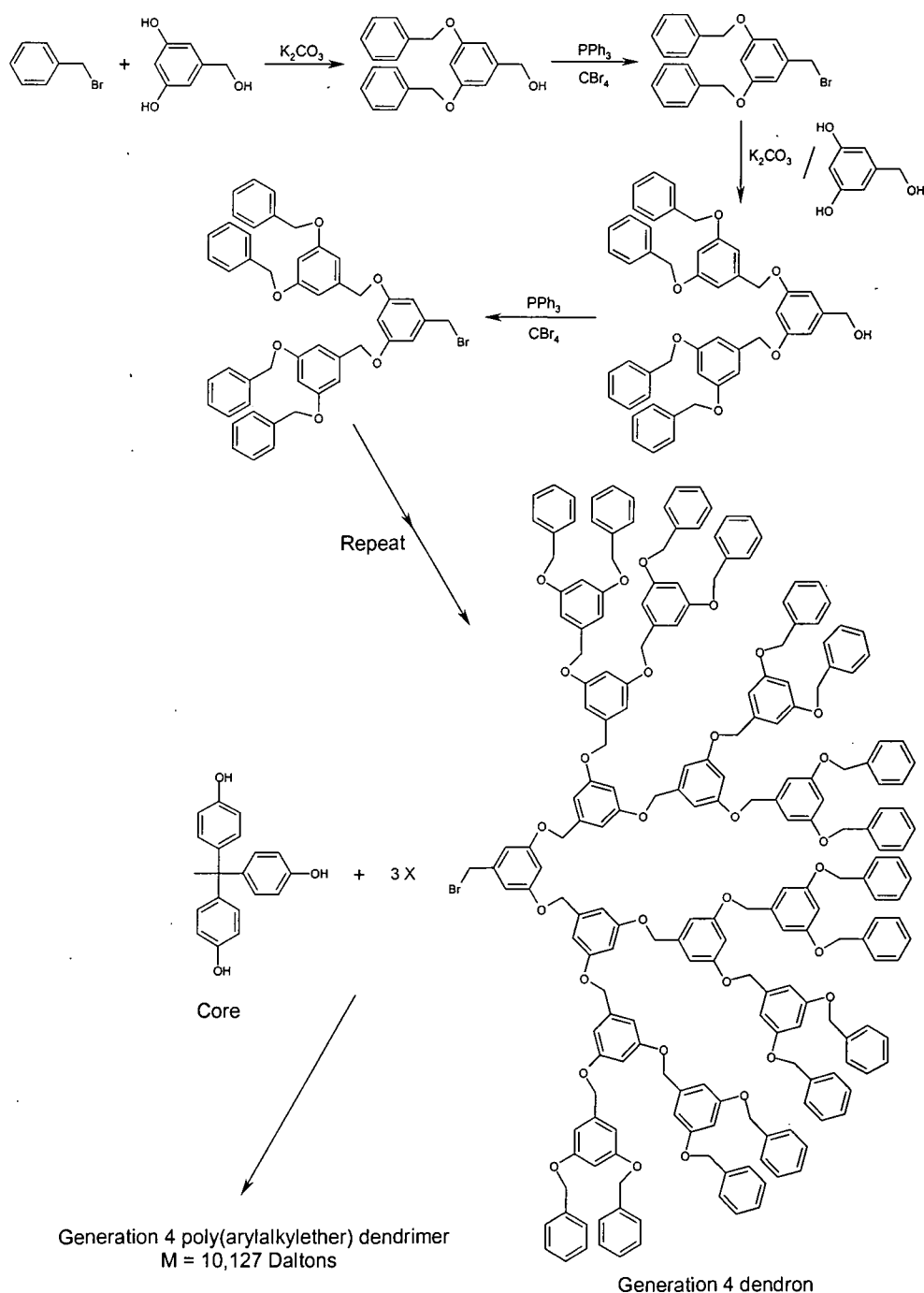


Figure 1.5. Convergent growth of Fréchet's poly(arylalkylether) dendrimer

1.2.3. Properties

The unique, perfectly symmetrical, globular shape of dendrimers gives rise to original and specific properties in comparison to those offered by other synthetic polymers. Dendrimers possess a monodisperse molecular weight distribution, whereas most synthetic polymers are polydisperse. This property is exhibited by size exclusion chromatography (SEC): while a synthetic polymer, like a polystyrene standard (prepared by anionic polymerisation) exhibits a narrow peak, it is found that SEC traces for dendritic macromolecules have appreciably narrower peak widths. The monodispersity of dendrimers can also be observed with MALDI-TOF (Matrix-Assisted Laser Desorption / Ionisation - Time Of Flight) Mass Spectroscopy. In the case of dendrimer samples, a unique peak is observed, proving that dendrimers possess a unique molecular weight, whereas polymeric samples show a distribution of peaks; each peak corresponds to a molecular weight within the molecular weight distribution of the considered polymer.⁷

Dendrimers exhibit unique solution behaviour. It is now well known that the intrinsic viscosity of linear polymers increases as their molecular weight increases, according to the Mark-Houwink-Sakurada equation:

$$[\eta] = K.M_v^\alpha$$

Where: $[\eta]$ is the intrinsic viscosity.

M_v is the viscosity average molecular weight.

K and α are constant for a given polymer/solvent/temperature system.

However, the behaviour of dendritic macromolecules does not obey this equation. The plot of $\log [\eta]$ vs. \log (molecular weight) gives a bell-shaped curve rather than the expected linear plot observed for linear polymers. This rather strange behaviour can be explained on the basis of the physical definition of the intrinsic viscosity: as inherent viscosity is concentration dependent, $[\eta]$ is obtained by extrapolation of the inherent viscosity to zero concentration. In the case of dendrimers, the value of $[\eta]$ is expressed in inverse concentration units (i.e. a volume divided by a mass). During generation growth, the volume of a supposed spherical dendrimer is expected to increase cubically ($V = 4/3 \pi r^3$), while its mass doubles at each successive

generation in an exponential way (the molecular weight is proportional to $2^{(G-1)}$).⁷ After reaching a critical generation, the mass term dominates and a bell-shaped curve is obtained. The maximum in intrinsic viscosity is correlated with a shape change of the dendrimer from an extended to a more compact globular shape.⁵ This change of conformation occurs when high generation numbers and therefore high molecular weights are reached.

Another characteristic of dendrimers is their enhanced solubility in comparison with their linear analogues. Miller and Neenan reported solubility enhancements of 10^5 for poly(phenylene) dendrimers in comparison with linear poly(phenylene).¹⁶ The increased solubility of dendritic macromolecules is due to their branched architecture, giving them a micelle-like shape, and to the solubilising contributions of their numerous end groups.⁷

The important branching of dendrimers provides the higher generations with an increasing number of cavities within the macromolecule. All those cavities can act as niches for specific guest-molecules. The surface congestion of high generation dendrimers can be used as a tool to trap those small molecules. They will be slowly delivered from the inner cavities of the dendrimer through its congested dense-packed surface.^{6, 17-20}

Their micelle-like shape and their ability to trap selectively small molecules allow amphiphilic dendrimers to be used as unimolecular micelles. Those dendritic micelles, which do not display any critical micelle concentration, are dendrimers possessing hydrophobic core and interior building blocks, which constitute an attractive environment for a hydrophobic molecule, and hydrophilic end groups, which allow the easy solubilisation of this host-guest system in water.²¹

The next category of dendritic macromolecules to be discussed is the family of hyperbranched polymers.

1.3. Hyperbranched polymers

In 1952, Flory elaborated a theoretical synthesis of highly branched structures from the one-step polycondensation of AB_x ($x \geq 2$) multifunctional monomers.²² These new polymers were predicted to have a broad molecular weight distribution, to be non-entangled, free of crosslinking and non-crystalline because of their highly branched structure.

Dendrimers offer very interesting material properties, but their synthesis is time-consuming. For use as engineering materials, they are far too difficult and expensive to produce, which makes the one-step synthesis of their hyperbranched analogues more and more attractive.²³

Kim and Webster wanted to use dendritic macromolecules as rheology control agents and as spherical multifunctional initiators. To obtain the material quickly and in large quantities, they developed a route for the one-step synthesis of hyperbranched polyphenylenes.²⁴⁻²⁷ They were synthesised by using Pd^0 or Ni^{II} catalysed coupling reactions. The monomers used were various dihalophenyl derivatives such as dibromophenylboronic acid (*Figure 1.6*).

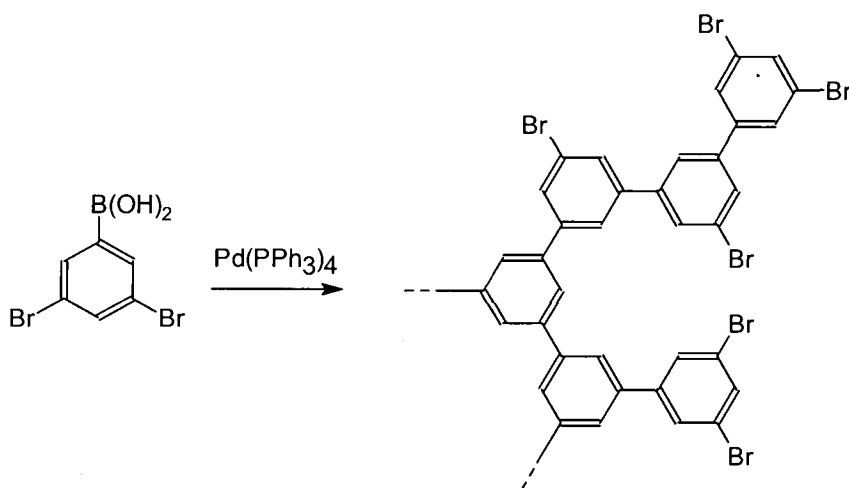


Figure 1.6. Synthesis of a hyperbranched polyphenylene by Suzuki coupling

The resulting polymers were polydisperse and highly branched macromolecules, but had defects in the form of built-in linear segments. These linear segments, the one-step strategy and the consequent imperfect growth and polydispersity are the fundamental differences between hyperbranched polymers and dendrimers (see *Figure 1.7*).

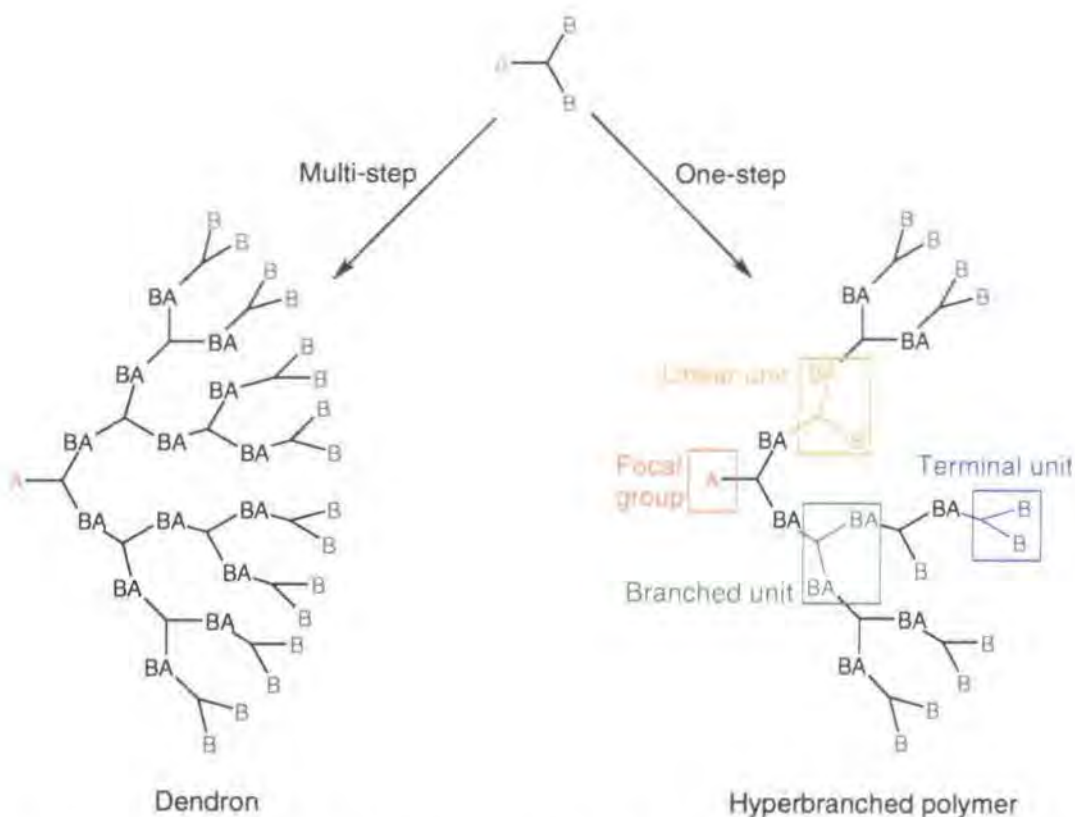


Figure 1.7. A comparison of a perfect dendron and a hyperbranched oligomer

While the step-by-step growth of macromolecules from AB_2 monomers gives rise to dendrimers, the one-step polymerisation of AB_2 monomers leads to complex hyperbranched products containing both branched and linear segments. The equal reactivity of the two B groups is modified when one of them reacts with an A group of another monomer to form a polymer linkage BA. The resulting steric constraint in the immediate vicinity of the unreacted B group decreases its accessibility and leads to the formation of defects; the linear units.

To define those intermediate structures, which stand between linear polymers and dendrimers, a new term: Degree of Branching (DB) has been introduced. It characterises the relative abundance of linear, terminal and branched units within a polymer. Fréchet's definition of DB was:²⁸

$$DB = (B + T) / (B + T + L)$$

Where: B is the number of branched units

T is the number of terminal units

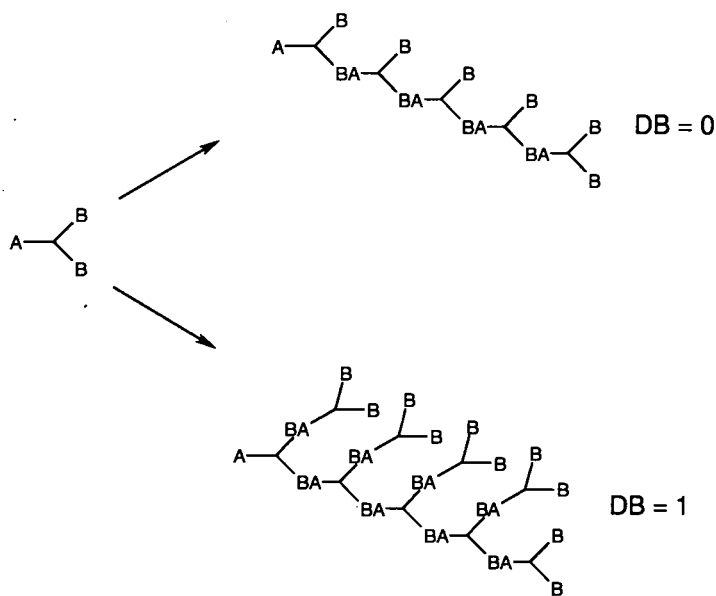
L is the number of linear units

Another definition was proposed by Frey:²⁹

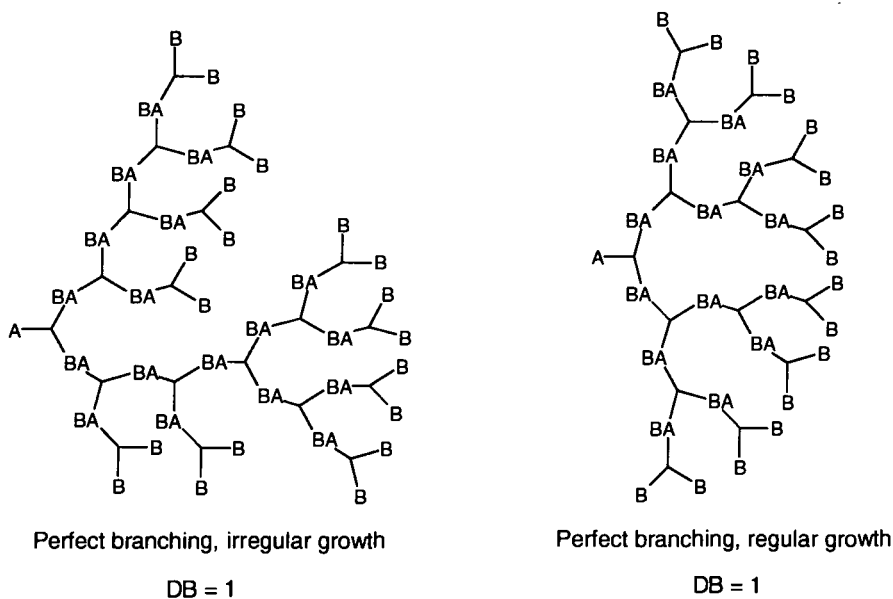
$$DB = 2B / (2B + L)$$

This latter definition is more widely accepted since it gives a more reasonable estimate of branching than the Fréchet method, which over emphasises residual monomer.

However, the degree of branching provides no useful information about the overall topology of the considered polymer. For example, it is possible to synthesise linear polymers with a DB equal to 0 or 1.



Furthermore, two dendritic macromolecules possessing a DB of 1 may display two different kinds of growth.



Statistical polymerisation of AB_2 monomers, i.e. where all B groups have equivalent reactivity independent of their location, is predicted to give hyperbranched polymers with a degree of branching of 0.5. Also, it was predicted that as the extent of consumption of A groups tends to completion, the polydispersity tends to infinity.²²

1.3.1. Synthesis strategies

Several conditions are required to achieve high molecular weight hyperbranched polymers from AB_x monomers. The A and B groups must only react with each other, there can be no A with A or B with B reactions. There must be no side reactions and there must be no AA bifunctional impurities. Three major polymerisation methods are used to synthesise hyperbranched polymers: step polymerisation, self-condensing vinyl polymerisation and ring-opening polymerisation.

• Step polymerisation

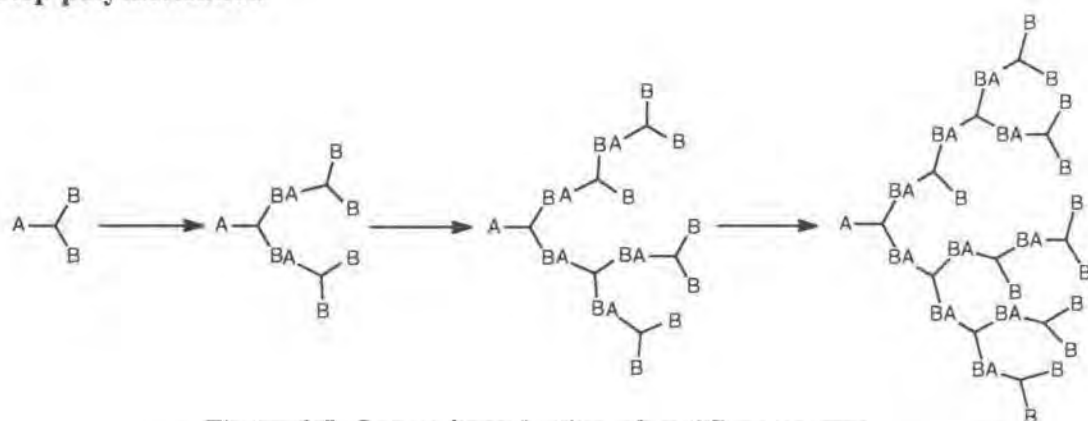
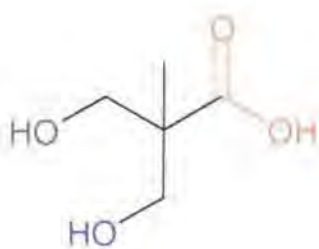
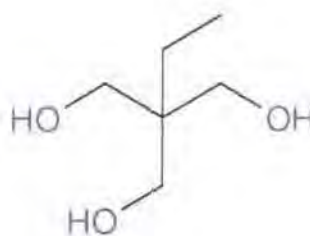


Figure 1.8. Step polymerisation of an AB_2 monomer

Hyperbranched aliphatic polyesters were obtained by condensation copolymerisation of 2,2-bis(hydroxymethyl)propionic acid (AB_2 monomer) and 2-ethyl-2-(hydroxymethyl)-1,3-propanediol (B_3 monomer used as a core), in the presence of an acid catalyst.^{30, 31}



2,2-bis(hydroxymethyl)propionic acid



2-ethyl-2-(hydroxymethyl)-1,3-propanediol

The polymers exhibited a degree of branching close to 0.45. This result is in accordance with an ideal statistical branching.³² The addition of small quantities of B₃ core units has been suggested as a good way to control the molecular weight distribution of hyperbranched polymers.³³ It can provide a one-step route to pseudo-dendrimers (*Figure 1.9*).

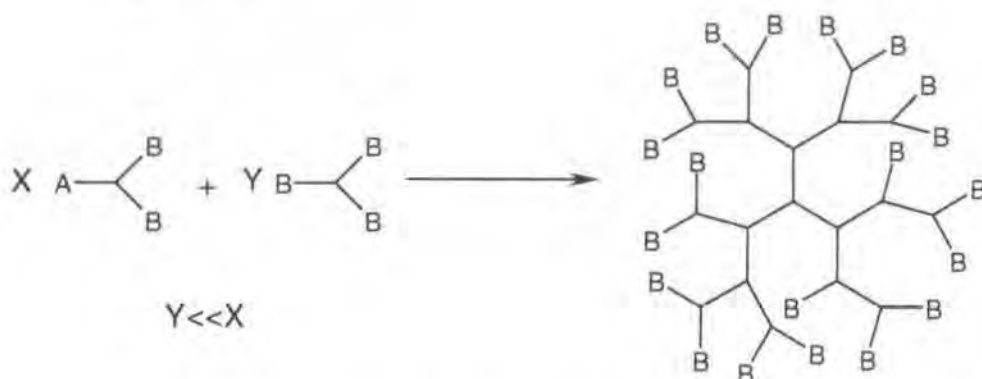


Figure 1.9. Formation of an AB₂/B₃ copolymer, a pseudo-dendrimer

In previous work in Durham, Lois Hobson synthesised hyperbranched poly(amidoamine)s, hyperbranched analogues of Tomalia's PAMAM dendrimers.^{34,39,40} Aminoacrylamide hydrochloride AB₂ monomers (*Figure 1.10*) were polymerised in the melt, using Michael addition chemistry. No evidence of cyclisation, due to the intramolecular reaction between a terminal group and the focal point, was found by MALDI-TOF, ¹H and ¹⁵N NMR spectroscopy. Using the n = 2 monomer lead to hyperbranched polymers exhibiting a degree of branching, determined by ¹⁵N NMR, close to 1.

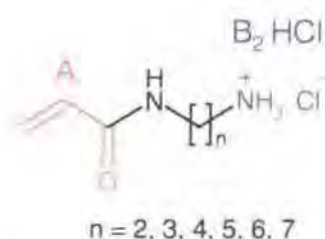


Figure 1.10. Monomers used in the synthesis of hyperbranched poly(amidoamine)s

• Self-condensing vinyl polymerisation

This polymerisation requires monomers containing both an initiating group and a propagating group. The monomers are usually vinyl monomers containing pendant groups B that can be transformed into initiating species by an activation step.

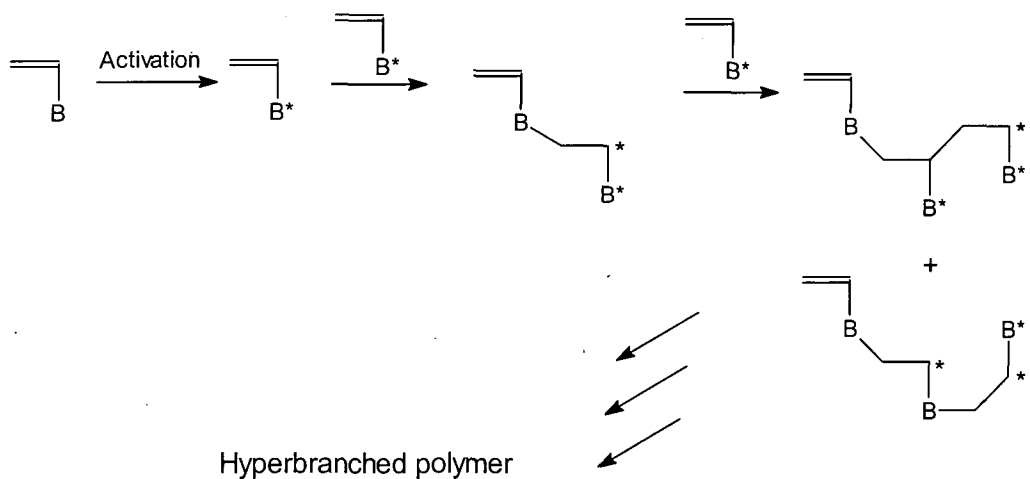


Figure 1.11. Self-condensing vinyl polymerisation

Hawker used this method to polymerise 4-[2-(phenyl)-2-(1-2,2,6,6-tetramethyl piperidinyloxy) ethoxy] methyl styrene³⁵ by TEMPO-assisted radical polymerisation (Figure 1.12) and Matyjaszewski applied the concept to *para*(chloromethyl)styrene³⁶ using Atom Transfer Radical Polymerisation (Figure 1.13).

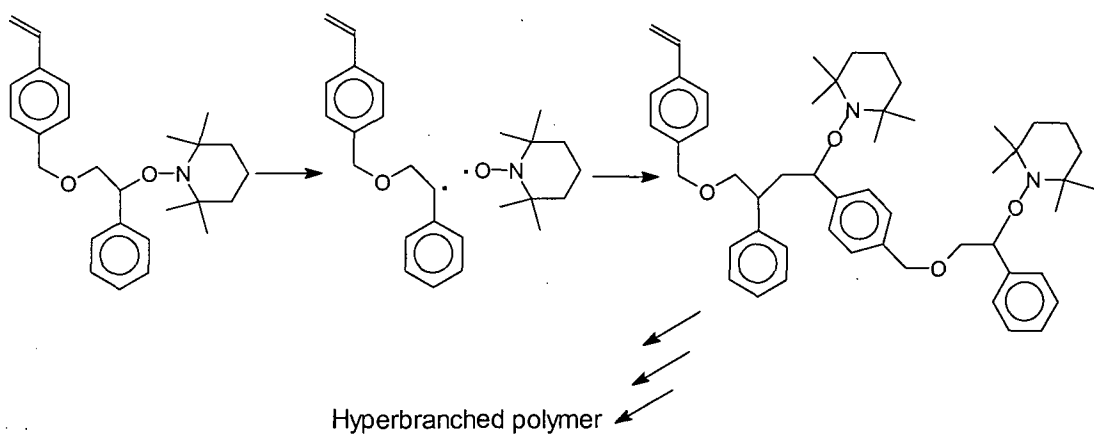


Figure 1.12. TEMPO-assisted activation and radical polymerisation of 4-[2-(phenyl)-2-(1-2,2,6,6-tetramethyl piperidinyloxy) ethoxy] methyl styrene

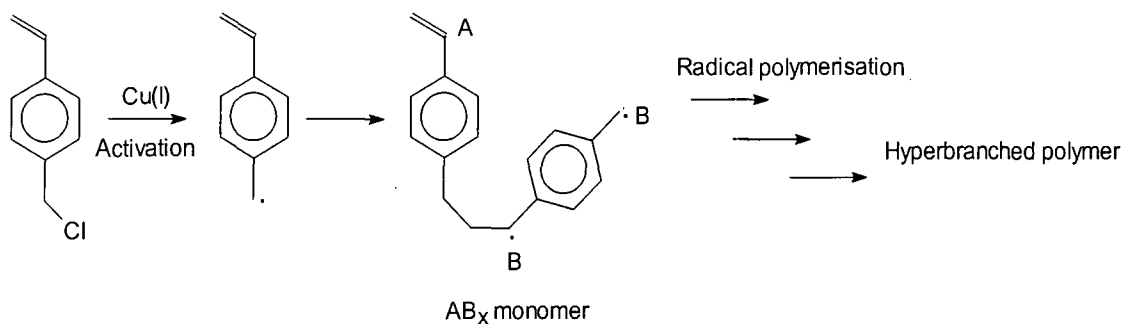


Figure 1.13. Activation and Atom Transfer Radical Polymerisation of *para*(chloromethyl)styrene

• Ring-opening polymerisation

This method involves the creation of an AB₂ monomer by ring-opening of a cyclic species. Suzuki reported the synthesis of hyperbranched polyamines with controlled molecular weights and low polydispersities (<1.3) using a cyclic carbamate, which reacted with a Pd⁰ catalyst and a primary amine to give rise to a diamino compound; the AB₂ monomer.³⁷ This diamino derivative contained a secondary amino group that reacted with the ring-opened carbamate to give branched units (1), while the primary amino group reacted with the carbamate to give linear units (2) (Figure 1.13). The combination and repetition of these two reactions lead to the synthesis of hyperbranched polymers.

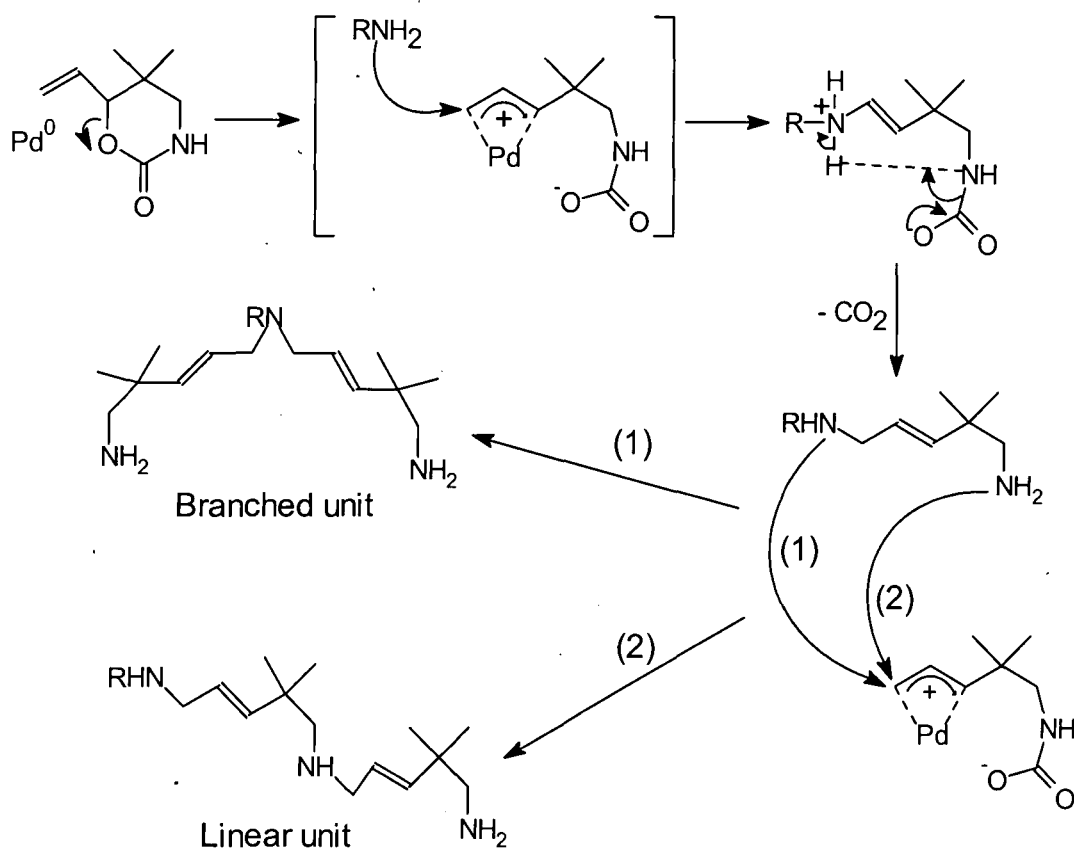


Figure 1.13. Synthesis of hyperbranched polyamines by ring-opening polymerisation

1.3.2. Properties

Hyperbranched polymers possess properties, which can be similar to those of dendrimers. At high molecular weights, hyperbranched polymers display an irregular globular shape, which is the direct consequence of the flexibility of their segments and their degree of branching. They possess a high chemical reactivity, especially with

regard to the chemical modification of their chain ends, but this reactivity is lower than the one observed for perfect dendrimers because some chain ends, buried inside the hyperbranched structure cannot easily be accessed for modification.

The solution behaviour of dendrimers does not follow the Mark-Houwink-Sakurada equation; by contrast, hyperbranched polymers, like linear polymers, do follow this equation, but with lower " α " values, hence they exhibit lower intrinsic viscosities than their linear counterparts.^{7, 23} The solubility of hyperbranched polymers is enhanced in comparison to that of their linear analogues. Kim and Webster reported that their hyperbranched polyphenylenes had very good solubility in various organic solvents whereas linear polyphenylenes had very poor solubility in the same solvents. The solubility of hyperbranched polymers is also dependent on the nature of their end groups; highly polar end groups, such as carboxylates, allowed hydrophobic hyperbranched polyphenylenes to become water-soluble. Like dendrimers, hyperbranched polymers possessing hydrophobic inner structures and hydrophilic end groups can behave as unimolecular micelles. Kim and Webster described their hyperbranched polyphenylenes with carboxylate end groups as unimolecular micelles.²⁴ Carboxylate end groups made their polymers water-soluble and the hydrophobic interior could host guest molecules. Hawker and Chu solubilised small hydrophobic molecules in water by using hyperbranched aromatic poly(ether-ketones) with carboxylic acid end groups.³⁸ They did not observe any critical micelle concentration, but an increase of the solubility of the hydrophobic molecules with increase of the polymer concentration.

The mechanical properties of hyperbranched polymers are the direct consequence of their highly branched structure. The lack of chain entanglements leads to reduced mechanical strength in comparison with analogous linear polymers. Their compact highly branched structure makes hyperbranched polymers amorphous. As a consequence, they are suitable as additives or components of thermosets, where resistance to compression or toughness is needed.

Hyperbranched polymers constitute a new field in polymer chemistry. Their highly branched structure and their large number of end groups make them very interesting materials for a large number of low-cost applications, where properties similar to those of dendrimers are desirable.

This project had the objectives of reproducing and extending the work that Dr. Lois Hobson had achieved in Durham. In order to achieve this goal, a thorough investigation of synthesis and characterisation of the monomer; N-acryloyl-1,2-diaminoethane hydrochloride was undertaken. Melt polymerisation of this monomer was found to be difficult to reproduce and simpler procedures were sought, aqueous solution polymerisation was considered and studied in detail using the following monomers: N-acryloyl-1,2-diaminoethane hydrochloride and N-acryloyl-1,2-diaminoethane. The resulting polymers were fully characterised.

Chapter Two

Monomer synthesis

2.1. Introduction

The synthesis and polymerisation of a new AB₂ monomer, N-acryloyl-1,2-diaminoethane hydrochloride was developed in Durham by Lois Hobson during the 1995–1998 period.^{34, 39, 40} The monomer was polymerised in the melt and the resulting hyperbranched poly(amidoamine)s exhibited degrees of branching close to 1. This polymerisation potentially represented an easier and cheaper way to synthesise hyperbranched polymers, which might exhibit properties similar to those of Tomalia's PAMAM dendrimers. She made a family of related monomers with longer methylene sequences but, although these also polymerised in the melt to give hyperbranched polymers, it was only the N-acryloyl-1,2-diaminoethane hydrochloride that gave a degree of branching of 1, the others tended towards statistical branching. The three-step synthesis of N-acryloyl-1,2-diaminoethane hydrochloride involved:

- i. The protection of one amino group of 1,2-diaminoethane.
- ii. The reaction of the remaining unprotected amino group with acryloyl chloride.
- iii. Acidic deprotection of the protected amino group.

The purity of the monomer is critical and has to be essentially 100% in order to obtain hyperbranched polymers without any possibility of intermolecular crosslinking. Each intermediate product must be as pure as possible before being used as a reagent in the next step. In particular, it is essential that any diacryloyl derivatives are excluded, since traces of such impurities inevitably lead to insoluble crosslinked products. Diamines and diammonium salt impurities or AB₂ oligomers are less critical. The synthetic route is shown in *Figure 2.1* and the details of the protocol developed in this work in order to obtain pure monomer are described in the next section and discussed in section 2.3.

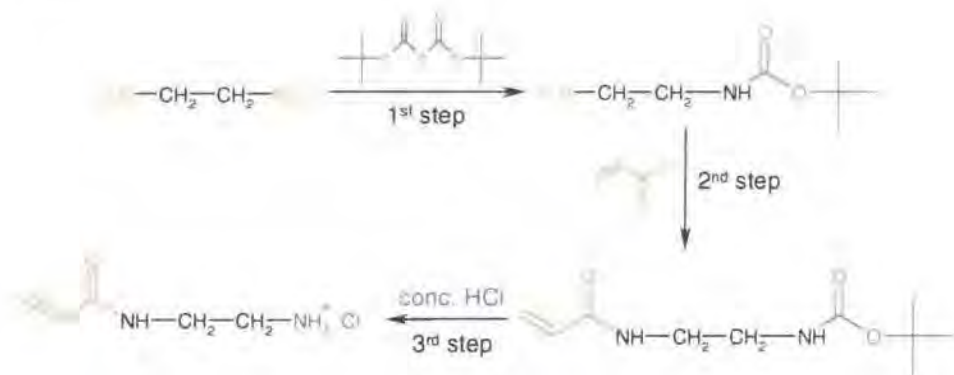


Figure 2.1. Three-step synthesis of N-acryloyl-1,2-diaminoethane hydrochloride

2.2. Experimental

All chemicals were purchased either from Aldrich Chemical Company or Lancaster Synthesis. Ethylenediamine and acryloyl chloride were distilled and stored under nitrogen prior to use. Di-*tert*-butyldicarbonate was used as received and stored in a fridge. Elemental analyses were performed using an Exeter Analytical Elemental Analyzer CE-440. Infrared spectra were recorded on a Perkin Elmer 1720X FTIR spectrometer. ^1H and ^{13}C NMR spectra were acquired on a Varian Unity 300 spectrometer at 299.91 MHz (^1H) and 75.41 MHz (^{13}C) or a Varian Mercury 400 spectrometer at 399.97 MHz (^1H) and 100.57 MHz (^{13}C) or a Varian Inova 500 at 499.78 MHz (^1H) and 125.67 MHz (^{13}C). Mass spectra, without chromatography, were recorded on a Micromass AutoSpec instrument. Gas chromatography – Mass spectroscopy (GC-MS) experiments were run on a Finnigan TRACE MS instrument possessing a HP 5 chromatography column (5% diphenyl–95% dimethylpolysiloxane). Electrospray (ES) mass spectra were recorded on a Micromass LCT instrument.

2.2.1. Step 1: *N-tert*-butoxycarbonyl-1,2-diaminoethane

Following the synthesis reported by Lois Hobson, the mono-protection of ethylenediamine was achieved by reaction of excess ethylenediamine with di-*tert*-butyldicarbonate, according to the following protocol.

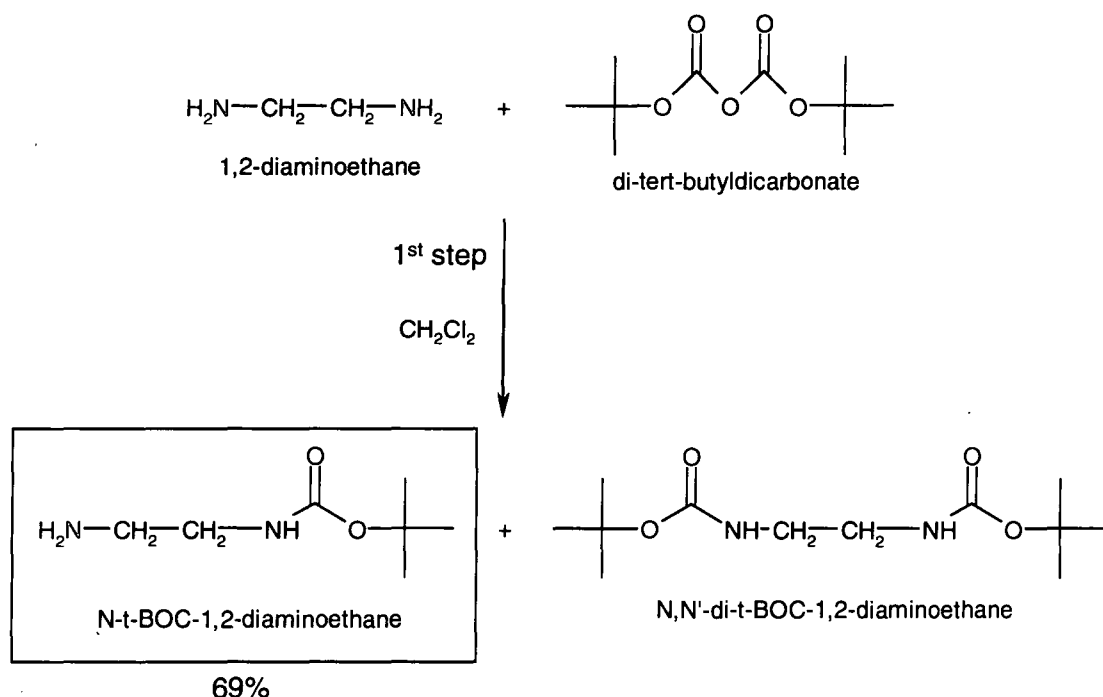


Figure 2.2. Synthesis of *N-tert*-butoxycarbonyl-1,2-diaminoethane

To a 2L three-necked flask cooled in an ice/salt bath (temperature between -10 and 0 °C), fitted with a condenser, a pressure equalising dropping funnel, a magnetic stirrer and a nitrogen inlet, was added a solution of ethylenediamine (45 g, 733 mmol) in dichloromethane (400 ml). A solution of di-*tert*-butyldicarbonate (45 g, 206 mmol) in dichloromethane (200 ml) was added dropwise over 2 hours while stirring. A white solid was formed during the addition. At the end of the addition, the temperature of the mixture was allowed to increase to room temperature and the mixture was left stirring at room temperature overnight. The solvent was removed by rotary evaporation and water (200 ml) was added to allow the complete precipitation of the white solid, *N,N'*-(bis-*t*-butoxycarbonyl)-1,2-diaminoethane, which was separated from the aqueous solution by filtration. Empirically, it was found that total removal of all the precipitate required the use of a Whatman® number 1 qualitative filter paper. The filtered aqueous solution was saturated with sodium chloride and the *t*-BOC monoprotected compound (*N-tert*-butoxycarbonyl-1,2-diaminoethane) was extracted from the aqueous phase with ethyl acetate (3 x 100 ml). The combined organic fractions were concentrated under reduced pressure to give an oil, which was dissolved in chloroform (100 ml). The residual sodium chloride precipitated and was removed by filtration using the procedure described above. The chloroform was removed under reduced pressure. A clear colourless oil was obtained. It was stirred and dried under vacuum overnight to afford pure *N-tert*-butoxycarbonyl-1,2-diaminoethane (22.70 g, 142 mmol; yield = 69%). Found: C, 51.85; H, 10.07; N, 17.19%. C₇H₁₆N₂O₂ requires: C, 52.48; H, 10.07; N, 17.49%. FTIR (liquid film on KBr): 3361 (br, primary amine N-H stretching, water?); 2976, 2932 and 2869 (s, CH₂ and CH₃ C-H stretching); 1698 (s, urethane C=O stretching); 1522; 1366; 1276 and 1174 cm⁻¹ (Appendix 1.1). ¹H NMR (CDCl₃, 299.91 MHz): δ (ppm): 1.11 (s, 2 H, NH₂); 1.39 (s, 9 H, CH₃); 2.74 (t, ³J_{HH} = 5.9 Hz, 2 H, CH₂); 3.11 (q, ³J_{HH} = 5.9 Hz, 2 H, CH₂) and 5.04 (bs, 1 H, urethane hydrogen) (see Appendix 1.2). ¹³C NMR (CDCl₃, 125.67 MHz): δ (ppm): 28.09 (CH₃); 41.53 (CH₂); 43.09 (CH₂ close to NH₂); 78.62 (quaternary C) and 156.04 (C=O) (see Appendix 1.3). MS (CI⁺): m/z: 161 (Molecular peak + H) and 105 (loss of H₂C=C(CH₃)₂) (see Appendix 1.4).

2.2.2. Step 2: *N-tert*-butoxycarbonyl-*N'*-acryloyl-1,2-diaminoethane

The second step of the monomer synthesis involved an addition-elimination reaction between the unprotected amino group of the monoprotected diamine with

acryloyl chloride in the presence of triethylamine to give *N-tert*-butoxycarbonyl-*N'*-acryloyl-1,2-diaminoethane as described in the following protocol.

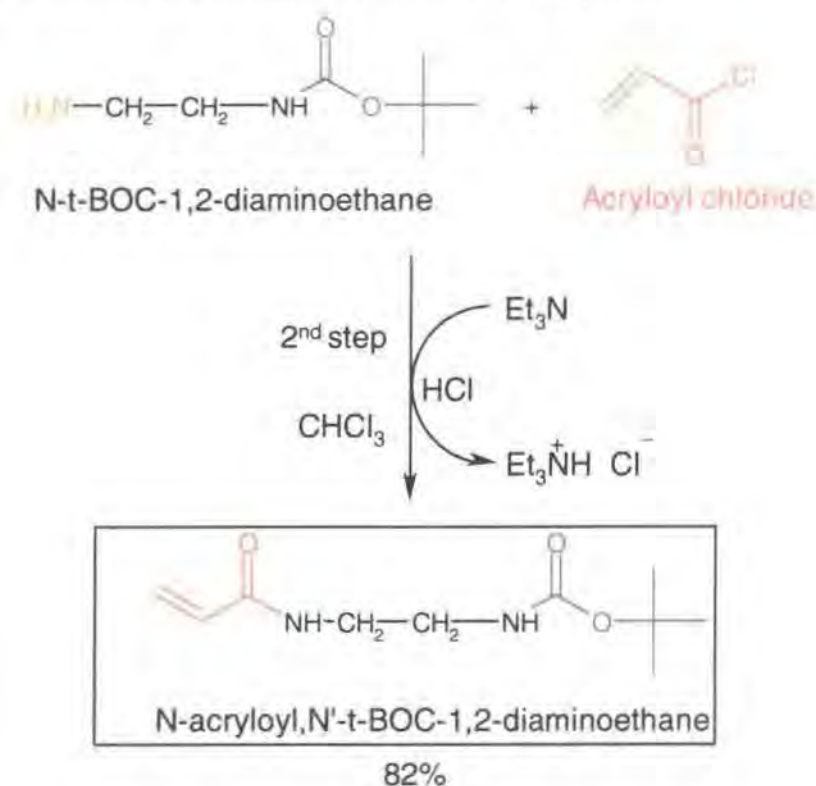


Figure 2.3. Synthesis of *N-tert*-butoxycarbonyl-*N'*-acryloyl-1,2-diaminoethane

To a well-stirred solution of acryloyl chloride (15.4g, 170 mmol) in chloroform (300 ml), cooled in an ice/salt bath (-10 to 0 °C), was added dropwise, over 1 hour, a solution of triethylamine (14.37 ml, 142 mmol) and *N-tert*-butoxycarbonyl-1,2-diaminoethane (22.70g, 142 mmol) in chloroform (150 ml). After the addition was completed, the reaction was allowed to equilibrate to room temperature and stirred for 2 hours. Then the chloroform was removed under reduced pressure. The white residue was washed with water (200 ml) and extracted with chloroform (3 x 150 ml). The organic fractions were concentrated under reduced pressure. A white solid was obtained and dried under vacuum during one day to give pure *N-tert*-butoxycarbonyl-*N'*-acryloyl-1,2-diaminoethane (25 g, 117 mmol, yield = 82%). Found: C, 55.25%; H, 8.48%; N, 13.33%. $\text{C}_{10}\text{H}_{18}\text{N}_2\text{O}_3$ requires: C, 56.06%; H, 8.47%; N: 13.07%. FTIR (KBr disc): 3307 (br, water); 3077 (m, vinyl double bond C-H stretching); 2979 (s, CH_2 and CH_3 C-H stretching); 1699 (s, urethane C=O stretching); 1557; 1451; 1286; 1177; 980 (s, vinyl double bond C-H out-of-plane deformation) and 689 cm^{-1} (see Appendix 1.5). $^1\text{H NMR}$ (CDCl_3 , 499.78 MHz): δ (ppm): 1.43 (s, 9 H, CH_3); 1.61 (s, water); 3.25 (q, $^3J_{\text{HH}} = 5.7 \text{ Hz}$, 2 H, CH_2); 3.38 (q, $^3J_{\text{HH}} = 5.7 \text{ Hz}$, 2 H, CH_2); 4.95 (bs, 1 H, urethane

hydrogen); 5.57 (d, $^3J_{\text{HH cis}} = 10.5$ Hz, 1 H, vinyl hydrogen); 6.02 (dd, $^3J_{\text{HH cis}} = 10.5$ Hz, $^3J_{\text{HH trans}} = 17$ Hz, 1 H, vinyl hydrogen); 6.20 (d, $^3J_{\text{HH trans}} = 17$ Hz, 1 H, vinyl hydrogen); 6.40 (bs, 1 H, amide hydrogen) (see Appendix 1.6). ^{13}C NMR (CDCl_3 , 125.67 MHz): δ (ppm): 28.31 (CH_3); 40.05 (CH_2); 40.97 (CH_2); 79.77 (quaternary C); 126.22 ($\text{H}_2\text{C}=\text{}$); 130.86 ($=\text{CH}$); 157.12 (urethane $\text{C}=\text{O}$); 166.22 (amide $\text{C}=\text{O}$) (see Appendix 1.7). MS (EI+): m/z : 158 (loss of $\text{H}_2\text{C}=\text{C}(\text{CH}_3)_2$); 141 (loss of $\text{O}-\text{C}(\text{CH}_3)_3$); 115 (loss of CO_2 , $\text{H}_2\text{C}=\text{C}(\text{CH}_3)_2$ and gain of $+\text{H}$); 97 (loss of NH_3 and H); 84 ($\text{H}_2\text{C}=\text{CHCO}-\text{NH}-\text{CH}_2$); 57 ($\text{C}(\text{CH}_3)_3$) (see Appendix 1.8).

2.2.3. Step 3: N-acryloyl-1,2-diaminoethane hydrochloride

The final step in the monomer synthesis involves the removal of the *t*-BOC protecting group using concentrated hydrochloric acid (HCl), releasing isobutene and carbon dioxide (biproducts of the deprotection) and leading to the synthesis of the ammonium salt as described in the following procedure.

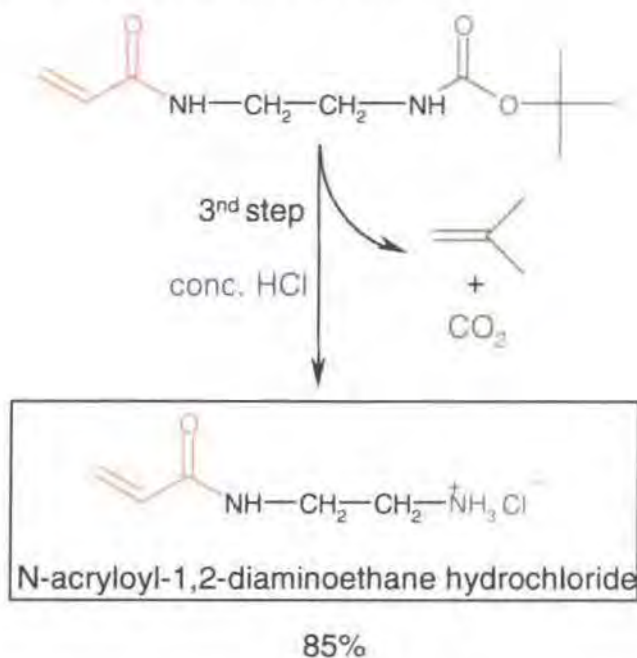


Figure 2.4. Third step: Cleavage of *t*-BOC protecting group

To the white powder of *N*-*tert*-butoxycarbonyl-*N'*-acryloyl-1,2-diaminoethane (10 g, 47 mmol) an aqueous solution of concentrated hydrochloric acid (37%, 10 ml) was added slowly. The powder, initially insoluble in water, slowly dissolved in the concentrated HCl solution, while strong bubbling was observed; a sign that the removal of the *t*-BOC protecting group was occurring. The solution was stirred for 30 minutes and the solvent was removed overnight under high vacuum (8×10^{-2} mbar) to afford a

clear white gum that was dissolved in ethanol (100 ml); the resulting mixture was filtered through a porosity 2 sinter. A white hygroscopic powder was obtained by reprecipitation in cold hexane and recovered by filtration using a porosity 2 sinter. The white solid was dried under vacuum to give pure N-acryloyl-1,2-diaminoethane hydrochloride (6 g, 40 mmol, yield = 85%). Found: C, 39.43; H, 7.41; N, 18.37%. $C_5H_{11}N_2OCl$ requires: C, 39.87; H, 7.36; N, 18.60%. FTIR (KBr disc): 3262 and 3062 (br, ammonium group N-H stretching, water?); 1661 and 1625 (s, C=O stretching); 1548; 1249; 1171; 982 (s, vinyl double bond C-H out-of-plane deformation); 806 and 668 cm^{-1} (see Appendix 1.9). $^1\text{H NMR}$ (D_2O , 499.78 MHz): δ (ppm): 3.02 (t, $^3J_{\text{HH}} = 6\text{ Hz}$, 2 H, CH_2); 3.43 (t, $^3J_{\text{HH}} = 6\text{ Hz}$, 2 H, CH_2); 5.64 (dd, $^3J_{\text{HH cis}} = 9.5\text{ Hz}$, $^2J_{\text{HH}} = 2\text{ Hz}$, 1 H, vinyl hydrogen); and a pseudo ABq, $\delta_A = 6.11\text{ ppm}$, $\delta_B = 6.07\text{ ppm}$, $J_{\text{AB}} = 17.25\text{ Hz}$, with the A limb split into doublets ($^3J_{\text{HH cis}} = 9.5\text{ Hz}$) and the B limb split into doublets ($^2J_{\text{HH}} = 2\text{ Hz}$) (see Appendix 1.10). $^{13}\text{C NMR}$ (D_2O , 125.67 MHz): δ (ppm): 36.93 (CH_2); 39.32 (CH_2); 128.17 ($\text{H}_2\text{C}=\text{}$); 129.65 ($=\text{CH}$); 169.59 ($\text{C}=\text{O}$) (see Appendix 1.11). MS (ES+): 115 (loss of $\text{HCl} + \text{H}$); 98 (loss of NH_3) (see Appendix 1.12).

2.2.4. Synthesis of N-acryloyl-1,2-diaminoethane

A second monomer, N-acryloyl-1,2-diaminoethane, more reactive than N-acryloyl-1,2-diaminoethane hydrochloride was synthesised using Dowex ion exchange resin beads that exchange their hydroxyl anion with the chloride anion of the N-acryloyl-1,2-diaminoethane hydrochloride, generating water and N-acryloyl-1,2-diaminoethane according to the following procedure.

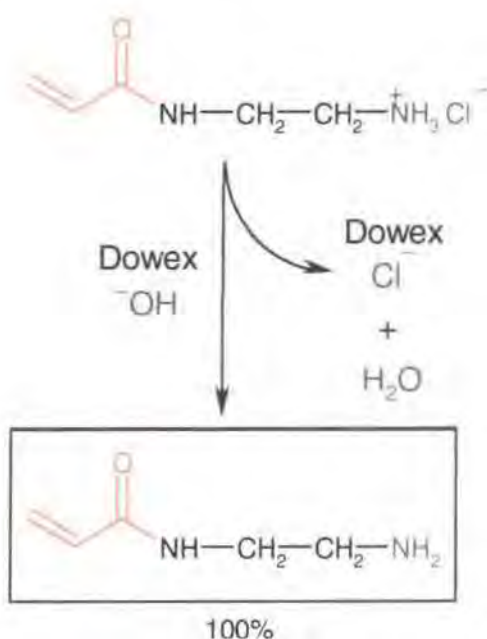


Figure 2.5. Synthesis of N-acryloyl-1,2-diaminoethane

To a well stirred aqueous solution (10 ml) of N-acryloyl-1,2-diaminoethane hydrochloride (0.5 g, 3.32 mmol, $\text{pH}_{\text{solution}} = 5-6$) in deionised water were added about 4 g of Dowex ion (OH) exchange resin beads. The mixture was stirred for 15 minutes and then filtered through a porosity 2 sinter. The pH of the solution was determined as 10 using pH paper. In order to characterise this new monomer (see 2.3.4), a solution of N-acryloyl-1,2-diaminoethane hydrochloride (0.1 g, 0.33 mmol) was prepared in D_2O (2 ml) instead of deionised water and stirred with about 1 g of Dowex ion (OH) exchange resin beads for 15 min. The solution was then filtered and the pH of the solution was determined as 10. This solution was analysed by NMR. ^1H NMR (D_2O , 399.97 MHz): δ (ppm): 2.57 (t, $^3J_{\text{HH}} = 6.2$ Hz, 2 H, CH_2); 3.14 (t, $^3J_{\text{HH}} = 6.2$ Hz, 2 H, CH_2); 5.56 (dd, $^3J_{\text{HH cis}} = 10$ Hz, $^2J_{\text{HH}} = 1.6$ Hz, 1 H, vinyl hydrogen); and a pseudo ABq, $\delta_{\text{A}} = 6.07$ ppm, $\delta_{\text{B}} = 6$ ppm, $J_{\text{AB}} = 17.4$ Hz, with the A limb split into doublets ($^3J_{\text{HH cis}} = 10$ Hz) and the B limb split into doublets ($^2J_{\text{HH}} = 1.6$ Hz) (see Appendix 1.13). ^{13}C NMR (D_2O , 100.57 MHz): δ (ppm) = 39 (CH_2); 42 (CH_2); 127 ($\text{H}_2\text{C}=\text{}$); 130 ($=\text{CH}$); 169 ($\text{C}=\text{O}$) (see Appendix 1.14).

2.3. Discussion

NMR spectroscopy was the key technique for establishing the structures and as a guide to the nature of contaminants. H-H and H-C COSY experiments were run when doubts about the exact assignment of the peaks observed by ^1H and ^{13}C NMR existed. Finally, the purity of the first and second step products, which is the key factor to ensure the purity of the final monomer, was checked by gas chromatography (GC) of chloroform solutions.

2.3.1. First step

In the case of the characterisation of N-*tert*-butoxycarbonyl-1,2-diaminoethane by NMR spectroscopy, each of the peaks observed in the ^1H and ^{13}C NMR spectra can be identified on the basis of its chemical shift and by running H-H and H-C COSY experiments. Thus, the H-H COSY experiment, run on a sample of N-*tert*-butoxycarbonyl-1,2-diaminoethane (see *Figure 2.6*) shows that the methylene hydrogens observed at 3.11 ppm are directly correlated to the urethane hydrogen observed at 5.40 ppm and to the two methylene hydrogens observed at 2.74 ppm. As a consequence, the latter is connected to the unprotected primary amino group, which

corroborates the first approach based on the chemical shifts and the fact that the proximity of the electron withdrawing urethane group will generate a larger shift to higher ppm values for the methylene hydrogens adjacent to it.

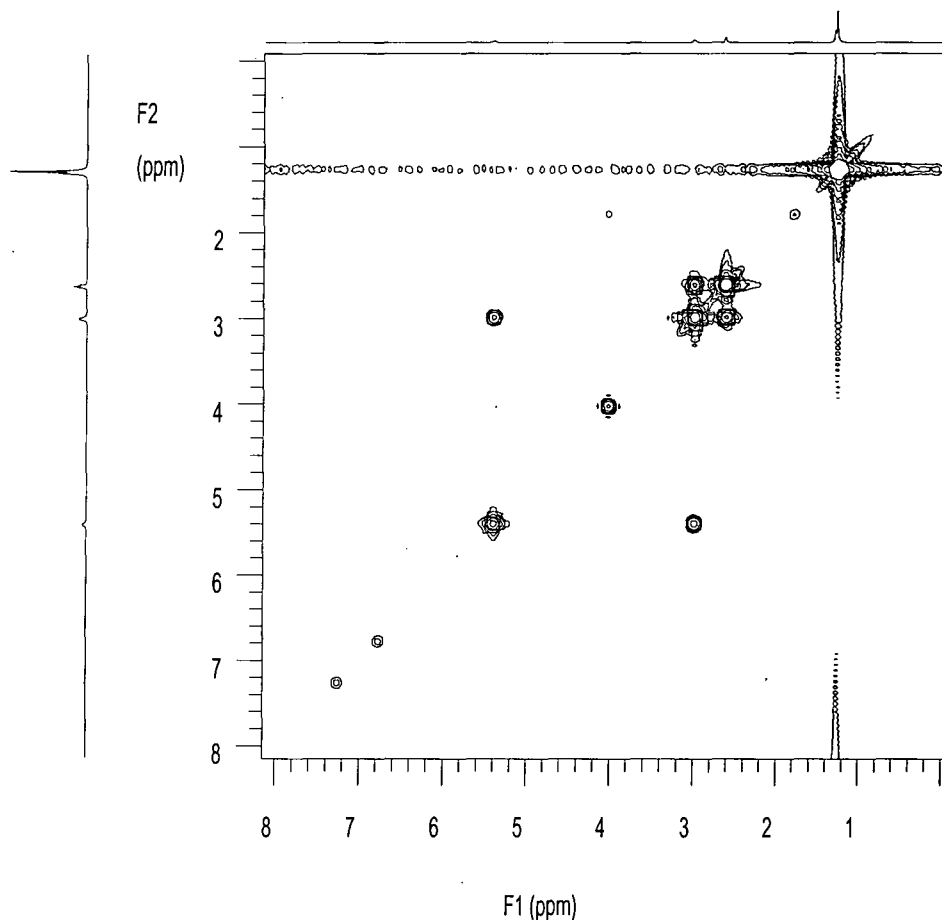


Figure 2.6. H-H COSY experiment on *N*-tert-butoxycarbonyl-1,2-diaminoethane

Using the H-C COSY experiment data, it is possible to assign each observed peak in the ^{13}C NMR spectrum to the corresponding carbon of the molecule, by correlating those peaks to the already assigned hydrogen peaks. In the ^{13}C NMR spectrum of *N*-tert-butoxycarbonyl-1,2-diaminoethane (see Figure 2.7 and Appendix 1.3), the peak observed at 28.09 ppm corresponds to the carbon of the CH_3 belonging to the *t*-BOC protecting group. The peak at 41.53 ppm originates from the carbon of the methylene close to the primary amine. The peak at 43.09 ppm is generated by the carbon of the methylene close to the urethane. At 76 ppm, a triplet corresponding to the carbon of CDCl_3 is observed. This signal appears as a triplet due to the direct coupling of the carbon atom with a deuterium atom. The carbonyl carbon is seen at

156.04 ppm (not shown here) and is not coupled to any hydrogen, as expected. Finally, the last carbon, not directly coupled to any hydrogen, is the quaternary carbon of the *t*-BOC protecting group that is observed at 78.62ppm.

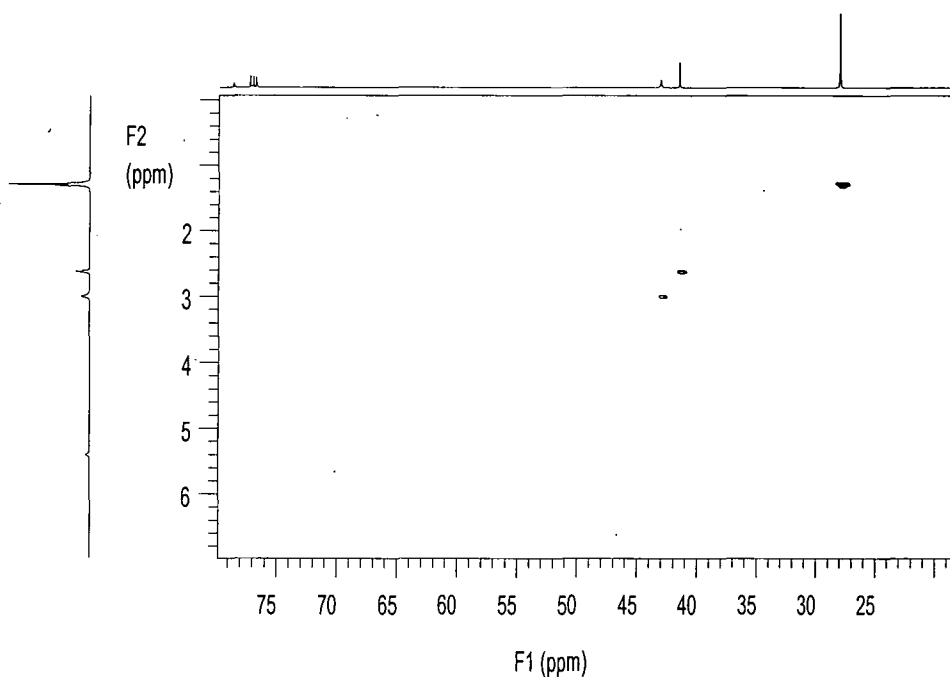


Figure 2.7. H-C COSY experiment on *N*-tert-butoxycarbonyl-1,2-diaminoethane

The analysis of the ^1H , ^{13}C , H-H and H-C COSY NMR spectra confirms the structural assignment. Analysis by gas chromatography (GC) in chloroform confirmed the purity of the product by displaying a unique and sharp peak with a tail, characteristic of amines, at an elution time of 11.51 minutes (see Figure 2.8).

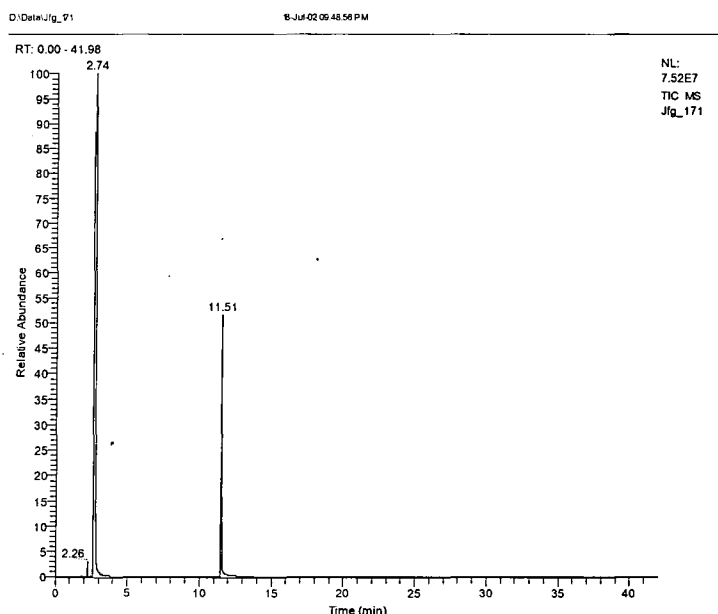


Figure 2.8. GC trace in chloroform of *N*-tert-butoxycarbonyl-1,2-diaminoethane

The elemental analysis, NMR and FTIR data were in agreement with those reported by Lois Hobson and confirmed the purity and the structure of the synthesised molecule. The yield, though, was lower than expected (69% instead of the 93% reported previously).

In this first step, it was found that distillation of ethylenediamine under reduced pressure, prior to its use as a reactant, was necessary in order to avoid any side product due to the slow degradation of amines left in contact with air and moisture. The distilled ethylenediamine was stable and remained colourless when stored under dry nitrogen for several weeks. Low temperature, excess of ethylenediamine and slow dropwise addition of di-*tert*-butyldicarbonate were necessary to minimise the formation of the diprotected product. The water-soluble monoprotected diamine was separated from the diprotected adduct by simple addition of water. The diprotected product precipitates in water as a fine white powder, which was easily removed from the solution by filtration. Unreacted excess of ethylenediamine (b.p. = 118 °C) remained to be removed. Most of it was removed by evaporation under reduced pressure. The rest was removed by saturation of the aqueous phase with sodium chloride and extraction with ethyl acetate. Ethylenediamine remained in water and *N-tert*-butoxycarbonyl-1,2-diaminoethane, less soluble in water, was displaced from the saturated aqueous solution to the organic phase. After separation and evaporation of ethyl acetate, a clear colourless oil was obtained. Though, a solid deposit of residual sodium chloride remained. The addition of chloroform and the filtration of the solution allowed the removal of the salt. The chloroform was evaporated and the oil was stirred overnight under high vacuum (8×10^{-2} mbar) at room temperature in order to remove the last traces of chloroform, ethyl acetate, ethylenediamine and water. The complete removal of ethylenediamine is crucial because its reaction with acryloyl chloride in the second step reaction can give *N,N'*-bis(-acryloyl)-1,2-diaminoethane that would not be easily separated from *N-t*-butoxycarbonyl-*N'*-acryloyl-1,2-diaminoethane. Contamination of the AB₂ monomer by *N,N'*-bis(-acryloyl)-1,2-diaminoethane (AA molecule) could lead to crosslinking by reacting with the terminal groups of the polymer.

2.3.2. Second step

For *N-tert*-butoxycarbonyl-*N'*-acryloyl-1,2-diaminoethane, the H-H COSY experiment (see *Figure 2.9*) allows the assignment of all the hydrogen signals. The

methylene hydrogens observed at 3.25 ppm are coupled with the urethane hydrogen at 4.95 ppm and the methylene hydrogens at 3.38 ppm are coupled to the amido hydrogen from the acrylamide moiety observed at 6.40 ppm. This corroborates the view that the conjugated acrylamide moiety will impose a bigger shift of the methylene hydrogens adjacent to it to higher ppm values than the urethane moiety. The H-H COSY experiment also allowed the precise assignment of the hydrogens observed in the vinyl region of the ^1H NMR spectrum. The vinyl hydrogen observed as a doublet at 5.57 ppm is mainly coupled to the hydrogen (doublet of doublets) at 6.02 ppm, which is coupled to the hydrogen (doublet) observed at 6.2 ppm. Therefore, the multiplet observed at 6.02 ppm corresponds to the =CH hydrogen and is coupled to both $\text{H}_2\text{C}=\text{C}$ hydrogens observed at 5.57 and 6.2 ppm respectively. It is also known that $^3J_{\text{trans}} > ^3J_{\text{cis}}$, which confirms that the hydrogen at 5.57 ppm is cis and that the hydrogen at 6.2 ppm is trans with respect to the =CH hydrogen.

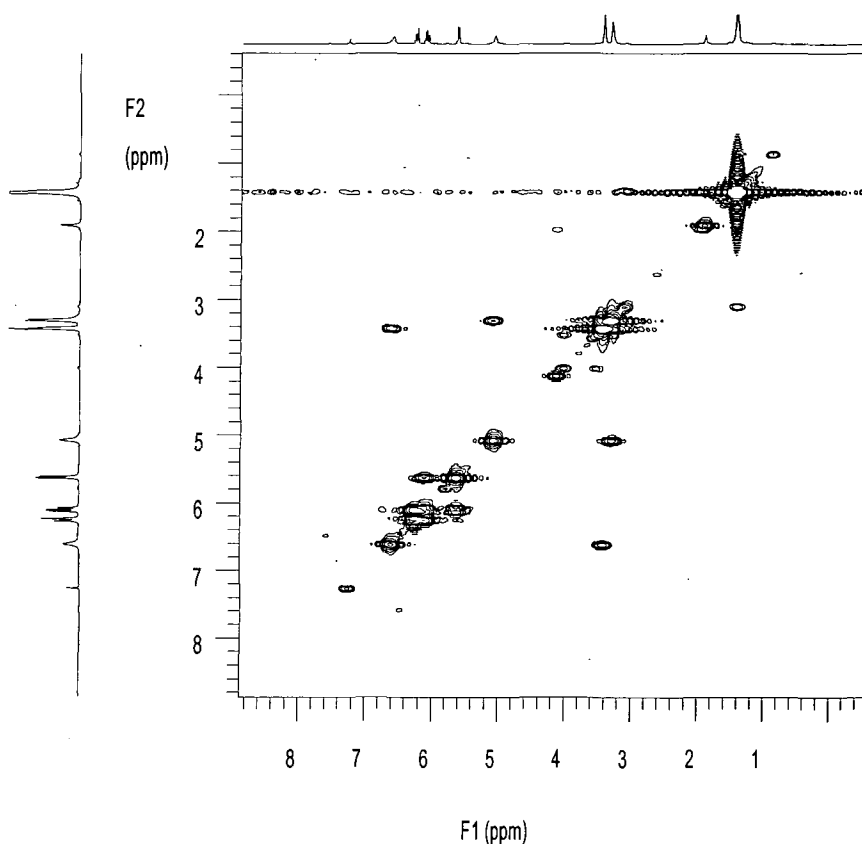


Figure 2.9. H-H COSY experiment on *N*-tert-butoxycarbonyl-*N'*-acryloyl-1,2-diaminoethane

The H-C COSY experiment (see *Figure 2.10*) allowed the precise assignment of the peaks observed by ^{13}C NMR. The peak observed at 28.31 ppm corresponds to the CH_3 carbons of the *t*-BOC protecting group. The peak at 40.05 ppm corresponds to the methylene carbon close to the urethane moiety, whereas the peak at 40.97 ppm corresponds to the methylene carbon close to the acrylamide moiety. As observed in the case of *N-tert*-butoxycarbonyl-1,2-diaminoethane, the peak at 79.77 ppm is not coupled to any hydrogen and as a consequence corresponds to the quaternary carbon of the *t*-BOC protecting group. The peak observed at 126.22 ppm is coupled with two vinyl hydrogens and therefore corresponds to the $\text{H}_2\text{C}=\text{C}$ carbon, while the peak at 130.86 ppm, coupled to the last vinyl hydrogen corresponds to the $=\text{CH}$ carbon. This assignment confirms the previous assignment of the vinyl hydrogens. Finally, the peak at 157.12 ppm corresponds to the urethane $\text{C}=\text{O}$ carbon because its chemical shift is similar to that of the similar urethane carbon observed for *N-tert*-butoxycarbonyl-1,2-diaminoethane and therefore, the last peak at 166.22 ppm corresponds to the amide $\text{C}=\text{O}$ carbon.

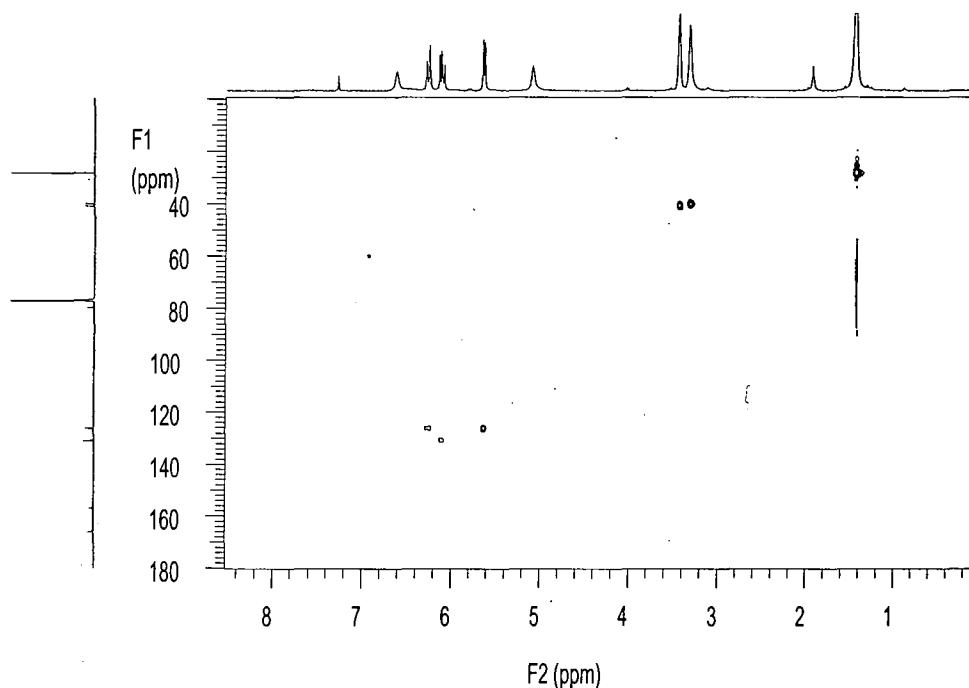


Figure 2.10. H-C COSY experiment on N-tert-butoxycarbonyl-N'-acryloyl-1,2-diaminoethane

The GC analysis in chloroform (see *Figure 2.11*) confirmed the purity of the compound by displaying a unique peak at an elution time of 17.51 minutes.

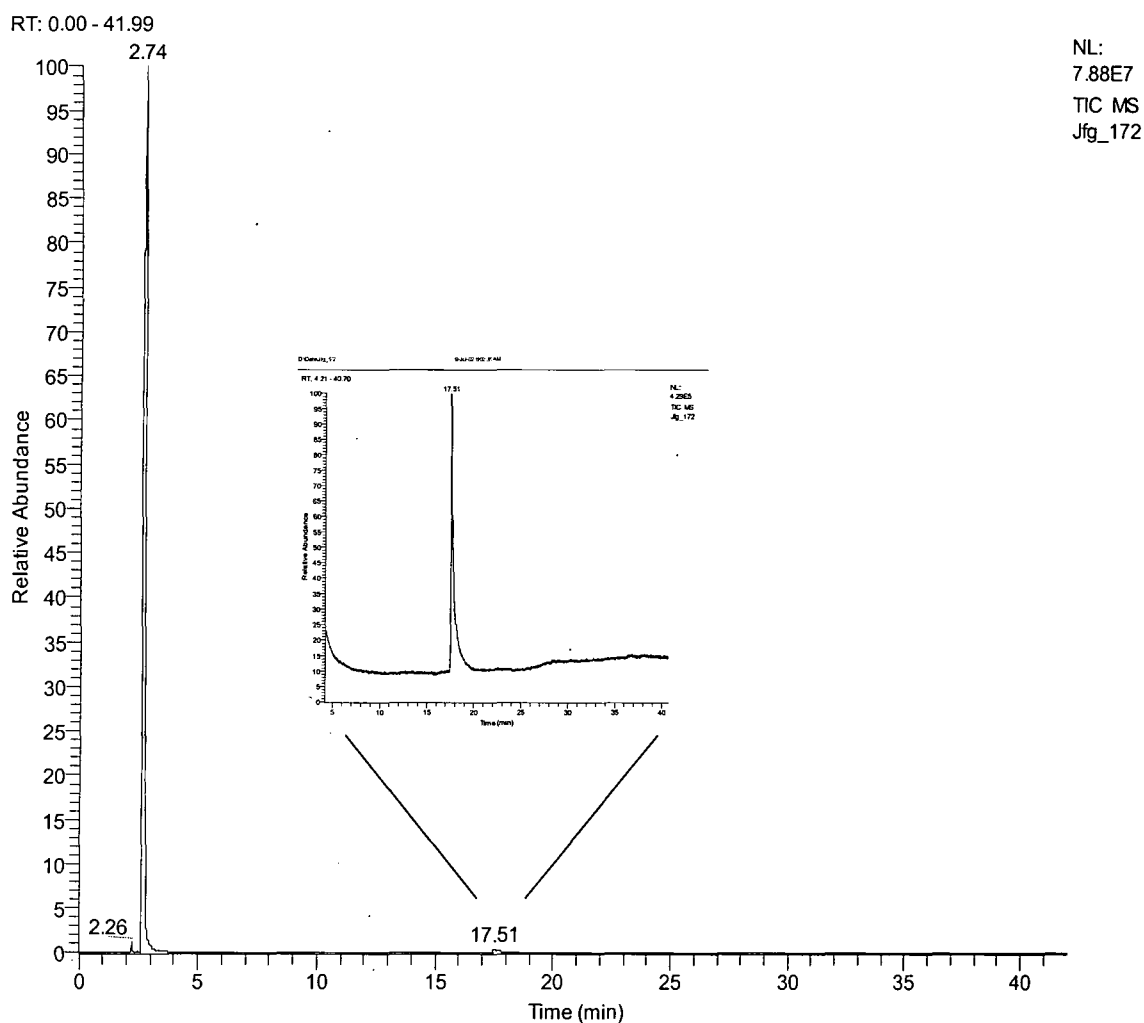


Figure 2.11. GC trace in chloroform of *N*-*tert*-butoxycarbonyl-*N'*-acryloyl-1,2-diaminoethane

The elemental analysis, NMR and FTIR data were in agreement with those published by Lois Hobson. Water was found by ^1H NMR and FTIR, proving the hygroscopic nature of this compound, which is presumably due to the presence of amido and urethane groups. In this step of the sequence, chloroform, unreacted acryloyl chloride (b.p. = 75°C) and triethylamine (b.p. = 88°C) were removed by rotary evaporation under reduced pressure at the end of the reaction. The residual white solid was washed with water in order to remove triethylammonium chloride and the traces of unreacted *N*-*t*-butoxycarbonyl-1,2-diaminoethane. The solid was extracted with chloroform. A pure white powder was obtained by simple evaporation of chloroform under reduced pressure and dried under high vacuum before characterisation. No side product was found so the final step in the monomer synthesis could be undertaken.

2.3.3. Third step

In the case of N-acryloyl-1,2-diaminoethane hydrochloride, the exchange that occurs between the amide / ammonium hydrogens and the deuterium of the NMR solvent rules out the use of a H-H COSY experiment to assign the different hydrogens. However, the high electron withdrawing nature of the acrylamide moiety compared to that of the ammonium salt should induce a large shift of the methylene hydrogens close to it towards higher ppm values. As a consequence, the methylene hydrogens close to the ammonium group are observed at 3.02 ppm, while the methylene hydrogens close to the acrylamide group are shifted to higher ppm and appear at 3.43 ppm. This hypothesis is backed-up by the H-C COSY (see *Figure 2.12*) experiment which shows that the carbon peak at 39.32 ppm corresponds to the methylene group close to the acrylamide. This value is close to that observed for the carbon close to the acrylamide moiety in N-acryloyl-N'-tert-butoxycarbonyl-1,2-diaminoethane (see *Figure 2.10* and *Appendix 1.7*); namely, 3.38 ppm. This proves that the carbon appearing at 36.92 ppm belongs to the methylene group close to the ammonium chloride salt and that the associated methylene hydrogens appear at 3.02 ppm in the ^1H NMR spectrum. The assignment of the vinyl hydrogens is similar to the one already made for the N-acryloyl-N'-tert-butoxycarbonyl-1,2-diaminoethane (see 2.3.2).

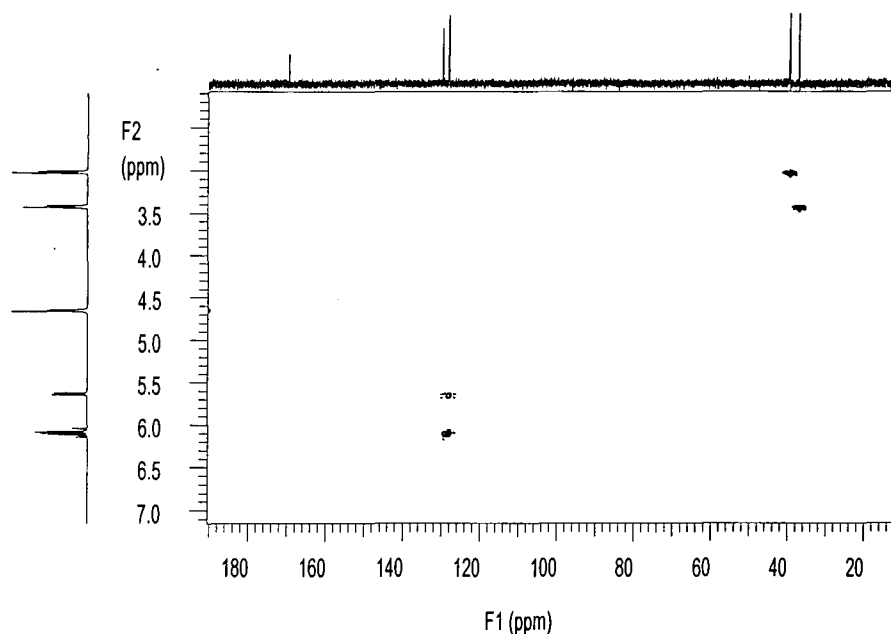


Figure 2.12. H-C COSY experiment on N-acryloyl-1,2-diaminoethane hydrochloride

The elemental analysis, NMR and FTIR data were in agreement with those found in the literature and confirm the synthesis of a pure monomer devoid of any impurity that could lead to crosslinking during the polymerisation process. Despite the much lower reactivity of the ammonium group in Michael addition to the double bond compared to that of the free amino group (see next section), this monomer was kept at low temperature in a freezer prior to its use.

2.3.4. Synthesis of the free-base monomer

In the case of N-acryloyl-1,2-diaminoethane, the aqueous solution made in deionised water was freeze-dried under high vacuum and a white powder was obtained. The characterisation of this powder by NMR and MALDI-TOF (see Chapters 3 and 5) revealed that the polymerisation process had already started at room temperature and that it was virtually impossible to isolate the monomer due to the high reactivity of free amino groups towards the vinyl double bond leading to the fast formation of polymers as the concentration increases during the freeze-drying process.

In order to characterise the monomer before any polymerisation process occurred, a low concentration aqueous solution was prepared to ensure that the polymerisation of this monomer at room temperature would not occur before the analysis was performed. This strategy allowed the easy characterisation by NMR of an otherwise very difficult-to-isolate monomer.

The ^1H NMR spectrum gave enough information to characterise the new monomer and confirm its purity. Based on our accumulated knowledge of the chemical shifts in these systems, the peak observed at 3.14 ppm corresponds to the methylene hydrogens adjacent to the acrylamide moiety, while the methylene hydrogens observed at 2.57 ppm are close to the primary amine hydrogens. The assignment of the vinyl hydrogens is similar to that in the related N-acryloyl-1,2-diaminoethane hydrochloride. In depth analysis of the ^{13}C NMR spectrum was not found to be necessary. The presence of two methylene, two vinyl and one carbonyl carbons was enough to confirm the 100% purity of the new compound. No residual trace of unconverted N-acryloyl-1,2-diaminoethane hydrochloride or other side product was found by either ^1H or ^{13}C NMR spectroscopy. The conversion of N-acryloyl-1,2-diaminoethane hydrochloride into N-acryloyl-1,2-diaminoethane was proved to be complete (100%).

N-Acryloyl-1,2-diaminoethane was synthesised immediately prior to its use in polymerisation experiments in order to avoid any uncontrolled polymerisation at room temperature or even at lower temperature because of the high reactivity of amino groups involved in the Michael addition with the double bonds.

In the next section, melt and aqueous solution polymerisations of N-acryloyl-1,2-diaminoethane hydrochloride will be described and compared, together with the aqueous solution polymerisation of N-acryloyl-1,2-diaminoethane.

Chapter Three

Polymerisation

3.1. Introduction

In this section, the polymerisation of N-acryloyl-1,2-diaminoethane hydrochloride in the melt and in aqueous solution as well as the aqueous solution polymerisation of N-acryloyl-1,2-diaminoethane will be discussed.

The polymerisation mechanism is based on Michael addition reactions between the amino (or ammonium) groups of a monomer molecule and the vinyl double bond of another monomer molecule. In the case of N-acryloyl-1,2-diaminoethane hydrochloride, the ammonium salt is in equilibrium with its free amine form. This free amino group is a nucleophile that attacks the electrophilic double bond of the α , β -unsaturated carbonyl group. In a conjugated α , β -unsaturated carbonyl system, there is a resonance structure that shows electrophilic character at the terminal carbon of the vinyl double bond (*Figure 3.1*).

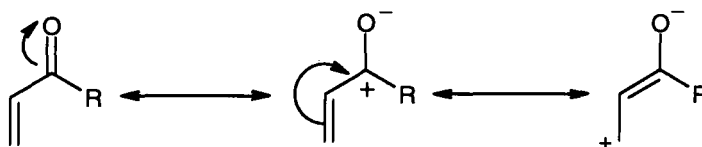


Figure 3.1. Resonance structures of a α , β unsaturated carbonyl compound

The general mechanism of a Michael addition reaction between a nucleophile (or Michael donor) Nu-H (e.g. amines) and an α , β -unsaturated carbonyl compound (or Michael acceptor) is described in *Figure 3.2*.

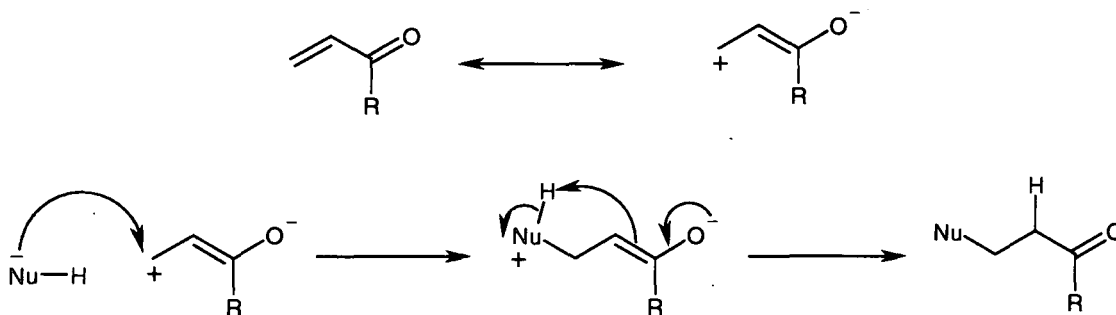


Figure 3.2. General mechanism for a Michael addition reaction

The polymerisation of both N-acryloyl-1,2-diaminoethane hydrochloride and N-acryloyl-1,2-diaminoethane is therefore a step-growth process that involves multiple Michael addition reactions between the amino groups of a monomer molecule or growing oligomers and the unreacted vinyl double bond of another monomer molecule or growing oligomer.

3.2. Experimental

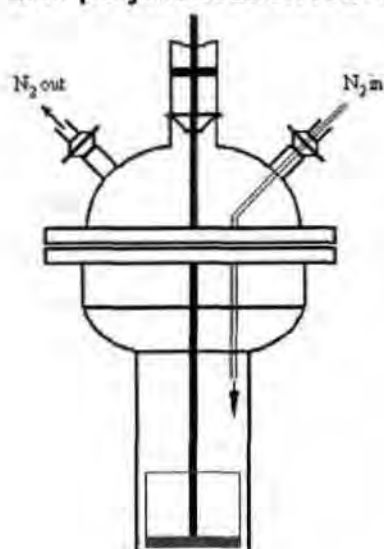
Elemental analyses were performed using an Exeter Analytical Elemental Analyzer CE-440. Infrared spectra were recorded on a Perkin Elmer 1720X FTIR spectrometer. ^1H and ^{13}C NMR spectra were acquired using a Varian Mercury 400 spectrometer at 399.97 MHz (^1H), 100.57 MHz (^{13}C) and 40.53 MHz (^{15}N). Thermogravimetric analyses were performed using a Perkin Elmer Pyris 1 TGA (5-10 mg, $10^\circ\text{C} \cdot \text{min}^{-1}$). Differential Scanning Calorimetry analyses were performed using a Perkin Elmer Pyris 1 Differential Scanning Calorimeter at $10^\circ\text{C} \cdot \text{min}^{-1}$. MALDI-TOF mass spectra were recorded using a Voyager-DE STR Mass Spectrometer (UV laser at 337 nm), in reflectron mode. The samples (2 mg. ml^{-1} , methanol) were analysed using α -cyano-4-hydroxycinnamic acid (10 mg. ml^{-1} , methanol) as the matrix. A volume of 6 μl of sample solution was mixed with 54 μl of matrix solution prior to analysis.

3.2.1. Melt polymerisation of N-acryloyl-1,2-diaminoethane hydrochloride

N-Acryloyl-1,2-diaminoethane hydrochloride (2 g, 13.3 mmol) was placed into the lower section of a polymerisation flask, consisting of a flat bottomed cylindrical vessel fitted with a three-necked flange head. The polymerisation reactor was fitted with a close-fitting stainless steel stirrer paddle powered by a high torque Heidolph stirrer motor, a nitrogen inlet and a nitrogen outlet (see *Figure 3.3*). The flask was then purged with nitrogen and placed in an oil bath containing of high temperature silicone oil heated by a 1kW-heating band. The temperature of the oil bath was regulated using a temperature controller / programmer. The oil bath was heated at a programmed rate of $10^\circ\text{C} / \text{min}$. up to 210°C and held at this temperature for 4 hours. The reaction mixture was stirred using an efficient mixer (see *Figure 3.3*) at a constant rate of 125 rpm under a constant nitrogen flux. After 4 hours, the reaction mixture was cooled to

room temperature and a clear brown sticky solid was obtained which was removed from the vessel by dissolution in deionised water. The solid reaction product was recovered by freeze-drying under vacuum. Found: C, 37.80; H, 7.35; N, 17.03; Cl, 22.52%. $C_5H_{11}N_2OCl$ (hydrochloride monomer) requires: C, 39.87; H, 7.36; N, 18.60; Cl, 23.54%. FTIR (KBr disc): 3422 and 2963 (br, ammonium N-H stretching, water?); 1655 (s, C=O stretching); 1560; 1458; 1384,1262; 1103; 1022; 799 and 579 cm^{-1} (see Appendix 2.1). 1H NMR (D_2O , 399.97 MHz): δ (ppm): 2.40-3.80 (m, CH_2); 5.6-6.2 (m, unreacted vinyl hydrogens) (see Appendix 2.2). ^{13}C NMR (D_2O , 125.67 MHz): δ (ppm): 20-56 (CH_2); 128 and 130 (vinyl Carbons); 160-178 (C=O carbons) (see Appendix 2.3).

Melt polymerisation reactor



Stirrer blades

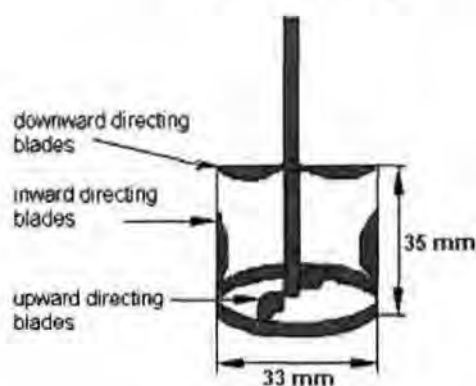


Figure 3.3. Schematic of the melt polymerisation reactor and the mechanical stirrer

3.2.2. Aqueous solution polymerisation of N-acryloyl-1,2-diaminoethane hydrochloride

An aqueous solution (10 ml) of N-acryloyl-1,2-diaminoethane hydrochloride (2.5 g, 16.6 mmol) was prepared in deionised water. The solution was divided into 10 x 1ml aliquots that were placed in 10 separate ampoules (5 ml) or Carius tubes (10 ml) fitted with magnetic stirrer bars. The solutions were freeze-thawed three times. The ampoules were closed under vacuum using Teflon taps. When Carius tubes were used,

they were permanently sealed under static vacuum (8×10^{-2} mbar). The ampoules or Carius tubes were mounted onto a specially designed rack fitted with ten metallic clamps. This rack, holding the ten clamped ampoules (or Carius tubes), was completely immersed in silicon oil at 100°C . The polymerisation experiment was performed at this temperature during 10 days. Every day, a sample was removed from the oil bath and cooled to room temperature. Clear yellow-green solids were recovered by freeze-drying and analysed. Found: C, 37.32; H, 7.46; N, 17.44; Cl, 23.21%. $\text{C}_5\text{H}_{11}\text{N}_2\text{OCl}$ (hydrochloride monomer) requires: C, 39.87; H, 7.36; N, 18.60; Cl, 23.54%. FTIR (KBr disc): 3430 and 3072 (br, ammonium N-H stretching; water?); 1655 (s, C=O stretching); 1551; 1458; 1384; 1262; 1173; 1106; 1026; 779 and 572 cm^{-1} (see Appendix 2.20). ^1H NMR (D_2O , 399.97 MHz): δ (ppm): 2.30-3.70 (m, CH_2); 5.6-6.2 (m, vinyl hydrogens) (see Appendix 2.21). ^{13}C NMR (D_2O , 125.67 MHz): δ (ppm): 28-58 (CH_2 carbons); 128 and 130 (vinyl carbons); 173 (C=O carbons) (see Appendix 2.22).

3.2.3. Aqueous solution polymerisation of N-acryloyl-1,2-diaminoethane

3.2.3.1. High concentration monomer solution

An aqueous solution (10 ml) of N-acryloyl-1,2-diaminoethane hydrochloride (2.5 g, 16.6 mmol) was prepared in deionised water. The solution was stirred with about 5 g of Dowex ion (OH) exchange resin beads for 20 minutes. The solution was then filtered using a porosity 2 sinter and the pH value was determined as 10 using pH paper. The solution was then divided into 10 x 1ml aliquots that were placed in 10 separate Carius tubes (10 ml) fitted with magnetic stirrer bars. Nine of these solutions were freeze-thawed three times and then the nine Carius tubes were sealed under static vacuum (8×10^{-2} mbar). These tubes were immersed in silicon oil preheated at 100°C . The polymerisation experiment was performed at this temperature for 90 minutes. Every 10 minutes, a sample was removed from the oil and cooled to room temperature. White powders were recovered by freeze-drying under vacuum and analysed. The content of the tenth tube was not heated; it was freeze-dried under vacuum and a white powder was obtained (see 3.3.3). Found: C, 40.28; H, 7.91; N, 18.09; Cl, 16.98%. $\text{C}_5\text{H}_{10}\text{N}_2\text{O}$ (free base monomer) requires: C, 52.61; H, 8.83; N, 24.54; Cl, 0%. FTIR

(KBr disc): 3419 and 3077 (br, N-H stretching; water?); 1652 (s, C=O stretching); 1557; 1456; 1384; 1266; 592 cm^{-1} (see Appendix 2.25). ^1H NMR (D_2O , 399.97 MHz): δ (ppm): 2.30-3.30 (m, CH_2); 5.6-6.2 (m, vinyl hydrogens) (see Appendix 2.26). ^{13}C NMR (D_2O , 125.67 MHz): δ (ppm): 30-50 (CH_2 carbons); signals for vinyl and C=O carbons expected at ca 130 and ca 170 ppm were too weak to be detected (see Appendix 2.27).

3.2.3.2. Low concentration monomer solution

An aqueous solution (10 ml) of N-acryloyl-1,2-diaminoethane hydrochloride (0.5 g, 3.32 mmol) was prepared in deionised water. This solution was stirred with about 3 g of Dowex ion (OH) exchange resin beads for 20 minutes. The solution was then filtered using a porosity 2 sinter and the pH value was determined as 10 using pH paper. The solution was divided into 10 x 1ml aliquots that were distributed between 10 separate Carius tubes (10 ml) fitted with magnetic stirrer bars. Nine of these solutions were freeze-thawed three times and the nine Carius tubes were sealed under static vacuum (8×10^{-2} mbar). These Carius tubes were then immersed in silicon oil preheated at 100°C . The polymerisation experiments were performed at this temperature for 90 minutes. Every 10 minutes, a sample was removed from the oil and cooled down to room temperature. White powders were recovered by freeze-drying under vacuum and analysed. The content of the tenth Carius tube was not heated but directly freeze-dried under vacuum. A white powder was obtained (see 3.3.4). Found: C, 42.79; H, 7.74; N, 19.87; Cl, 10.13%. $\text{C}_5\text{H}_{10}\text{N}_2\text{O}$ (free base monomer) requires: C, 52.61; H, 8.83; N, 24.54; Cl, 0%. FTIR (KBr disc): 3422 and 3307 (br, N-H stretching; water?); 2925 (C-H stretching); 1637 (s, C=O stretching); 1560; 1437; 1384; 1309; 1202; 1119; 1027; 979; 927; 796 and 615 cm^{-1} (see Appendix 2.30). ^1H NMR (D_2O , 399.97 MHz): δ (ppm): 2.20-3.30 (m, CH_2); 5.6-6.2 (m, vinyl hydrogens) (see Appendix 2.31). ^{13}C NMR (D_2O , 125.67 MHz): δ (ppm): 32-55 (CH_2 carbons); 128 and 130 (vinyl carbons); 174-176 (C=O carbons) (see Appendix 2.32).

3.3. Discussion

NMR Spectroscopy was the main technique used to determine the extent of polymerisation and the structure of the hyperbranched polymers. ^1H NMR spectroscopy was used to follow the kinetics of polymerisation (see Chapter 4) and to calculate both the degree of polymerisation (DP) and the number average molecular weight (M_n) of the hyperbranched polymers. ^{15}N NMR Spectroscopy was used to determine the degree of branching (DB) of the hyperbranched structures. MALDI-TOF Mass Spectrometry was used to determine and to follow the evolution of the molecular weight distribution of the various oligomers and polymers with respect to the reaction time (see Chapter 5).

3.3.1. Melt polymerisation of N-acryloyl-1,2-diaminoethane hydrochloride

The Michael addition reactions between ammonium groups and vinyl double bonds give rise to new methylene groups that can be observed by NMR spectroscopy and the consumption of vinyl groups due to these reactions can be observed using FTIR and NMR spectroscopy.

In the FTIR spectrum of the polymer (see Appendix 2.1), the peak observed at 982 cm^{-1} in the FTIR spectrum of the monomer, N-acryloyl-1,2-diaminoethane hydrochloride, does not appear. This peak corresponds to the out-of-plane deformation of the vinyl C-H bonds and the fact that it could not be observed in the polymer FTIR spectrum is evidence that most, if not all, of the vinyl groups of the monomer molecules have been consumed during the polymerisation process. It was anticipated that the $\text{CH}_2=\text{CH}$ - stretching vibration mode could also be used as a probe of reaction but, in the event, this weak absorption could not be identified with certainty and the absorptions in the 1400 to 1630 cm^{-1} region were not sufficiently well resolved to be of use.

In the ^1H NMR spectrum in D_2O of the polymer, new methylene hydrogens can be observed in the region between 2.40 and 3.80 ppm , in addition to the methylene hydrogens already observed in the monomer at 3.00 and 3.40 ppm respectively (see

Appendix 1.10 and 2.2). The relative intensities of the vinyl hydrogens observed in the region between 5.6 and 6.2 ppm have considerably decreased and have almost completely disappeared in comparison with those of the vinyl hydrogens observed in the monomer ^1H NMR spectrum. This observation confirms that most of the vinyl groups have been consumed by the Michael addition reactions and were converted into new methylene units within the polymer structure. The observed peaks are very broad compared to the fine and detailed peak structures observed in the monomer spectrum. This broadening of the peaks is a characteristic of a high molecular weight polymer. In order to confirm this view, it is possible to determine the degree of polymerisation, from the ^1H NMR spectrum of the polymer, by using the relationship between the DP and the ratio of the total relative intensity of all the methylene hydrogens over the total relative intensity of all the vinyl hydrogens. A poly(amidoamine) hyperbranched polymer, can be represented as its linear counterpart (see *Figure 3.4*).

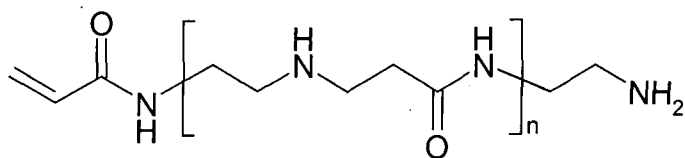


Figure 3.4. General representation of a polyamidoamine macromolecule

In that representation, $\text{DP} = n + 1$. There is only one unreacted vinyl group per polymer molecule. The higher the value of n becomes, the higher the relative intensity of methylene units observed by NMR will be and the lower the relative intensity of the vinyl group. This analysis assumes that the vinyl group is not consumed in competitive side reactions such as cyclisation or free radical polymerisation (see later).

In that representation, the total number of CH_2 groups ($N_{\text{methylene}}$) is related to the total number of vinyl groups (N_{vinyl}) by:

$$N_{\text{methylene}} = (4n + 2) N_{\text{vinyl}}$$

where: $n = \text{DP} - 1$.

As a consequence, $N_{\text{methylene}} = (4\text{DP} - 2) N_{\text{vinyl}}$ and the expression for DP becomes:

$$\text{DP} = [(N_{\text{methylene}} / N_{\text{vinyl}}) + 2] / 4$$

The ^1H NMR spectrum allows the determination of the total relative intensity (or integration) of the methylene hydrogens ($I_{\text{methylene}}$) and the total relative intensity of the vinyl hydrogens (I_{vinyl}). As a methylene group generates two hydrogen signals and a vinyl group generates three hydrogen signals, it is possible to calculate the respective values of $N_{\text{methylene}}$ and N_{vinyl} :

$$N_{\text{methylene}} = I_{\text{methylene}} / 2$$

$$N_{\text{vinyl}} = I_{\text{vinyl}} / 3$$

The expression for DP then becomes:

$$\text{DP} = [(3 I_{\text{methylene}} / 2 I_{\text{vinyl}}) + 2] / 4$$

Using this expression and the relative intensities observed in the ^1H NMR spectrum shown in Appendix 2.2, a value of 188 was found for the DP for this polymer. The number average molecular weight (M_n) was obtained using the following expression $M_n = \text{DP} \times 150.5$ (molecular weight of the monomer unit) giving a value of 28,000 Daltons. However, the determination of the values of DP and M_n depend on the ability to see and integrate the residual vinyl signal. At very high conversion, these signals become almost impossible to distinguish from the base line of the spectrum and the determination of DP becomes unreliable. A systematic error is associated with the integration of each signal observed by ^1H NMR spectroscopy. This error is 10% of the integration value. As a consequence, the absolute error in the calculated values of DP and M_n equals the sum of the absolute errors in the values of $I_{\text{methylene}}$ (10%) and I_{vinyl} (10%), i.e. 20% of the DP value. The relative error on the calculated value of DP (see above) becomes ± 38 (DP x absolute error) and the relative error on the M_n value can be estimated as $\pm 5,500$ Daltons, that is a value of $28,000 \pm 5,500$ Daltons.

The ^{13}C NMR spectrum in D_2O shows that many new carbon signals have appeared in the region of the methylene carbons (20 to 60 ppm), where the ^{13}C NMR spectrum of the monomer showed only two signals at 37 and 39 ppm (see Appendices 1.11 and 2.3). As observed in the ^1H NMR spectrum, the carbon signals related to the

vinyl groups, normally observed at 128 and 130 ppm, have decreased in intensity in comparison to the relatively much more intense methylene carbon signals. The diversity of environments in which the methylene groups are located (i.e. focal, linear, branched or terminal units) within the newly generated hyperbranched structure gives rise to the large number of the chemical shifts observed in the ^1H and ^{13}C NMR spectra. A precise assignment of all the peaks observed in the methylene region is impossible. However, from our accumulated knowledge of chemical shifts in this systems, it is possible to assume that, in the ^1H NMR spectrum, the peaks observed between 3.4 and 3.8 ppm correspond to the hydrogens of the methylene groups close to the amides ($\text{CH}_2\text{-NH-C=O}$), while on the other hand, the peaks observed between 2.4 and 2.8 ppm correspond to the methylene hydrogens close to the carbonyls ($\text{CH}_2\text{-CO-NH}$). Therefore the peaks observed between 3 and 3.8 ppm correspond to the hydrogens belonging to methylene groups close to ammonium salts. The ^{15}N NMR spectrum in D_2O of this polymer (see Appendix 2.4) allowed the determination of the degree of branching exhibited by this hyperbranched structure. Due to the extremely low natural abundance of ^{15}N , the whole sample (2 g) had to be used in this analysis. Despite the relatively high level of noise, it was possible to distinguish after an acquisition time of 60 hours three peaks at 55.30, 67.32 and 140.56 ppm. Based on the work previously published by Hobson³⁴, it was possible to assign each of these observed peaks. The peak at 55.30 ppm corresponds to a primary ammonium group (terminal units, T). The peak at 67.32 ppm corresponds to a tertiary ammonium group (branched units, B) and the peak at 140.56 ppm corresponds to a secondary amide (A). There is one amide group per repeat unit, therefore the number of amide groups is equal to the total number of units: $A = B + L + T$. If there were linear units, they would be observed as a unique peak located between the two peaks observed for the branched and terminal units respectively. No linear unit (L) could be found using this characterisation method. The relative intensities of the terminal and branched units are similar and the relative intensity of the amide groups represents about twice the intensity of the branched units. The degree of branching, using Fréchet's formula ($\text{DB} = B + T / A$) was found to be equal to 0.97. However, the high level of noise made it difficult to have an absolutely accurate integration of the peaks. As a consequence, this value of 0.97 may not be the exact value of DB for this polymer. Using Frey's definition for DB gives a DB of 1 since no linear unit could be found. Those two values are close to the value reported by Hobson. The complete absence of linear units (^{15}N NMR spectrum) and the presence

of remaining vinyl hydrogens (^1H NMR spectrum) suggest the absence of cyclic polymers, which contrasts with most hyperbranched systems where cyclisation occurs by reaction of an end group with the focal point of the polymer. If significant cyclisation had occurred it would be impossible to observe any remaining vinyl hydrogens.

Figure 3.4 shows a representation of a hyperbranched polymer molecule that can be generated by melt polymerisation at $210\text{ }^\circ\text{C}$ for 4 hours under nitrogen, where no linear unit can be found. The real sample of the polymer would, of course, consist of a mixture which was polydisperse in both molecular weight and structure.

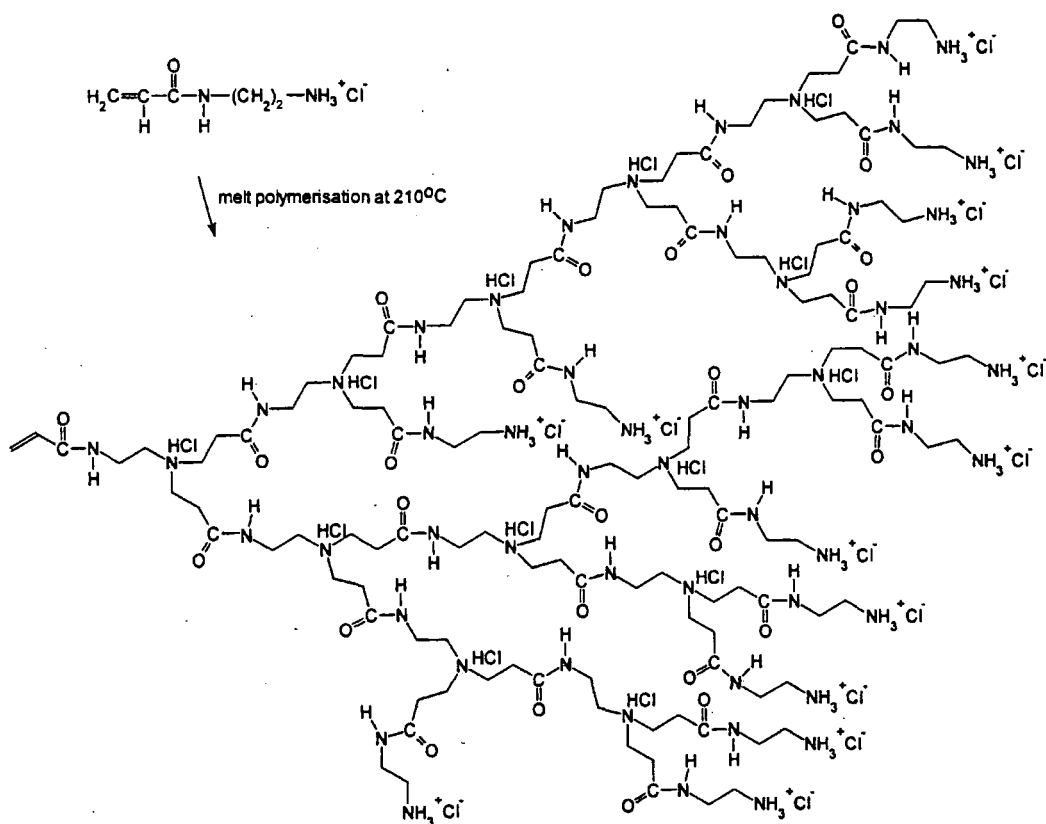


Figure 3.4. A possible structure for the hyperbranched poly(amidoamine) polymers synthesised by melt polymerisation of *N*-acryloyl-1,2-diaminoethane hydrochloride

A possible explanation for this high degree of branching and the absence of cyclisation might lie in the structure of the monomer and the growing oligomers. Once the dimer is formed, the repulsion between the two ammonium units results in a preference for a “stretched conformation” in which hydrogen transfer from $-\text{NH}_2^+$ to the adjacent amide carbonyl via a six-membered ring is preferred over transfer from the

terminal -NH_3^+ via a seven-membered ring, see *Figure 3.5*. Additionally, the marginally greater nucleophilicity of the secondary amine ($\text{pK}_a = 11.1$) as compared to the primary amine ($\text{pK}_a = 10.8$) favours the higher reactivity of the newly formed dialkylammonium unit and, hence, the high degree of branching observed. For monomers where the number of internal CH_2 is greater than 2, the formation of a six-membered ring is no longer favoured and the differentiation in the hydrogen transfer no longer exists, leading to statistically hyperbranched structures.³⁴

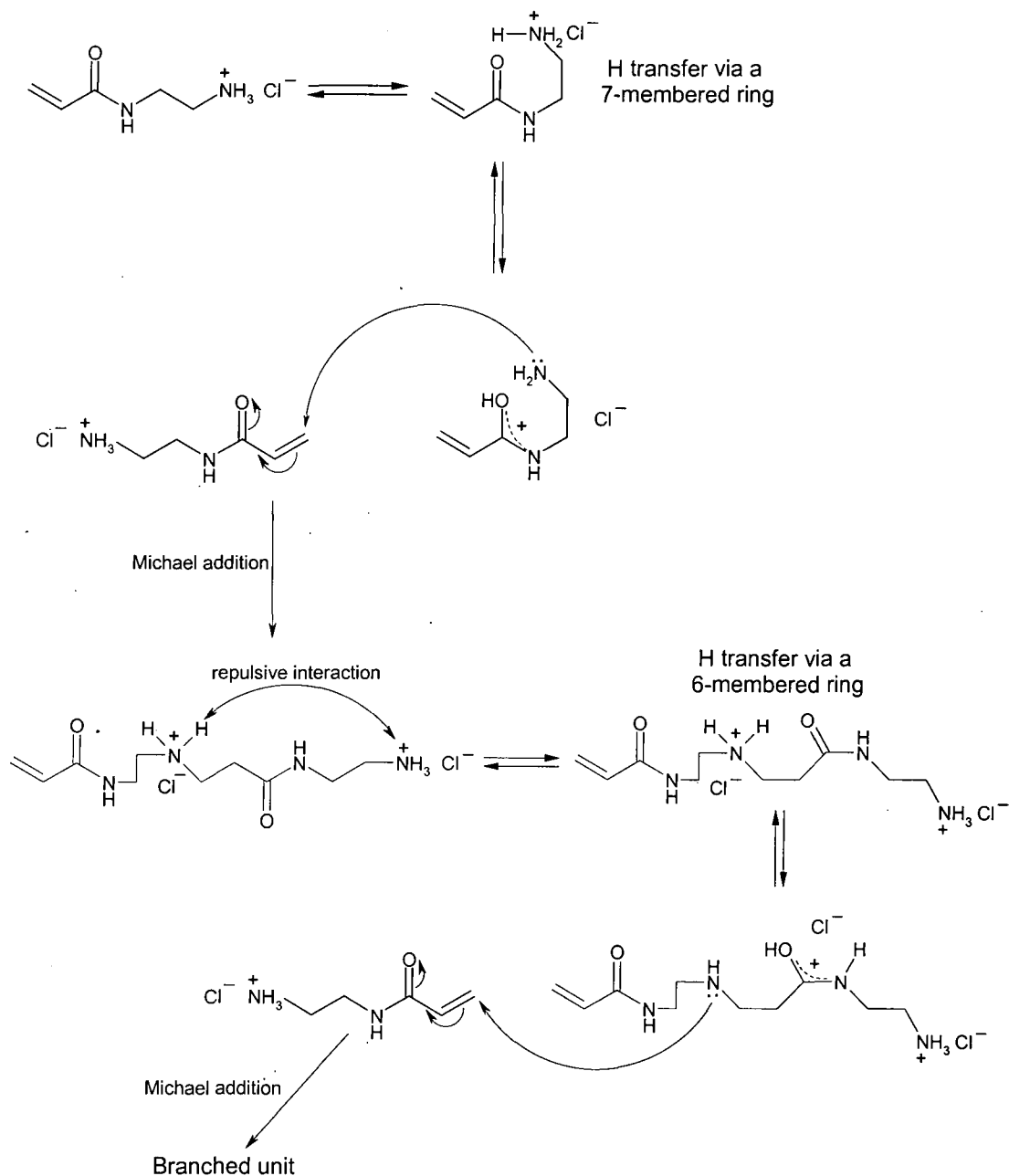


Figure 3.5. Possible explanation for the high degree of branching observed for polymers formed in the melt polymerisation of N-acryloyl-1,2-diaminoethane hydrochloride.

Thermogravimetric analysis indicated that the dry polymer was thermally stable displaying less than 4% weight loss up to 260°C, after which extensive degradation and weight loss occur. Differential Scanning Calorimetry (DSC) failed to reveal any crystalline melting point. This lack of crystallinity is due to the disruption of packing by the branched segments. A value for the glass transition temperature (T_g) was observed at 1.6°C, which is much lower than the value reported by Hobson.³⁴ The difficulty to reproduce this observation may be due to plasticisation of the polymer by absorption of water; the monomer and polymer are hygroscopic, a factor that prevented reliable elemental analysis in this work.

Unfortunately, the melt polymerisation of N-acryloyl-1,2-diaminoethane hydrochloride proved to be somewhat difficult to reproduce in the author's hands. Although Hobson had previously managed to control the process, others had experienced difficulties as well.⁴¹ On occasion, the author was able to reproduce the result reported by Hobson, but for the overwhelming majority of attempts, this procedure gave rise to a product completely different to the one previously described. In these cases, mechanical stirring during the polymerisation process was usually inhibited by the formation of a bulky solid on the stirrer. The products from these reactions could only be partially dissolved in deionised water; insoluble suspensions of gel particles were formed. After filtration, brown solids were recovered by freeze-drying the solution and amounted to about 80 wt-% of the starting material. They were dissolved in D₂O and analysed by ¹H, ¹³C and ¹⁵N NMR spectroscopy.

A ¹H NMR spectrum of the soluble fraction of this new product shows that virtually all the monomer hydrogens have been consumed and two new signals have appeared at 3.2 and 3.8 ppm in the approximate intensity ratio 1:3. This suggests that the monomer has undergone a solid state conversion into a new compound with a relatively simple structure since there are only two signals (traces of residual monomer are marked on the spectrum of the product) and both are relatively sharp and well resolved, compare Appendices 1.10, 2.2 and 2.5. Analysis of the ¹³C NMR spectrum of this product is consistent with the conclusion that virtually all the monomer was consumed and a product with a relatively simple structure was formed; compare Appendices 1.11, 2.3 and 2.6. The ¹⁵N NMR spectrum was also recorded but, since ¹⁵N is in low abundance, the spectrum is rather noisy, see Appendix 2.7, and the integration

is unreliable; however, there were only two peaks, with that at 140 ppm being assigned to amide nitrogen and that at 56 ppm being assigned to an ammonium nitrogen. Attempts to record a MALDI-TOF mass spectrum of this new product failed, although the melt polymerisation of the monomer gave a MALDI-TOF mass spectrum, which, as expected, displayed the features of the material previously reported by Hobson.³⁴

The author has struggled to provide a plausible rationalisation of these observations but has been unable to reach a definite convincing conclusion. However, it is felt that enough reliable data have been accumulated to justify some speculative comment. As the reader can easily imagine, the failure to consistently reproduce the melt polymerisation results of Hobson were very disappointing and the author made strenuous efforts to ensure that the monomer, N-acryloyl-1,2-diaminoethane hydrochloride, was very pure. Despite these efforts, the thermal solid state conversion of the purified monomer into the new unidentified product was the result of the overwhelming bulk of the polymerisation attempts and, as a consequence, the melt polymerisation approach was abandoned and alternative strategies were investigated, see Sections 3.3.2 and 3.3.3.

It was felt that the failure to reproduce Hobson's results probably indicated that impure monomer was being produced; thus, for example, N,N'-bis-acryloyl-1,2-diaminoethane, present in small quantities would result in a crosslinked mass. However, on reflection, it might be that the monomer prepared by the author was more pure than that used by Hobson and, as a consequence, had a higher melting point. If this was the case, and if the packing of the monomer in the crystal was appropriate, a solid state Michael addition polymerisation to give a linear polymer might have occurred; the concept is illustrated in *Figure 3.6*. Such a linear polymer would have four methylene groups in the repeat unit and only two nitrogen environments, which is consistent with the 3:1 intensity ratio for the two signals in the ¹H NMR spectrum if three of the peaks overlap and with two signals in the ¹⁵N NMR spectrum corresponding in shift with amide and ammonium environments, as required.

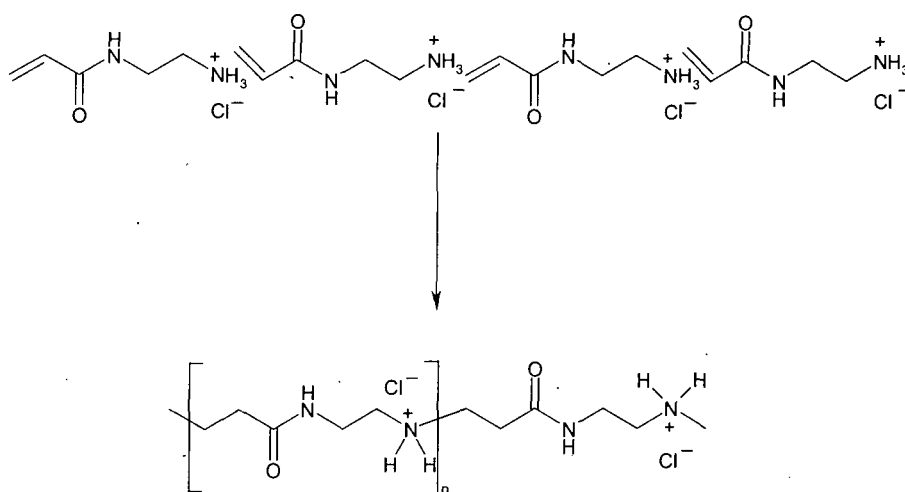


Figure 3.6. Hypothetical solid state thermal polymerisation of *N*-acryloyl-1,2-diaminoethane hydrochloride.

This new material constituted 80 wt-% of the product with the remainder of the mass appearing as gel particles arising from some other reaction(s). It would have been advantageous to test this hypothesis by measuring the molecular weight of the product but it did not fly in the MALDI-TOF experiment and although it was soluble in water, the author did not have access to aqueous GPC (a technique which, in any event, is notoriously difficult with polyelectrolytes).

The melt polymerisation approach was abandoned in favour of solution methods but the speculations given above suggest that the solid state thermal process may merit further investigation.

3.3.2. Aqueous solution polymerisation of *N*-acryloyl-1,2-diaminoethane hydrochloride

The first experiments were run in water at 100 °C for 10 days, instead of 4 hours in the melt. Reactions were carried out using 5 ml ampoules that could be connected to a vacuum line for degassing and closed with Teflon taps. Ten ampoules were loaded with 1ml of a 0.25g/ml solution of monomer in deionised water and freeze-thawed three times under vacuum (8×10^{-2} mbar). This was necessary in order to remove oxygen that might initiate the free radical polymerisation at the vinyl double bond. Such chain-growth polymerisation could compete with the main step-growth

polymerisation in the consumption of vinyl groups, preventing a correct estimation of the degree of polymerisation. Then, each ampoule was closed under vacuum using a Teflon tap. The polymerisation experiment was run for 10 days at 100°C, removing a sample each day for analysis by NMR spectroscopy.

The polymer obtained after 10 days was analysed by elemental analysis, FTIR, ^1H NMR spectroscopy and ^{13}C NMR spectroscopy. The four analyses gave results similar to those observed for the polymerisation of N-acryloyl-1,2-diaminoethane hydrochloride in the melt (compare Appendices 2.1-2.3 with Appendices 2.13-2.15). However, minor differences can be observed in the relative intensities and broadening of the different peaks observed by ^1H NMR spectroscopy. A much lower degree of polymerisation was found in the solution case, 23 instead of 188. This low DP and the relatively sharp peaks observed indicate that only low molecular weight hyperbranched oligomers were synthesised as opposed to the high molecular weight polymers synthesised in the melt reaction. This view was confirmed by the MALDI-TOF analysis of the polymers obtained in aqueous solutions (see Chapter 5).

Free radical polymerisation of the vinyl double bonds could not always be avoided. In some samples, broad peaks were detected in the ^1H NMR spectra between 1.5 and 2 ppm. It was, never the less, possible to follow the polymerisation process by NMR spectroscopy and FTIR (see Appendices 2.8 to 2.15). In the early stages of the polymerisation (1 day), a DP of 2 was reached and new peaks started to appear in the aliphatic regions of the ^1H and ^{13}C NMR spectra, see Appendices 2.9 and 2.10; in this sample, both FTIR and NMR spectra confirmed the presence of unreacted vinyl groups. This is in agreement with the relatively lower reactivity of ammonium groups in concentrated aqueous solution as opposed to the melt. Even at this stage, it was possible to observe the presence of methylene hydrogens due to free radical polymerisation. However, the peaks between 1.5 and 2 ppm appeared in the spectra of samples in a random manner; thus, after 5 days (DP = 15), such peaks could be seen (Appendix 2.11), whereas, after 10 days (Appendix 2.14), such peaks could not be detected. This proves that the occurrence of free radical polymerisation is not only due to the long periods of exposure of the monomer to high temperatures, but also to the presence of oxygen by leakage into the ampoules, via the Teflon taps; presumably via

surface scratches. In order to eliminate the risk of free radical polymerisation, the ampoules and their Teflon taps were replaced by Carius tubes that were sealed under static vacuum after three freeze-thaw cycles. The sealed tubes were completely immersed in preheated oil at 100°C. This new procedure produced polymers that did not exhibit signs of contamination by free radical polymerisation of the monomer (see Appendices 2.16-2.22), until prolonged heating, when very low levels could be detected. This modification in the experimental protocol confirmed the view that oxygen leakage via the Teflon taps was mainly responsible for the observed free radical polymerisation, presumably the imperfection of the Teflon tap seals was statistically distributed. When the products of reaction in leaky ampoules were compared with the analogous products produced from reactions in sealed Carius tubes, it was found that the Carius tube samples had lower degrees of conversion and DPs. The free radical polymerisation, initiated by oxygen biradicals, consumed vinyl hydrogens and caused the value of DP observed by ^1H NMR to increase. However, when well-sealed ampoule results were compared with Carius tube results, the same extent of reaction was observed; compare Appendices 2.14 and 2.21.

Due to the small quantities of polymer present in each sample (0.25 g) and the long reaction times required to obtain a low molecular weight sample, a large quantity of high molecular weight polymer could not be synthesised in order to carry a ^{15}N NMR spectroscopy experiment. As a consequence, it was not possible to determine the degree of branching of these new polymers. However, it was possible to perform thermogravimetric and DSC analyses on two different samples of polymers obtained after 9 days reaction time in aqueous solution; one in Carius tube and the other in an ampoule. Both the polymers were found to be thermally stable up to 250°C, which is very close to the result observed for the melt polymer. The DSC analysis on the other hand gave rise to differences between the two polymers. For the polymer obtained in an ampoule and exhibiting signs of free radical polymerisation, value of 42.7°C was found for the T_g as opposed to the 1.6°C found for the melt polymer sample. For the polymer obtained in a Carius tube, a value of 2.1°C was found for the T_g , which is very close to the value observed for the melt polymer. Although slight decreases in the value of T_g can be explained by the presence of water that acts as a plasticiser, such a huge difference, as observed between those two samples, is most likely due to the

introduction of linear segments through free radical polymerisation in the final structure of the polymer. As for the melt polymer, no melting point could be observed for both polymeric samples, suggesting the dominant hyperbranched nature of both polymeric structures.

Thus, the author has established a new and more reproducible way of producing hyperbranched poly(amido amine)s. However, the long reaction times required so that relatively low degrees of conversion can be reached, constituted a major disadvantage of this new method if large amounts of high molecular weight polymers were to be produced. A rational next step in developing the protocol would be to increase the monomer concentration up to 0.5g/ml. This was tried and was successful up to a DP of 95, obtained after 4 days polymerisation in closed ampoules at 100°C. In that case, because of the use of ampoules, free radical polymerisation could not be avoided as shown in Appendix 2.33 and signs of this process were observed in every collected sample (one per day). Unfortunately, these high concentration reactions with the ionic monomer gave solid gels (after 4 days reaction) from which it proved very difficult to extract the desired hyperbranched polymers; consequently a new protocol was investigated. The aqueous solution polymerisation of N-acryloyl-1,2-diaminoethane was studied. This new method is discussed in the following sections.

3.3.3. Aqueous solution polymerisation of N-acryloyl-1,2-diaminoethane

Free amino groups are much more reactive towards α,β -unsaturated carbonyl groups than their ammonium salts. Their use could therefore help to synthesise high molecular weight hyperbranched poly(amidoamine)s in aqueous solution. A highly concentrated solution (10 ml) of N-acryloyl-1,2-diaminoethane hydrochloride (2.5 g) was prepared in deionised water and mixed with Dowex ion (^-OH) exchange resin beads in order to generate the free amine monomer and water. This treated solution was filtered, the pH was determined as 10 and the solution was divided into 10 x 1 ml aliquots, each of which was placed in a Carius tube fitted with a magnetic stirrer bar. After three freeze-thaw cycles, in order to remove oxygen, nine of these tubes were sealed under static vacuum (8.10^{-2} mbar). With the tenth sample, an attempt was made to recover the free unreacted N-acryloyl-1,2-diaminoethane monomer (see 3.2.3).

However, Michael addition reactions could not be prevented as seen in the ^1H and ^{13}C NMR spectra for this sample. A value of 4, was calculated for the DP and new methylene peaks were observed as a result of the consumption of vinyl groups by Michael additions (see Appendix 2.23 and 2.24). This confirms the expected higher reactivity of free amines compared to that of ammonium salts. Even at low temperatures, it is impossible to slow down and/or prevent the Michael addition reactions. The difficulty in regulating the polymerisation process increases as the concentration of the monomer solution increases.

After 90 minutes at 100°C , the vinyl hydrogens and carbons have almost completely disappeared after being converted into new methylene groups as shown in the ^1H and ^{13}C NMR spectra for this sample; see Appendices 2.26 and 2.27. A degree of polymerisation of 62 was calculated from the values of the relative intensities of the peaks observed in the ^1H NMR spectrum as explained in the previous sections. The FTIR spectrum showed no sign of the out-of-plane C-H deformation of the vinyl double bond, as shown in the Appendix 2.25, confirming the virtually complete consumption of the vinyl groups by the polymerisation process. The elemental analysis of the resulting polymers showed that the conversion of ammonium groups into free amines was not complete. This could be the consequence of the high concentration of the hydrochloride solution, making it difficult to efficiently convert all the ammonium salts. However, only a few amino groups are necessary to increase the overall kinetic of the polymerisation process, thanks to the permanent exchange of protons between the ammonium salts and free amines. The coexistence of both species in solution gives rise to a ^1H NMR spectrum completely different in terms of relative intensities of the observed CH_2 peaks, when compared with the spectrum observed for the hydrochloride polymers in solution; compare Appendices 2.21 and 2.26. A shift of the chemical shifts of the methylene hydrogens towards lower ppm values can also be observed. This is the consequence of the partial conversion of ammonium salts into free amines. The observed difference in terms of relative intensities of the methylene peaks suggests a great difference in terms of structure between the partially free amine polymer and the hydrochloride polymer. The relatively sharp and well-resolved peaks could suggest that only low molecular weight oligomers were synthesised. Analysis by MALDI-TOF mass spectrometry confirmed this observation, as the highest molecular weight that

could be observed did not exceed 2,500 Daltons; see chapter 5. The small weight of each sample (0.25 g) made the analysis by ^{15}N NMR spectroscopy, in order to determine the value of DB, impossible. The thermogravimetric analysis revealed that this new polymer was thermally stable up to 200°C, which is a lower value than that observed for the more thermally stable hydrochloride polymers. The DSC analysis revealed no melting point for this polymer, confirming its hyperbranched structure and a value of 14.7°C was found for the T_g .

In order to solve the problem of the incomplete conversion into a free base monomer and to slow down the kinetic of the reaction, it was decided to decrease the concentration of the monomer solution. A solution (10 ml) of N-acryloyl-1,2-diaminoethane hydrochloride (0.5 g, 3.32 mmol) was then prepared in deionised water and the procedure described in Section 3.2.4 above was applied. The sample that wasn't polymerised was analysed using NMR spectroscopy. The ^1H NMR spectrum for this sample confirmed that new methylene groups were created and a DP of 5 was calculated; see Appendix 2.28. This observation was confirmed by the analysis of the ^{13}C NMR spectrum that revealed the creation of new aliphatic carbons; see Appendix 2.29. The calculated value for DP is similar to that observed in the case of the more concentrated free base solution. This confirms that the reactivity of the free amino groups is the driving force of the polymerisation, independently of the HCl content. Even at low temperature, the polymerisation occurs quickly. It is therefore almost impossible to control the process as the concentration increases and all attempts to isolate the free base monomer are vain. The fact that the N-acryloyl-1,2-diaminoethane could only be isolated and spectroscopically identified in a very dilute solution (see Chapter 2) confirms the view that the polymerisation occurs during the freeze-drying process, when the concentration of monomer increases. These observations tend to confirm not only the high reactivity of amino groups, but also the view that reducing the concentration allows a better control over the polymerisation kinetics.

After 90 minutes at 100°C, a polymer was obtained and characterised by elemental analysis. Chlorine was found (10%), which is lower than the percentage found for higher concentration monomer solution experiments. This confirms the difficulty in converting all ammonium salts into free amino groups even at very lower concentration. The FTIR spectrum is similar to the FTIR spectra already obtained for

the previously analysed and discussed polymers. However, some residual vinyl peaks are observed at 979 and 927 cm^{-1} , as shown in the Appendix 2.30. The ^1H NMR spectrum shows a typical structure of a supposedly hyperbranched polymer, namely virtually complete absence of vinyl hydrogens and creation of new methylene hydrogens in addition to those already observed for the monomer. However, all chemical shifts are shifted to lower ppm values; this observation confirms the partial conversion of ammonium salts into amino groups; see Appendix 2.31. A value of 80 was calculated for the DP of this polymer. Such a high value for DP contradicts the relatively well-resolved structure of the observed peaks (no broadening). This could suggest that the value of DP is artificially increased by the consumption of vinyl double bonds through cyclisation reactions. This view is also suggested by the MALDI-TOF analysis (see Chapter 5) of these polymers. The ^{15}N NMR analysis could not be performed on the small quantities of polymers that were obtained and the values of DB could not be determined for these polymers. The ^{13}C NMR spectrum confirmed the formation of a hyperbranched polymer, due to the creation of numerous new methylene signals and the relatively important decrease of the intensities of the vinyl carbons, as seen in the Appendix 2.32. The thermogravimetric analysis of this sample revealed no thermal decomposition before 200°C. DSC analysis showed no evidence of a melting temperature and no T_g value could be determined, which was attributed to the presence of water in the sample.

In the next Chapter, the kinetics of the polymerisations of N-acryloyl-1,2-diaminoethane hydrochloride and N-acryloyl-1,2-diaminoethane in aqueous solutions at different concentrations will be discussed. The analysis of the various polymer samples using MALDI-TOF mass spectrometry will be discussed in Chapter 5.

Chapter Four

Kinetic study

4.1. Introduction

In this chapter, the ^1H NMR data accumulated over time for each different polymer will be analysed in order to study the kinetics of the polymerisation in aqueous solution of the two different monomers; N-acryloyl-1,2-diaminoethane hydrochloride and N-acryloyl-1,2-diaminoethane at different concentrations. As explained in Chapter 3, it is possible to determine the DP of the various polymers using their corresponding ^1H NMR spectra. A sample was taken and analysed every day over 10 days in the case of the aqueous polymerisations of N-acryloyl-1,2-diaminoethane hydrochloride and every 10 minutes over 90 minutes in the case of the solution polymerisations of N-acryloyl-1,2-diaminoethane. This allowed the author to follow the evolution of DP values as a function of time and whenever possible to determine the rate constant associated with each polymerisation experiment. For each monomer, the influence of monomer concentration was studied, using two different concentrations: 0.5 and 0.25 g/ml (3.32 and 1.66 mmol/ml) for N-acryloyl-1,2-diaminoethane hydrochloride, 1.66 and 0.33 mmol/ml for N-acryloyl-1,2-diaminoethane.

4.2. Kinetic study of the aqueous solution polymerisation of N-acryloyl-1,2-diaminoethane hydrochloride

In this section the kinetics of the solution polymerisation of N-acryloyl-1,2-diaminoethane hydrochloride in aqueous solution will be discussed. Four cases will be studied:

- i. Case 1: Aqueous solution polymerisation of a 0.5 g/ml (3.32 mmol/ml) solution of monomer in D_2O . The polymerisation was performed in 5ml ampoules over 4 days at 100°C . All the recorded ^1H NMR spectra for the analysed samples revealed the strong presence of side-products due to free radical polymerisation, as discussed in Chapter 3.
- ii. Case 2: Aqueous solution polymerisation of a 0.25 g/ml (1.66 mmol/ml) solution of monomer in D_2O performed in 5ml ampoules over 10 days at 100°C . All the recorded ^1H NMR spectra showed strong signs of free radical polymerisation.

iii. Case 3: Aqueous solution polymerisation of a 0.25 g/ml (1.66 mmol/ml) solution of monomer in D₂O performed in 5ml ampoules over 10 days at 100°C. Six out of ten recorded ¹H NMR spectra showed strong signs of free radical polymerisation while the four other ¹H NMR spectra did not show any sign of free radical polymerisation.

iv. Case 4: Aqueous solution polymerisation of a 0.25 g/ml (1.66 mmol/ml) solution of monomer in D₂O performed in 10ml Carius tubes over 10 days at 100°C. Very weak signs of free radical polymerisation could only be found after long reaction times.

4.2.1. Case 1: High concentration of monomer in aqueous solutions, polymerisations performed in closed ampoules

In this case, the polymerisation of N-acryloyl-1,2-diaminoethane hydrochloride in highly concentrated solution (0.5g/ml; 3.32 mmol/ml) in D₂O was performed at 100°C over 4 days in 10 separate 5ml ampoules degassed and closed under static vacuum with Teflon taps. The use of D₂O allowed a direct analysis of the samples using ¹H NMR spectroscopy, as the liquid samples could be directly transferred from the ampoules to the NMR tubes with no intermediate freeze-drying process. However, such a procedure prevented the use of these samples for accurate MALDI-TOF analysis due to the hydrogen/deuterium exchanges between the NH groups of the products and the deuterated solvent, which resulted in very complex spectra. After 4 days, solid gels were formed and the reaction was stopped, since the formation of such gels prevented homogeneous stirring of the reaction mixtures. The four collected ¹H NMR spectra allowed the author to follow the evolution of the degree of polymerisation of the analysed polymeric sample as a function of elapsed reaction time. It was possible to determine the value of DP for each of the analysed samples, since remaining vinyl hydrogen signals could be observed and integrated. For each sample, strong hydrogen signals due to free radical polymerisation were observed and the relative intensities of the new methylene hydrogens generated by this process were included in the calculation of the DP values. The plot of the calculated DP values *versus* the corresponding polymerisation times is shown in *Figure 4.1*.

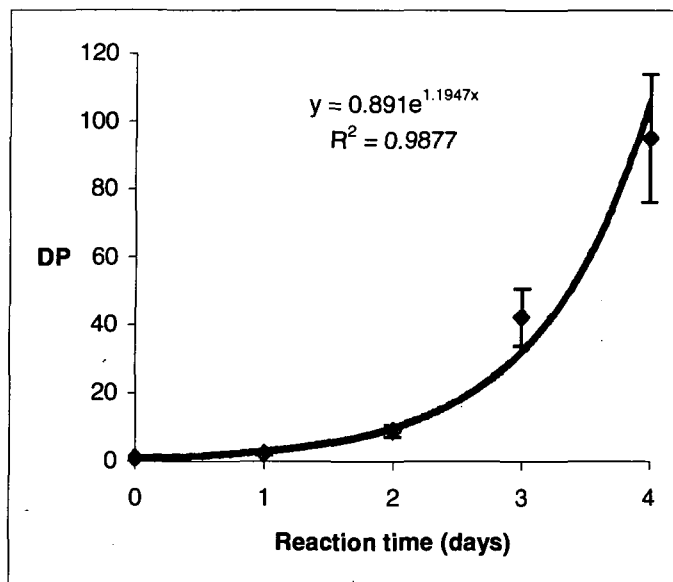


Figure 4.1. Plot of DP vs reaction time for case 1

The variables in these experiments are DP and time and we need to derive a relationship between them. The polymerisation involves successive Michael additions of one unreacted double bond (A group) of an AB_2 monomer molecule or growing oligomer with one unreacted $-NH-$ (B group) of another AB_2 monomer or growing oligomer. Thus, the rate of conversion (r) can be expressed as follow:

$$r = k [A] [B]$$

where:

k is the rate constant

$[A]$ is the concentration of unreacted A groups in the system at a time t

$[B]$ is the concentration of unreacted B groups in the system at a time t .

In order to determine the equation linking the value of DP to the reaction time, it is necessary to exploit the relationship existing between $[A]$, $[B]$ and DP and to transfer this relationship into the expression for r . Figure 4.2 shows that a hyperbranched molecule, obtained by AB_2 polymerisation with one unreacted A group (focal point) and 11 repeat units ($DP = 11$), will possess $DP + 1 = 12$ unreacted B groups (end groups).

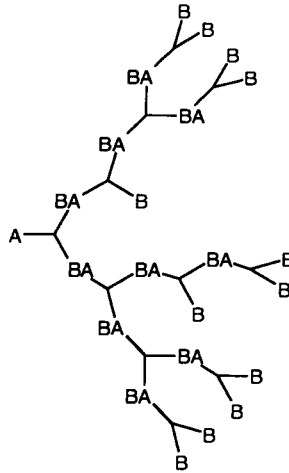


Figure 4.2. Representation of a hyperbranched molecule with a DP of 11

As a consequence, if no cyclisation occurred, the number of moles of B groups (n_B) present at a time t in the analysed sample can be expressed as a function of the number of moles of unreacted A groups present at the same time in the same sample:

$$n_B = n_A(DP + 1)$$

Thus, as the volume of the solution remains constant, the expression for [B] becomes:

$$[B] = [A](DP + 1)$$

And the expression for r becomes:

$$r = k[A]^2(DP + 1)$$

Now, it is necessary to express [A] as a function of DP:

$$[A] = n_A/V$$

where V is the volume of the solution.

If no cyclisation had occurred, the number of unreacted A groups should be equal to the number of molecules present in the system at a given time t . Furthermore, as there is no loss of any molecule during the polymerisation process, the law of

conservation of matter dictates that the mass of the final product equal the initial mass (m) of the monomer; therefore:

$$N_A = m/M_n = m/(150.5 \text{ DP})$$

The expression for [A] becomes:

$$[A] = m/(150.5 V \text{ DP}) = C/\text{DP}$$

where: C is the initial concentration of monomer in aqueous solution (in mol.ml⁻¹).

As A groups are being consumed by the polymerisation process, r represents the rate of consumption of A groups over time, therefore, after replacing [A] with its expression as a function of DP in the initial expression for r, it can be written that:

$$r = - d[A]/dt = kC^2(\text{DP} + 1)/\text{DP}^2$$

The derivation of the expression for [A] as a function of time gives:

$$d[A]/dt = C d(1/\text{DP})/dt = - C d\text{DP}/(\text{DP}^2 dt)$$

As a consequence, the expression for r becomes:

$$r = - d[A]/dt = C d\text{DP}/(\text{DP}^2 dt) = kC^2(\text{DP} + 1)/\text{DP}^2$$

The simplification of this equation gives:

$$d\text{DP}/dt = kC(\text{DP} + 1)$$

Therefore, by rearranging this equation, it is possible to write:

$$d\text{DP}/(\text{DP} + 1) = kC dt$$

Thus, by integrating the left side of this equation from the value DP at the time t=0 ($DP_{(t=0)}$) and the value of DP at a considered time t ($DP_{(t)}$), and the right side of the equation between the time t=0 and the time t, the following expression can be written:

$$\int_{DP_{(t=0)}}^{DP_{(t)}} \frac{dDP}{DP+1} = kC \int dt$$

which gives:

$$[\ln(DP+1)]_{DP_{(t=0)}}^{DP_{(t)}} = kC[t]_0^t$$

thus, giving:

$$\ln(DP_{(t)}+1) - \ln(DP_{(t=0)}+1) = kCt$$

Or:

$$\boxed{\ln(DP_{(t)}+1) = kCt + \ln(DP_{(t=0)}+1)} \quad (1)$$

which indicates a linear relationship between $\ln(DP+1)$ and reaction time, where kC represents the slope of the line, allowing for an easy determination of k , the rate constant of polymerisation. Applying an exponential relationship to both sides of the equation gives:

$$\boxed{DP_t = [(DP_0 + 1) e^{kCt}] - 1} \quad (2)$$

which confirms the exponential trend observed in *Figure 4.1* between DP and the reaction time. The plot of $\ln(DP+1)$ against reaction time verified the equation (1) as shown in *Figure 4.3*.

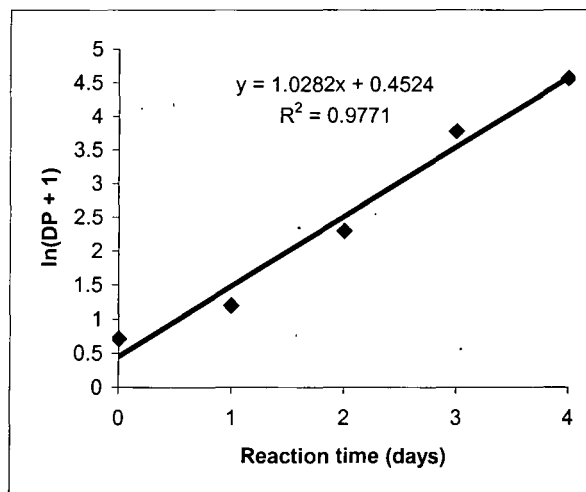


Figure 4.3. Plot of $\ln(DP + 1)$ vs reaction time for the case 1

From the value of the slope, it was possible to calculate the value of k_1 , the rate constant for the case 1. A value of $310 \text{ mol}^{-1} \text{ ml day}^{-1}$ ($3.6 \cdot 10^{-6} \text{ mol}^{-1} \text{ L s}^{-1}$) was found for k_1 . Each step in the polymer growth involves two species and the units of the growth rate constant are those of a second order reaction. The polymerisation of this monomer in aqueous solutions is a relatively slow process. Although for this data analysis many assumptions and approximations were made, such as the fact that possible cyclisation could have occurred was not considered and that the relative intensities of the methylene signals generated by free radical polymerisation were included in the calculation of DP, reasonably good fits were obtained and the two previously established equations were verified in this case. However, in order to confirm the calculated value for k and establish that this value is independent of the concentration and the approximations made to obtain it, the kinetics of the polymerisation of N-acryloyl-1,2-diaminoethane hydrochloride in more dilute aqueous solutions was studied, as described in the next two sections.

4.2.2. Cases 2 and 3: Lower concentration of monomer in aqueous solutions, polymerisations performed in closed ampoules

The solution polymerisation of N-acryloyl-1,2-diaminoethane hydrochloride was performed over 10 days at 100°C in 5ml ampoules, using more dilute aqueous solutions of monomer ($C = 0.25 \text{ g/ml}$ or 1.66 mmol/ml). For direct characterisation of the synthesised products using ^1H NMR spectroscopy, the polymerisation was first performed in D_2O (case 2), but, in order to characterise these products using MALDI-TOF mass spectrometry, the same experimental procedure was repeated in deionised water and the polymers were first recovered as yellow solids by freeze-drying and then analysed (case 3). However, these two identical reaction protocols gave rise to different results. In the case 2, all the synthesised polymers and oligomers showed signs of contamination by free radical polymerisation using ^1H NMR spectroscopy. In the second case (case 3), free radical polymerisation was randomly observed in the different samples. In both cases, no formation of solid gels was observed at high degrees of conversion. This gave an opportunity to study the influence of free radical polymerisation on the overall kinetics of the polymerisation. In both cases, the kinetics of polymerisation was studied using the same approach as described in 4.2.1.1; the

values for DP were calculated using the relative intensities of all the methylene hydrogens, including those formed by free radical polymerisation. In the case 2, the calculated values for DP were plotted against their corresponding reaction times, as shown in *Figure 4.4*.

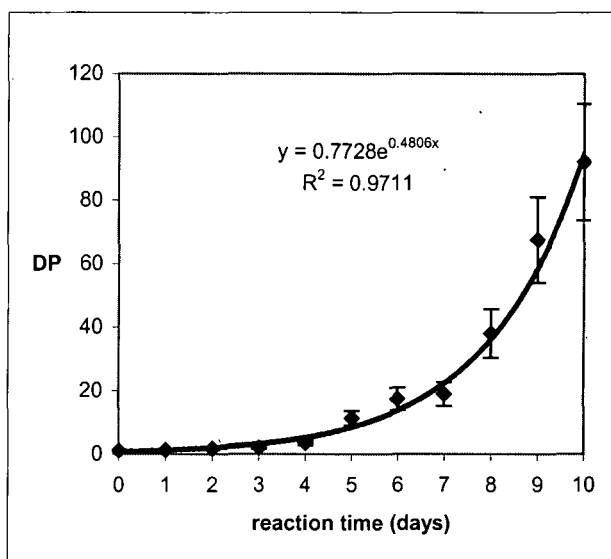


Figure 4.4. Plot of DP vs time for the case 2

Despite the approximations made in that case, an exponential relationship could also be found between DP and reaction time. The plot of $\ln(\text{DP} + 1)$ against reaction time confirms that the equation (1) applies to this case; see *Figure 4.5*.

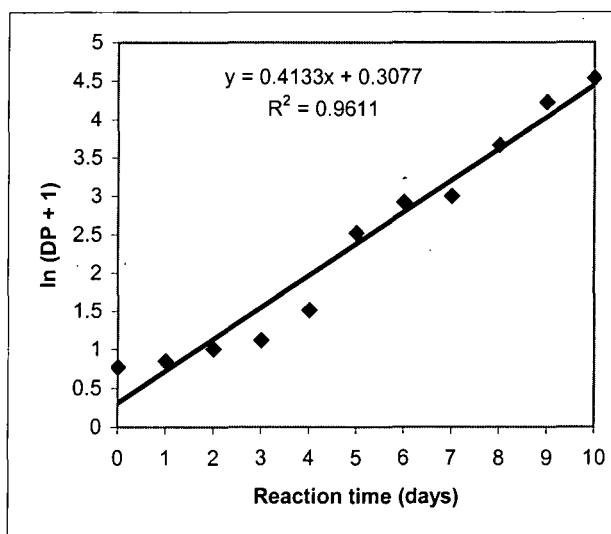


Figure 4.5. Plot of $\ln(\text{DP} + 1)$ vs reaction time for the case 2

From this plot and the value of the slope, the rate constant, k_2 , associated with the case 2, could be determined and a value of $249 \text{ mol}^{-1} \text{ ml day}^{-1}$ ($2.9 \times 10^{-6} \text{ mol}^{-1} \text{ L s}^{-1}$) was found. The value obtained for k_2 is lower than that calculated for k_1 , but the values are essentially the same within the error of the experiment. The experimental factors, such as the formation of solid gels at high concentration in monomer and the occurrence of parasitic free radical polymerisation render such a perfect match impossible to achieve. It is also possible that the error associated with calculation of DP using NMR data is responsible for the difference observed between these two values. If this is the case, an average value of $3.25 \times 10^{-6} \text{ mol}^{-1} \text{ L s}^{-1}$ could be assigned for k , the rate constant of polymerisation of N-acryloyl-1,2-diaminoethane hydrochloride in aqueous solution.

In the “case 3”, the same experimental procedure as “case 2” was reproduced, with only one change made in the protocol used for the case 2; the use of deionised water as a solvent instead of D_2O . Such a change should not modify the outcome of the reaction. However, the occurrence of free radical polymerisation was statistically distributed whereas, for the previously studied cases 1 and 2, this phenomenon was observed for each analysed sample. This confirms that the reproducibility of the aqueous solution polymerisation experiments performed for this monomer in closed ampoules depends on the non-predictable fatigue of the Teflon taps used. As a consequence, a non-exponential plot of DP *versus* reaction time was observed for the case 3, as shown in *Figure 4.6*.

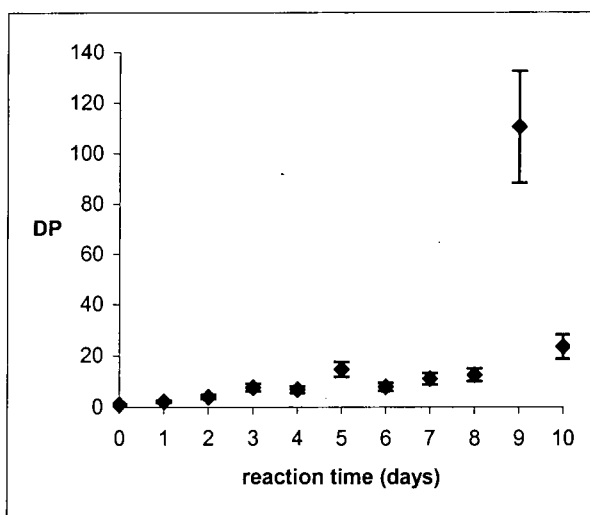


Figure 4.6. Plot of DP vs reaction time for the case 3

As the reader can easily imagine, the plot of $\ln(DP + 1)$ versus reaction time could, in no event, give the desired linear plot, as shown in *Figure 4.7*.

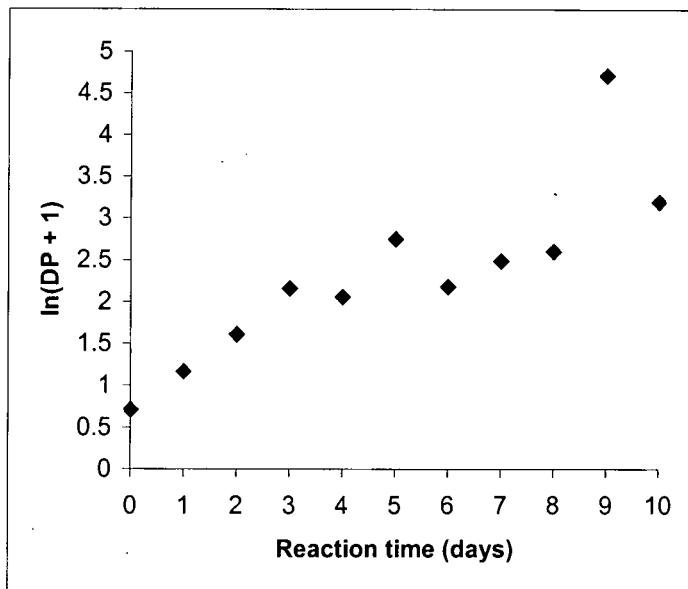


Figure 4.7. Plot of $\ln(DP + 1)$ vs reaction time for the case 3

However, removal from *Figures 4.6* and *4.7* of the data points collected after 3, 5 and 9 days reaction times respectively, produced two new plots much closer to those predicted by the theory; see *Figures 4.8* and *4.9*.

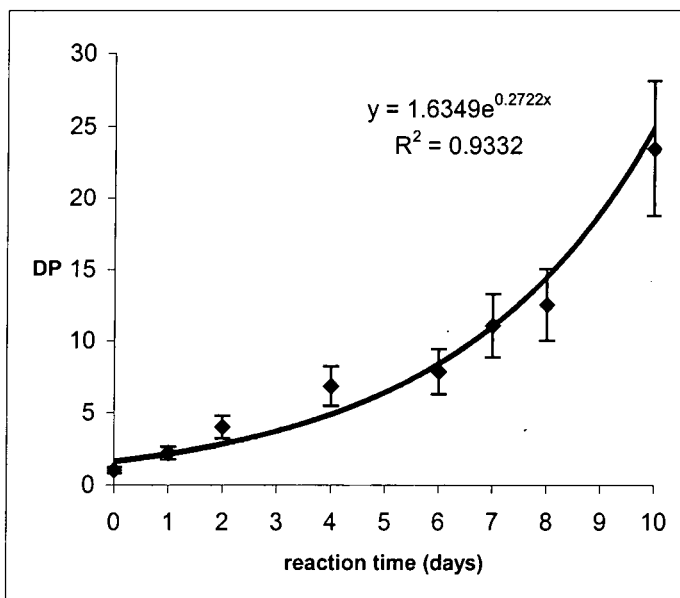


Figure 4.8. Second plot of DP vs reaction time for the case 3

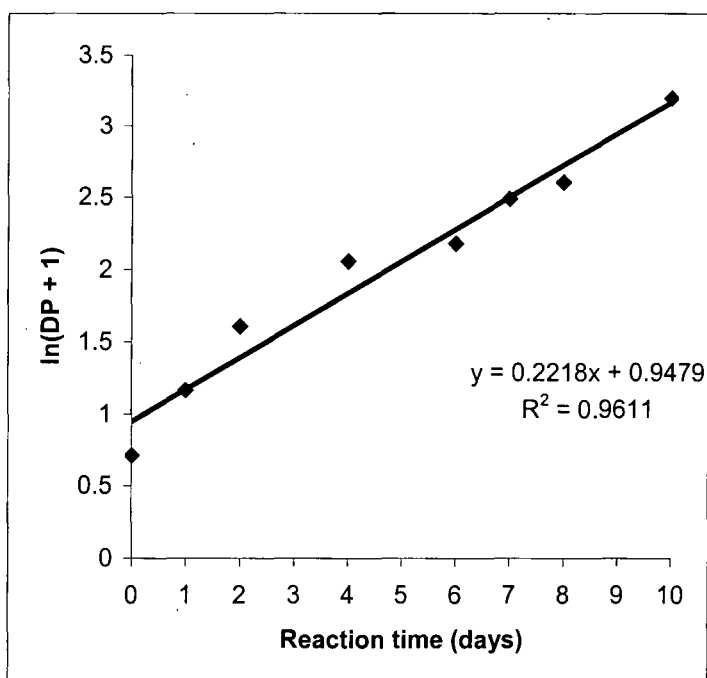


Figure 4.9. Second plot of $\ln(DP + 1)$ vs reaction time for the case 3

The plot in *Figure 4.8* shows the expected exponential dependence of DP with regard to the polymerisation time. As expected, the plot in *Figure 4.9* confirms the linear relationship between $\ln(DP + 1)$ and the polymerisation time. A value of $134 \text{ mol}^{-1} \text{ ml day}^{-1}$ ($1.55 \times 10^{-6} \text{ mol}^{-1} \text{ L s}^{-1}$) was found for the rate constant (k_3) corresponding to this experiment. This value is about half the average value found for k_1 and k_2 . This is easily explained by the random occurrence of free radical polymerisation observed in this case. Furthermore the values of DP that were removed from the final plots corresponded to samples strongly contaminated by free radical polymerisation, thus giving abnormally high values for DP. The values used in *Figures 4.8* and *4.9* correspond to samples where the relative intensities of the methylene hydrogen peaks due to free radical polymerisation were insignificant if not null. Therefore, it is very likely that the value calculated for k_3 is much closer to the true value of k than the higher values calculated for k_1 and k_2 but, within the precision of the DP measurements, the agreement between k_1 , k_2 and k_3 is encouraging.

As the use of Teflon taps was found to be the main source of oxygen leakage responsible for the observed free radical polymerisation, ampoules were replaced by Carius tubes. Their use virtually prevented free radical polymerisation from occurring. It was therefore necessary to study the kinetics of polymerisation for this new

procedure (case 4) and determine the true rate constant value associated with the polymerisation of N-acryloyl-1,2-diaminoethane hydrochloride in aqueous solution.

4.2.3. Case 4: lower concentration of monomer in aqueous solution, polymerisation performed in sealed Carius tubes

This polymerisation experiment was performed using 10ml Carius tubes loaded with 0.25g/ml (1.66 mmol/ml) 1ml-solutions of N-acryloyl-1,2-diaminoethane hydrochloride dissolved in deionised water. After three freeze-thaw cycles, these tubes were sealed under static vacuum and the polymerisation was carried out at 100°C for 10 days. Each day, a sample was collected and the content was free-dried under dynamic vacuum (8×10^{-2} mbar) to give a yellow solid that was analysed using ^1H and ^{13}C NMR spectroscopy as well as MALDI-TOF mass spectrometry. From the analysis of the data collected using ^1H NMR spectroscopy the plot of DP *versus* polymerisation time could be drawn, showing the expected exponential trend predicted by the theory, see *Figure 4.10*.

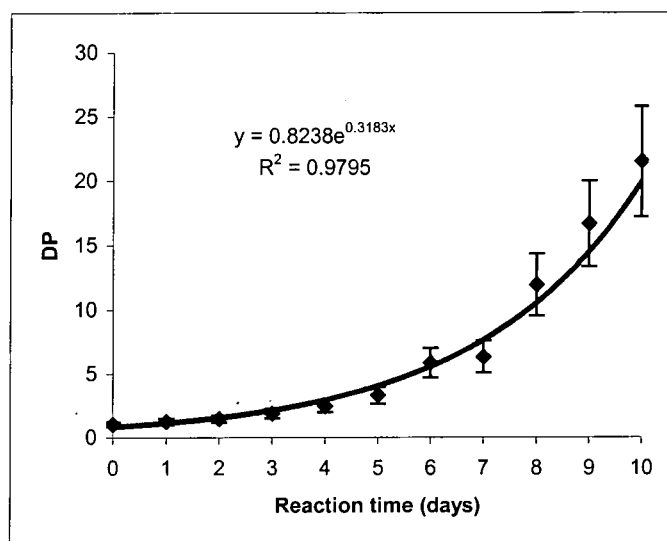


Figure 4.10. Plot of DP vs Reaction time for the case 4

The plot of $\ln(\text{DP} + 1)$ with respect to the reaction time gave rise to a quasi-linear plot, as shown in *Figure 4.11*.

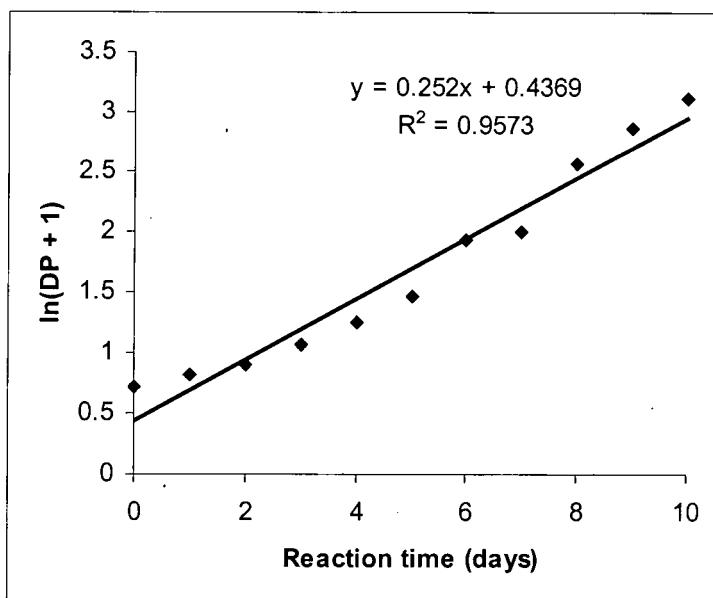


Figure 4.11. Plot of $\ln(DP + 1)$ vs reaction time for the case 4

This plot confirms that the equation (1) applies to this case and, as a consequence, it is possible to determine the rate constant (k_4) for this case; a value of $152 \text{ mol}^{-1} \text{ ml day}^{-1}$ ($1.76 \times 10^{-6} \text{ mol}^{-1} \text{ L s}^{-1}$) was found for k_4 . This value represents the true value of the rate constant of polymerisation of N-acryloyl-1,2-diaminoethane hydrochloride in aqueous solutions. This value is close to that observed for k_3 , when data collected from samples highly contaminated by free radical polymerisation were discarded, which supports the view that this value calculated for k_4 is the true value of the rate constant associated to the solution polymerisation of N-acryloyl-1,2-diaminoethane hydrochloride in water.

This kinetic study strengthened the conclusions expressed in Chapter 3; namely, that the polymerisation of N-acryloyl-1,2-diaminoethane hydrochloride performed in aqueous solutions at relatively low concentration using Carius tubes provides a reproducible method to obtain hyperbranched molecules without the contamination induced by free radical polymerisation and the formation of solid gels at high degrees of conversion observed in the case of highly concentrated solutions. However, the relatively long reaction times required so that relatively high degrees of conversion can be reached lead to the study of the aqueous solution polymerisation of the *in situ* generated free base monomer, N-acryloyl-1,2-diaminoethane hydrochloride as

described in Chapter 2 and discussed in Chapter 3. The kinetics of the polymerisation of this new monomer in aqueous solutions will be discussed in the next section.

4.3. Kinetics of the polymerisation of N-acryloyl-1,2-diaminoethane in aqueous solutions

In this section, the kinetics of two different polymerisation experiments will be analysed; namely, case 1' or the polymerisation of N-acryloyl-1,2-diaminoethane in solution in deionised water at relatively high concentration (1.66 mmol/ml) and case 2' or the polymerisation of the same monomer in more dilute solution (0.33 mmol/ml) in deionised water.

4.3.1. Case 1': High concentration of N-acryloyl-1,2-diaminoethane in deionised water, polymerisation in sealed Carius tubes

In this case, the polymerisation experiment was performed on a 1.66 mmol/ml solution of N-acryloyl-1,2-diaminoethane in deionised water. This monomer was synthesised *in situ* by preparing a 1.66 mmol/ml 10ml-solution of N-acryloyl-1,2-diaminoethane hydrochloride (2.5g, 16.6 mmol) in deionised water. The volume of the solution was made up to 10 ml using a 10ml volumetric flask. Dowex ion exchange resin beads (5g) were then added to the solution (see 3.2.3.1). The mixture was stirred for 20 minutes. After filtration, the pH of the solution was determined as 10. The solution was equally distributed between 10 Carius tubes fitted with magnetic stirrers. After three freeze-thaw cycles, nine of these tubes were sealed under vacuum and immersed in a preheated oil bath at 100°C. After 10 minutes a sample was picked and the content was freeze-dried to give white powders that were analysed by ¹H NMR spectroscopy and MALDI-TOF mass spectrometry.

The analysis of the data obtained using ¹H NMR spectroscopy confirmed that no sign of free radical polymerisation could be observed due to the short reaction times and the use of Carius tubes. The values for DP could be calculated for each sample, allowing drawing the following plot of DP *versus* reaction time, see *Figure 4.12*. The corresponding plot of ln(DP + 1) *versus* reaction time is shown in *Figure 4.13*.

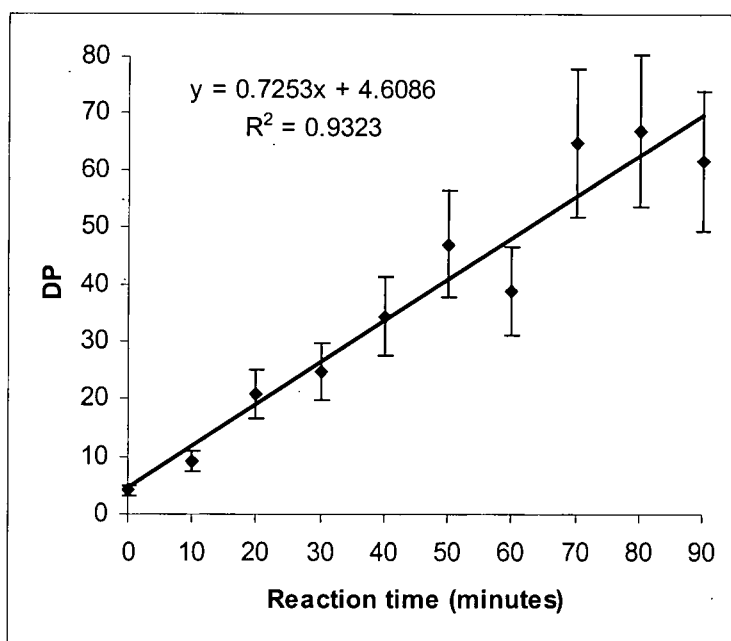


Figure 4.12. Plot of DP vs reaction time for the case 1'

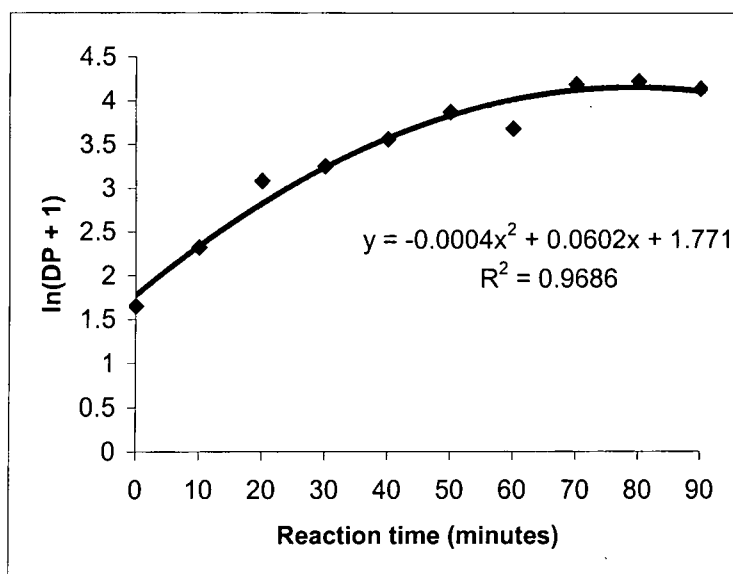


Figure 4.13. Plot of $\ln(DP + 1)$ vs reaction time for the case 1'

The plot in Figure 4.12 shows a linear dependence of DP with reaction time rather than the expected exponential trend. This is confirmed by the plot of $\ln(DP + 1)$ versus time (Figure 4.13) that shows a polynomial trend rather than the expected linear fit. Since all the samples were free from contamination by radical processes, the only possible explanation for such anomalies lies in the method used to obtain the dry polymers. As demonstrated in Chapter 3, it is virtually impossible to isolate the monomer due to the high reactivity of the free amino groups towards the vinyl

double bonds. As a consequence, Michael additions occurred during the freeze-drying of each sample and the DP must have increased with increase in the concentration as the samples became drier and drier. It is therefore impossible to stop the polymerisation during the freeze-drying process and during the analysis. As a consequence, it is irrelevant to try to determine the rate constant of polymerisation for this monomer. Furthermore, the possibility of cyclisation suggested by the MALDI-TOF analysis of these samples (see Chapter 5) make such a study even more complicated as the formula used for the determination of DP can only be used for non-cyclised hyperbranched polymers and oligomers.

However, by considering only the data accumulated up to 50 minutes reaction time, the following plot of DP *versus* time could be obtained, which showed a possible exponential trend, see *Figure 4.14*.

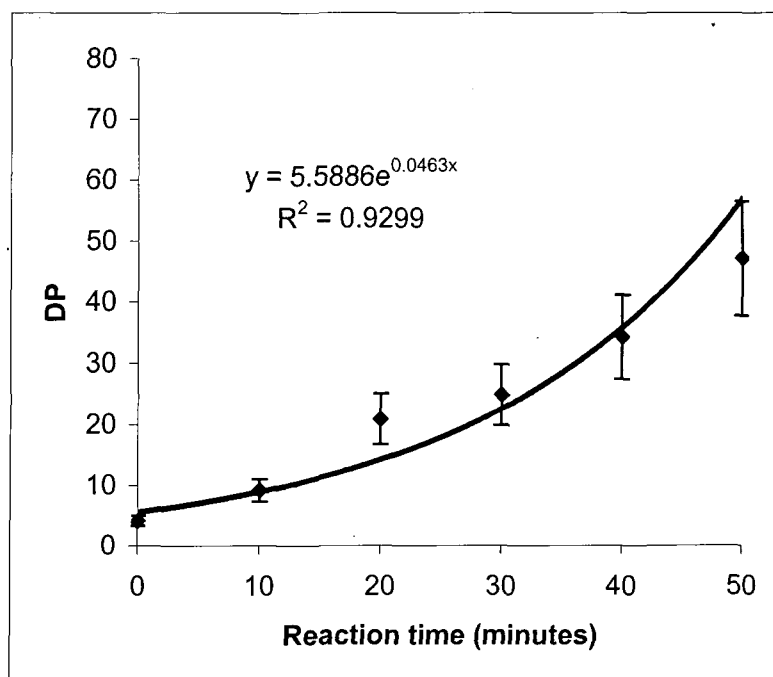


Figure 4.14. Second plot of DP vs reaction time for the case 1'

This exponential trend is confirmed by the plot of $\ln(\text{DP} + 1)$ *versus* reaction time, which, as one would expect, shows a fairly good linear trend, as shown in *Figure 4.15*.

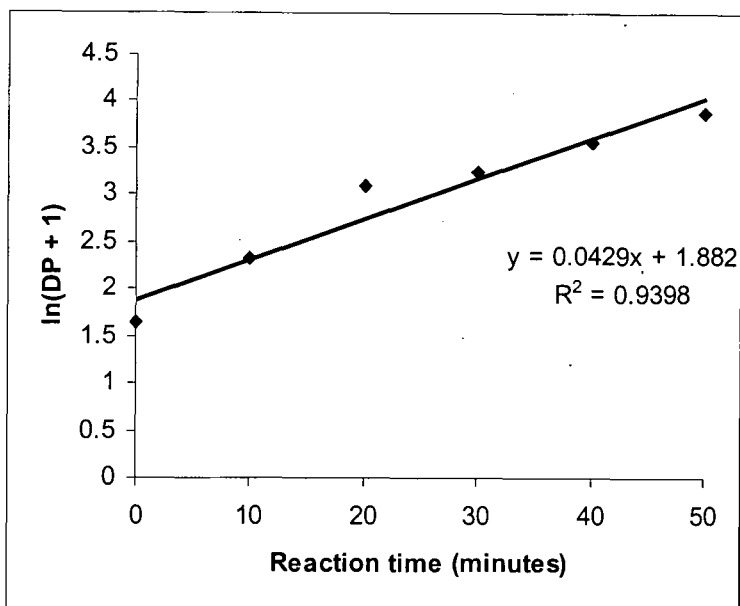


Figure 4.15. Second plot of $\ln(DP + 1)$ vs reaction time for the case 1'

From this extrapolated linear plot, it is possible to determine the value for k_1 , the rate constant associated with the case 1'; a value of $25.8 \text{ mol}^{-1} \text{ ml min}^{-1}$ ($4.3 \times 10^{-4} \text{ mol}^{-1} \text{ L s}^{-1}$), which means that this polymerisation is about 2.5×10^2 times faster than the solution polymerisation of N-acryloyl-1,2-diaminoethane hydrochloride performed at the same concentration. This observation confirms the relatively higher reactivity of the free base monomer as compared to its hydrochloride counterpart.

In order to establish a possible influence of the concentration for this monomer, the observations and results found for the case 1' will have to be compared with those found for the polymerisation of the same monomer in more dilute aqueous solutions (case 2'), see next section.

4.3.2. Case 2': Lower concentration of N-acryloyl-1,2-diaminoethane in deionised water, polymerisation in sealed Carius tubes

Exactly the same experimental procedure as described for the case 1' was used, with the only difference that a more dilute solution of N-acryloyl-1,2-diaminoethane in deionised water was used. For the case 2', the plot of DP *versus* reaction time is shown in Figure 4.16 and the plot of $\ln(DP + 1)$ *versus* reaction time can be seen in Figure 4.17.

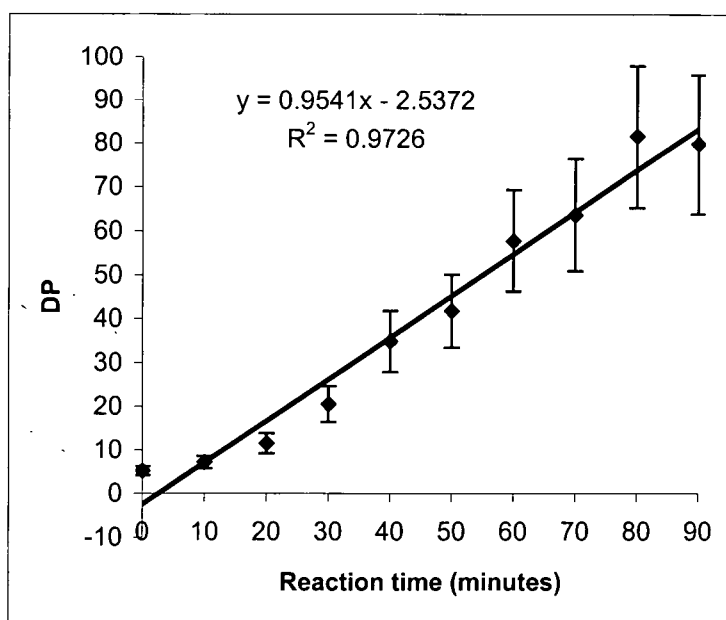


Figure 4.16. Plot of DP vs reaction time for the case 2'

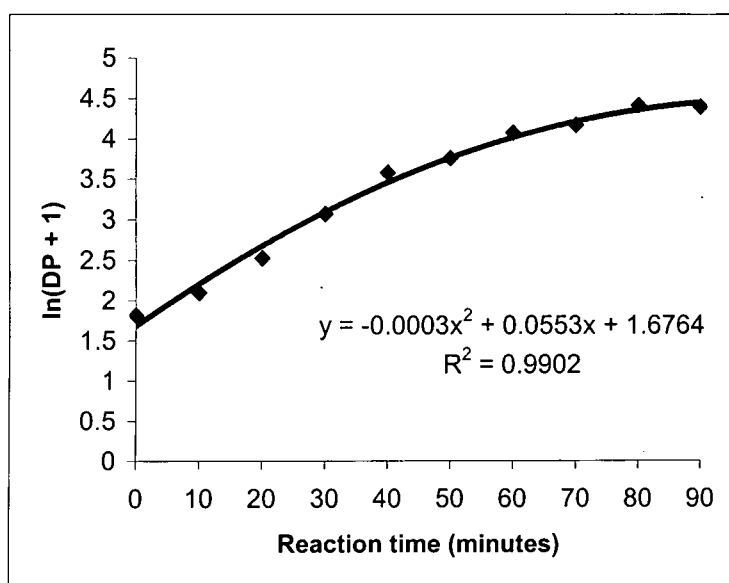


Figure 4.17. Plot of $\ln(DP + 1)$ vs reaction time for the case 2'

Similar observations to those made for case 1' can be made for case 2'; no exponential trend can be found for the plot of DP vs time considering all the data points while a linear trend is easily observed for this plot. As a consequence, the plot of $\ln(DP + 1)$ does not give the expected linear trend but a polynomial one. A slightly higher DP is achieved after 80 minutes in case 2' (DP = 82) than in case 1' (DP = 67), but the order of magnitude remains the same. Furthermore, a comparison of DP is irrelevant because of the possible cyclisation that can occur with these polymers and the fact that

polymerisation continues at room temperature. As it was observed for case 1', an exponential trend can be found for data points up to 50 minutes, as shown in *Figure 4.18*.

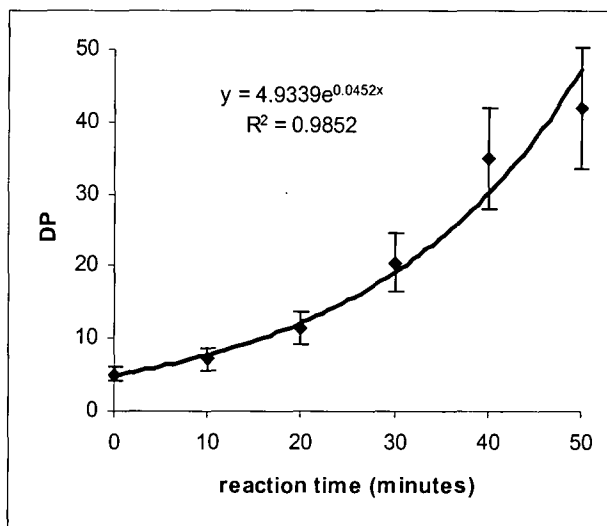


Figure 4.18. Second plot of DP vs reaction time for the case2'

As the reader can expect, the corresponding plot of $\ln(\text{DP} + 1)$ versus time shows a linear trend, see *Figure 4.19*, from which a value for the rate constant k_2 can be calculated, giving a value of $127 \text{ mol}^{-1} \text{ ml min}^{-1}$ ($2.12 \times 10^{-3} \text{ mol}^{-1} \text{ L s}^{-1}$).

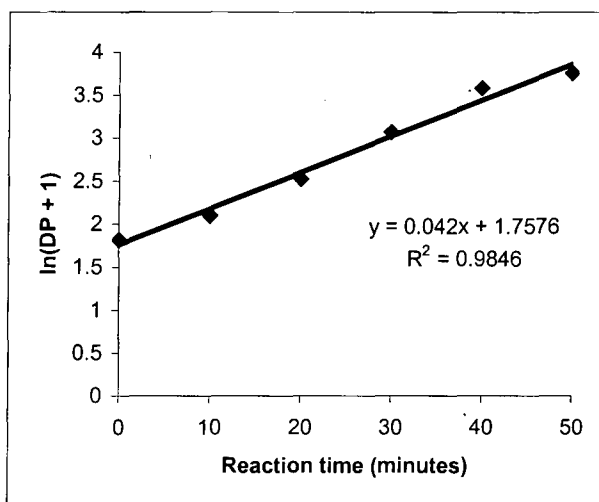


Figure 4.19. Second plot of ln(DP + 1) vs reaction time for the case2'

The first striking observation is all the Figures obtained for the case 1' are absolutely identical to all the Figures obtained for 2', as if it was exactly the same experiment, which is not the case. Therefore, this would suggest that the two polymerisation rates are identical and do not depend on the concentration in monomer,

which is impossible. That explains why two different values, k_1 and k_2 , were found for the same rate constant. All these observations confirm that although this polymerisation must obey a kinetic profile of 2nd order in monomer, the method used to isolate and analyse the samples did not allow the author to follow the real kinetics for the polymerisation of the free base monomer due to the high reactivity of amino group vis-à-vis the vinyl double bonds, preventing to take the real picture of the system at any chosen time. This relatively high reactivity may also be responsible for the cyclisation suggested by the analysis of the MALDI-TOF spectra obtained for these polymers, see next chapter.

The analysis of the kinetics of polymer growth presented above is entirely consistent with the mechanism proposed for the aqueous step-growth polymerisation of N-acryloyl-1,2-diaminoethane hydrochloride. When the aqueous polymerisation of the free base was studied, the analytical method broke down because the free amine is much more reactive and the polymerisation continues in isolated samples. However, an attempt to extract some numerical data from the experiments with the free base monomer suggests that the rate of polymer growth in this case is two or three orders of magnitude faster than for the hydrochloride monomer.

Chapter Five

MALDI-TOF analysis

5.1. Introduction

The MALDI-TOF MS (Matrix Assisted Laser Desorption / Ionisation – Time Of Flight Mass Spectrometry) technique was developed in the 1980s as a means of measuring high mass ions of biomolecules with m/z (mass of ion/charge) over 100kDa.⁴² This technique is based on a soft ionisation process with little fragmentation. This ability to detect high mass ions of relatively intact molecules makes the technique useful for the analysis of polymers.

For use of the MALDI technique, the sample to be analysed is uniformly mixed with a large excess of a matrix; a relatively low molecular weight organic compound that strongly absorbs at the wavelength of the laser used to generate the gas phase ions for analysis (see Figure 5.1). The mixture is placed in a vacuum chamber where it is subjected to the laser pulse that causes the rapid heating and vaporisation of the sample molecules (M). The ions generated in the process are generally of the type $[M + H]^+$ or $[M + \text{cation}]^+$, where the cation is K^+ and/or Na^+ .

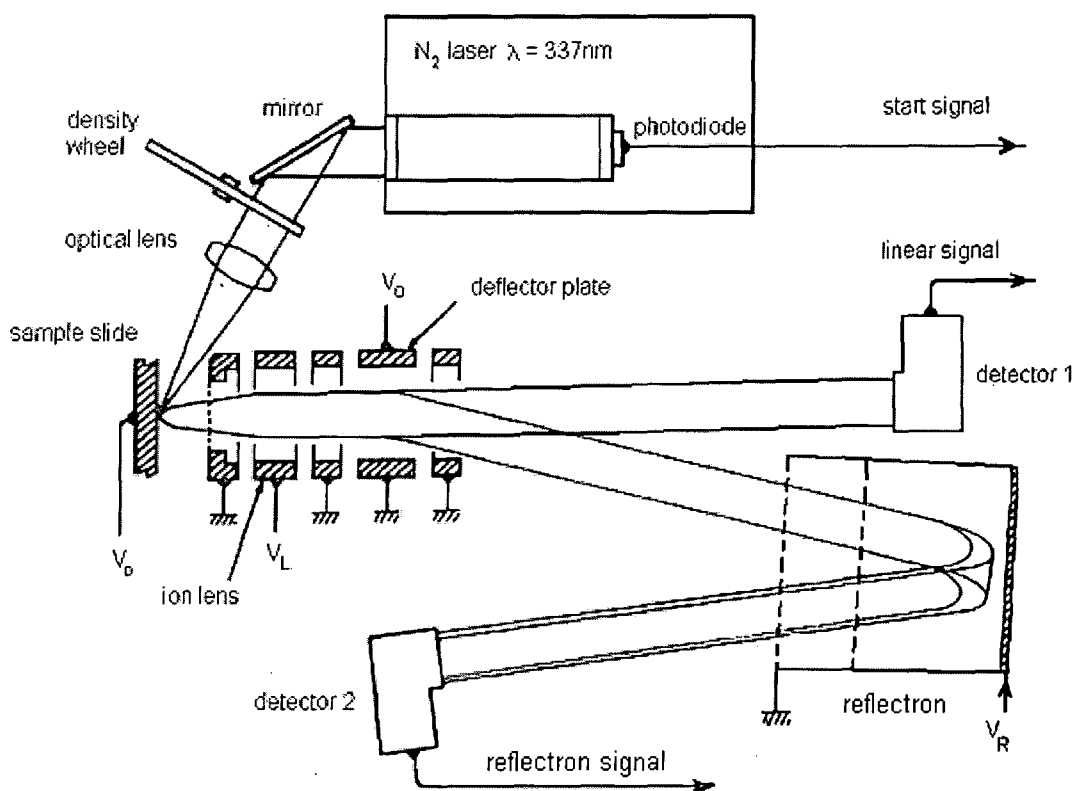


Figure 5.1. Schematic representation of a MALDI-TOF mass spectrometer

The singly charged ions generated are subjected to a potential difference between the sample slide and an extraction grid. This potential causes the acceleration at constant energy of each ion that then passes into a region free of electric field, called the drift space. The ions then “fly” to the detector 1, through the drift space, with velocities inversely proportional to the square root of their respective masses. As a consequence, lighter ions are detected sooner than heavier ions. The mass to charge ratio (m/z) of an ion is related to its “time of flight” by the following expression:

$$\frac{m}{z} = \frac{2V_0 t^2}{L^2}$$

where, m is the ion mass

z is the ion charge

t is the time of flight

V_0 is the potential difference between the sample slide and the extraction grid

And L is the length of the flight tube.

This acquisition method, called the linear mode, has high sensitivity but low mass resolution due to the fact that all ions arrive at detector 1 with the same kinetic energy. However, a second method used in this study, known as the reflectron mode, uses an energy-focussing device, the reflectron. In this case, the ions extracted from the sample are diverted by a deflector towards the reflectron and then measured at detector 2 (see *Figure 5.1*). With this method, the distribution in the time of flight, caused by the difference in kinetic energy when the ions were created, is eliminated for ions of the same mass. Ions having a higher kinetic energy advance deeper into the reflectron while lower energy ions have a longer time of flight through the drift space. As a consequence, ions with equivalent m/z ratios are detected at the same time, independently of their initial kinetic energy, thus providing an improved mass resolution but lowering the mass sensitivity.

For the analysis of polymers, this method has the potential to allow the direct identification of oligomers, the determination of structures and end groups in polymer samples as well as the measurement of distributions and molecular weight averages. Although the determination of molecular weight averages for low-polydispersity

polymer samples gives results in good agreement with other analytical methods, the application of this method to polydisperse materials failed to provide reliable results for the calculation of molecular weight averages.⁴³ Consequently, for the study of hyperbranched poly(amidoamine)s, which are polydisperse by nature, no attempt was made to determine the molecular weight averages using MALDI-TOF data. As described previously, ¹H NMR spectroscopy was the only method that could be used to determine the degree of polymerisation and the number average molecular weight (M_n) of the synthesised macromolecules, since no aqueous GPC was available at the time of study.

In the next sections, the samples synthesised by the aqueous solution polymerisations of N-acryloyl-1,2-diaminoethane hydrochloride and N-acryloyl-1,2-diaminoethane will be analysed. The distribution of oligomer molecular weights will be determined for each sample and the evolution with time of the oligomer distribution will be established for comparison with the expected distribution.

5.2. Analysis of the samples synthesised by the aqueous solution polymerisation of N-acryloyl-1,2-diaminoethane hydrochloride

MALDI-TOF mass spectra were recorded using a Voyager-DE STR Mass Spectrometer (UV laser at 337 nm), in reflectron mode. The samples (2 mg.ml⁻¹, methanol) were analysed using α -cyano-4-hydroxycinnamic acid (10 mg.ml⁻¹, methanol) as the matrix. The samples were presented to the spectrometer as previously described, see Chapter 3 page 38. These conditions were found to be the best suited for the analysis of these samples.

Two mass spectra were recorded for each sample, one from 0 to 1000 mass units (m/z values) and one from 300 to 5000 mass units. However, the spectra recorded from 0 to 1000 amu (see *Figure 5.2*) typically showed mainly the spectrum of the matrix (see *Figure 5.3*) and masked the spectrum of the sample itself, making the precise attribution of the observed peaks and the determination of the molecular weight distribution difficult to achieve. As a consequence, only spectra recorded from 300 to 5000 mass units were studied.

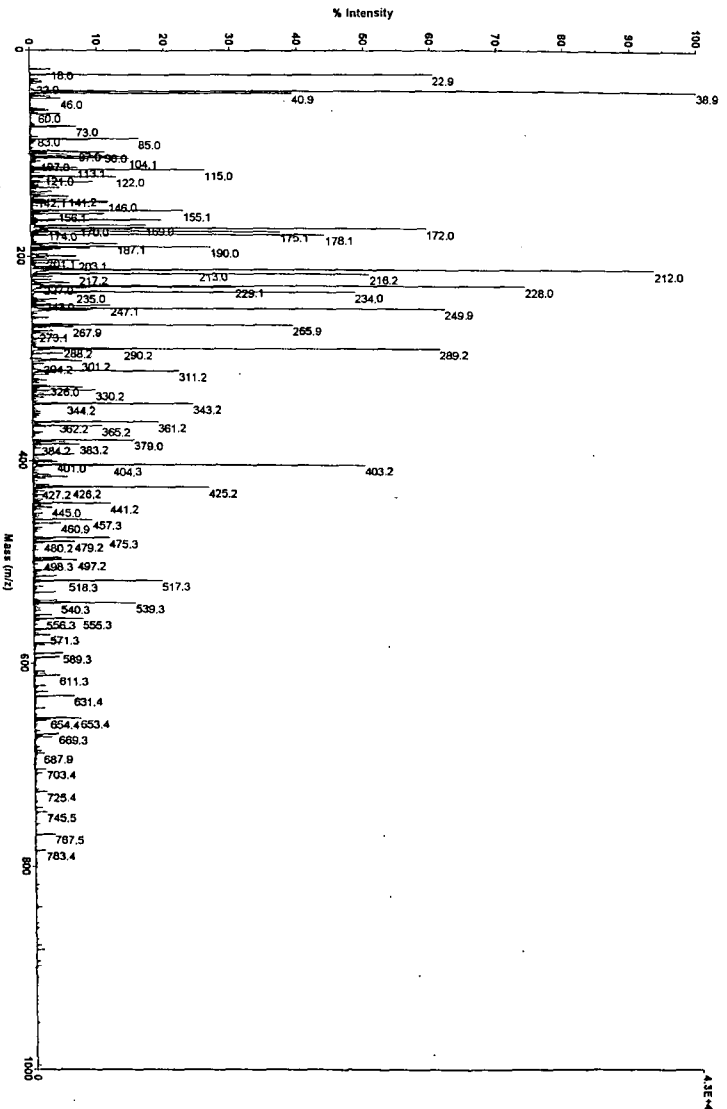


Figure 5.3. MALDI-TOF spectrum of the matrix: α -cyano-4-hydroxycinnamic acid

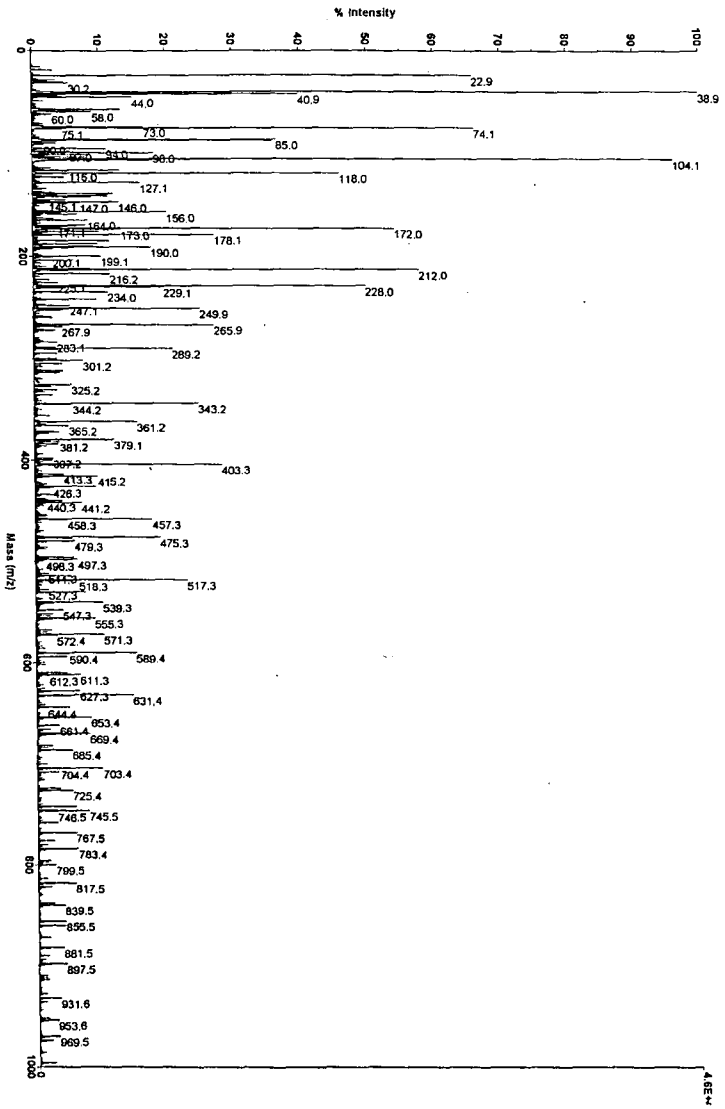


Figure 5.2. Typical MALDI-TOF spectrum of a polymer sample recorded between 0-1000 amu

As observed by Hobson³⁴, oligomeric and polymeric molecules do not fly as hydrochloride salts but as free bases. The same observation was made for the polymers obtained by polymerisation of 0.25g/ml solutions of monomer in deionised water in ampoules and Carius tubes. A typical MALDI-TOF spectrum, recorded for a 10 day reaction product is shown in *Figure 5.4*. A series of peaks at m/z values of $[114n + H]$, $[114n + Na]$, and $[114n + K]$, where $n = DP$ and 114 is the molecular weight (in Daltons) of the free base monomer, N-acryloyl-1,2-diaminoethane, is produced.

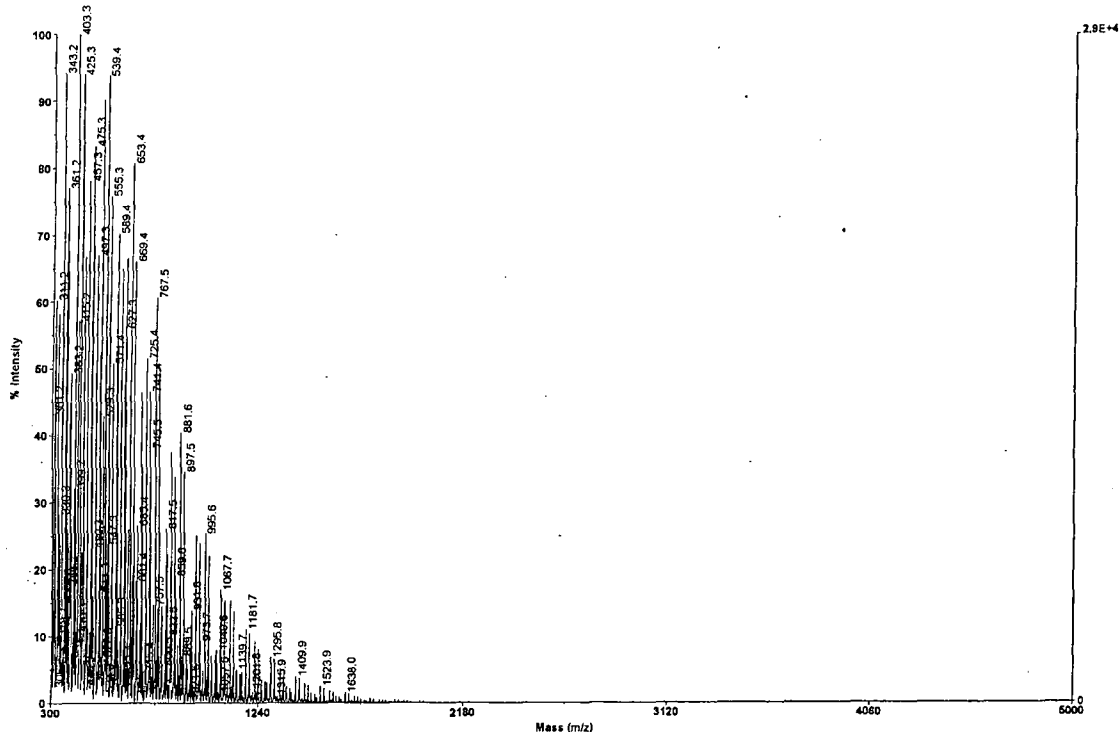


Figure 5.4. Typical MALDI-TOF spectrum obtained after 10 days of aqueous polymerisation of N-acryloyl-1,2-diaminoethane hydrochloride

A second series of peaks was observed at m/z values of $[(114n - 54) + H]$, $[(114n - 54) + Na]$, and $[(114n - 54) + K]$. These m/z values are equal to the m/z values of the first series minus 54, which corresponds to the loss of the focal unit ($m/z = 55$) (see route (1) in *Figure 5.5*) and transfer of one hydrogen to the charge carrying fragment.

In the earlier investigation of the MALDI-TOF spectra of hyperbranched poly(amidoamine hydrochlorides) produced by melt polymerisation³⁴, it was reported that this series of ions had m/z values of $[144n - 55]$ and the focal unit $H_2C=CH-CO-$ has a mass of 55.

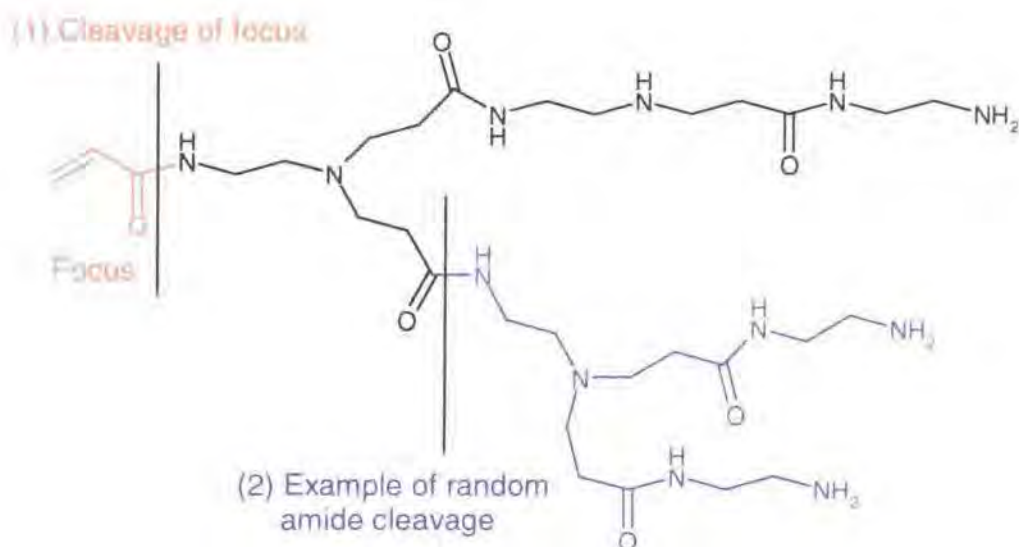
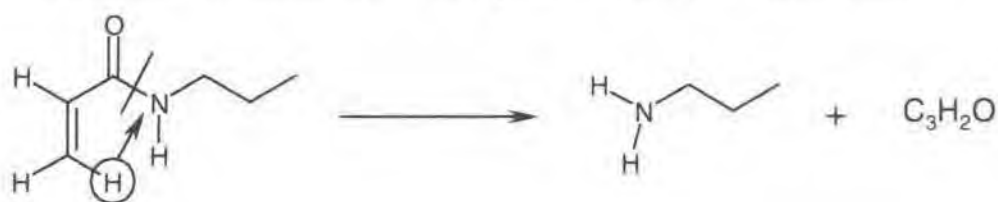


Figure 5.5. Possible fragmentation occurring in the MALDI-TOF mass spectrometer

However, the instrument and the conditions used to generate the spectra in that case were different to those used in the present work. In particular, the resolution of the spectrometer used in the earlier work was only 1 amu, whereas the present instrument has very high resolution and in favourable cases, m/z values can be determined to three places of decimal. Consequently, we can be certain that the series in question has m/z values of $[114n - 54]$ and not $[114n - 55]$. Nevertheless, this ion series is assigned to the molecular ions that have lost their focal unit. This raises the question of the process by which the fragmentation of the focal unit occurs, since it involves hydrogen transfer to the main fragment. Commonly in mass spectrometry, hydrogen transfer occurs in the direction of the oxygen bearing fragment, whereas the opposite appears to be the case here. A plausible rationalisation of the fragmentation route is shown below.



The loss of a neutral C_3H_2O fragment is surprising and may indicate some kind of enhanced stability, for example, a cyclopropanone may be lost, see below.



Oxygenated cyclopropenyl units have been postulated as contributors to mass spectrometry fragmentation pathways previously.⁴⁴ However, this rationalisation cannot be more than a speculation.

Fragmentation in MALDI is usually minimal but, in this case, we observe it quite unambiguously. Polyamides are known to fragment at the peptide link and, if this was happening randomly, the ions arising from the processes shown in *Figure 5.5* should be detected. We have discussed the fragmentation route (1) above. The ions corresponding to the fragments generated by the route (2) could not be found, which lead the author to favour the explanation provided by the route (1).

On the basis of these observations, a spreadsheet (see *Figure 5.6*) could be made listing the different peaks observed in the MALDI-TOF spectra of the samples synthesised by the aqueous polymerisation of the hydrochloride monomer. No significant peaks could be observed for DP above 15, see *Figure 5.4*.

DP (#mer)	[M + H]	[M-54 + H]	[M + Na]	[M-54 + Na]	[M + K]	[M-54 + K]
3	343.25	289.25	365.25	311.25	381.25	327.25
4	457.33	403.33	479.33	425.33	495.33	441.33
5	571.4	517.4	593.4	539.4	609.4	555.4
6	685.48	631.48	707.48	653.48	723.48	669.48
7	799.56	745.56	821.56	767.56	837.56	783.56
8	913.64	859.64	935.64	881.64	951.64	897.64
9	1027.72	973.72	1049.72	995.72	1065.72	1011.72
10	1141.8	1087.8	1163.8	1109.8	1179.8	1125.8
11	1255.88	1201.88	1277.88	1223.88	1293.88	1239.88
12	1369.96	1315.96	1391.96	1337.96	1407.96	1353.96
13	1484.04	1430.04	1506.04	1452.04	1522.04	1468.04
14	1598.12	1544.12	1620.12	1566.12	1636.12	1582.12
15	1712.2	1658.2	1734.2	1680.2	1750.2	1696.2

Figure 5.6. Spreadsheet showing m/z values for the peaks observed in the MALDI-TOF spectra of poly(amidoamine hydrochlorides) synthesised by aqueous polymerisation

In order to determine the oligomer molecular weight distribution for each sample, the relative areas of the peaks at [M + H], [M + Na] and [M + K] plus the areas of the peaks corresponding to their respective isotopes (+1 ¹³C, + 2 ¹³C, etc) were summed for each oligomer and this sum was normalised by reference to the most abundant oligomer. Thus, the integrated intensity of the set of oligomer peaks was

divided by the value for the most abundant species and multiplied by 100 to give a relative percentage for each oligomer within the distribution. In the case of the aqueous polymerisation performed in closed ampoules (see Chapter 4, case 3), the plot of these percentages against the DP values can be seen in *Figure 5.7* for the following reaction times: 1, 4, 7 and 10 days.

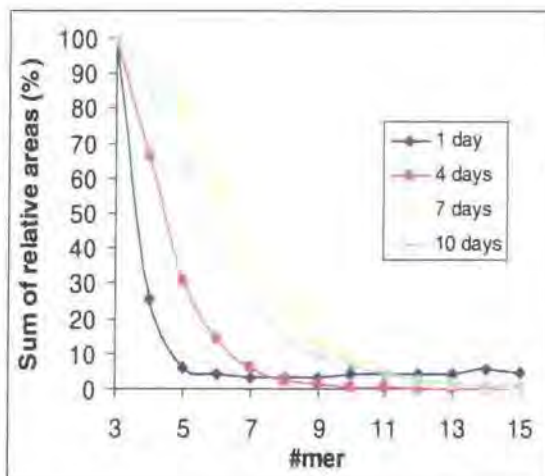


Figure 5.7. Distribution of molecular weights in some samples synthesised by aqueous polymerisation of the hydrochloride using ampoules, Chapter 4 - case 3

Figure 5.7 clearly shows that the distribution in molecular weights becomes more and more polydisperse with time, and the average of the distribution shifts to higher DP values as confirmed by the analysis of the ^1H NMR spectra for the same experiment (see Chapter 3 and case 3 in Chapter 4). However, the curve obtained after 10 days seems to contradict the trend indicated by the three other curves. Two reasons can be postulated to explain this behaviour. During the ^1H NMR analysis of this experiment, it was observed that for the sample obtained after 10 days, no signs of free radical vinyl polymerisation were found, while other spectra from the same series showed evidence of such side-reactions. Consequently, it is not really appropriate to compare the data for the 10 day sample with the data for the 1, 4 and 7 day samples. The other reason may be that the choice of matrix and solvent for this MALDI-TOF analysis does not allow high molecular weight sample to fly. The data points accumulated for this experiment allowed the author to follow the evolution of the respective percentages of each oligomers present in the sample with time, as shown in *Figure 5.8*. For clarity, only the results obtained for DP = 3 to DP = 6 are displayed.

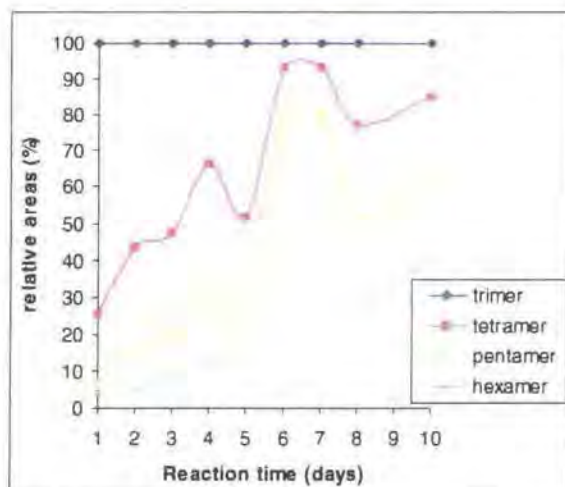


Figure 5.8. Evolution of the oligomers with time for the case 3

The trimer remains the most abundant species and the relative proportions of the other oligomers follow a similar trend, steadily increasing with time, reaching about 50-60% of the trimer value after 10 days. This confirms the general increase in polydispersity and DP observed in *Figure 5.7* and expected on the basis of theoretical prediction.²² The same analyses can be performed on the data related to the peaks corresponding to a loss of focal point by the different oligomers. As the peak expected for the [trimer - 54] (289 amu) could not be observed, it was necessary to start the analysis of the distribution from DP = 4. The resulting distribution for the oligomer minus focal point species is shown in *Figure 5.9*.

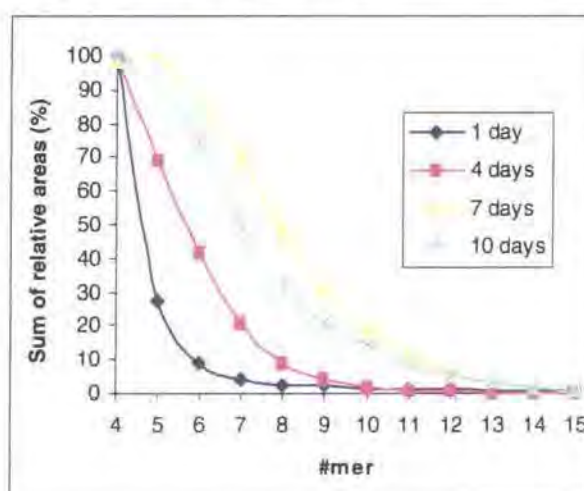


Figure 5.9. Distribution of the oligomers minus focal points for the case 3

The distributions observed after 1 and 4 days are similar to the distributions of the complete oligomers observed for identical reaction times. At 7 and 10 days, the

distributions of the oligomers minus their focal point are more polydisperse and exhibit slightly higher DP values than those of the complete oligomers at the same times. Similarly, the evolution of the oligomer minus focal point species with time shows a similar trend to that observed for the complete oligomers, compare *Figure 5.8* with *Figure 5.10*.

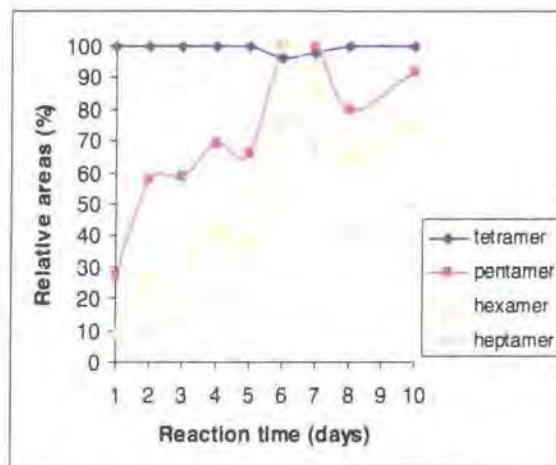


Figure 5.10. Evolution of oligomers without focus with time for the case 3

It seems from the peak intensities that there are as many if not slightly more ions corresponding to oligomers without focal units than ions corresponding to complete oligomers. This view is confirmed by the spectrum shown in *Figure 5.4*, where the most intense peaks observed correspond to the oligomers without focal units and by the following plot, *Figure 5.11*, of the distribution of the ratio of the sum of all the peaks associated with an oligomer over the sum of all the peaks associated with this oligomer plus those associated with the oligomer minus its focal point, that is $[M]/([M] + [M-f])$, where $([M] + [M-f])$ represents the total ion current associated with the peaks.

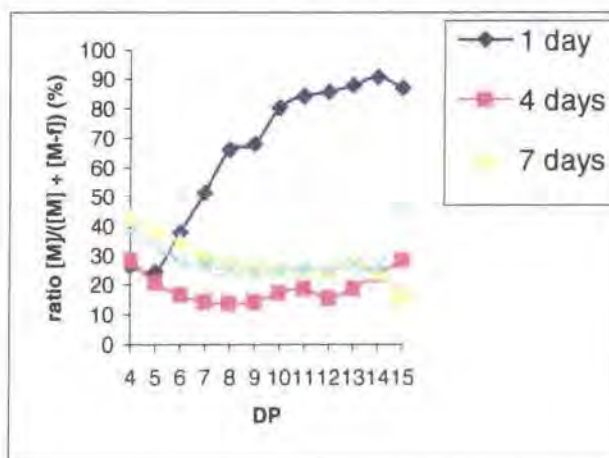


Figure 5.11. Distribution of the ratio $[M]/([M] + [M-f])$ for the case 3

For the plots corresponding to the samples obtained after 4, 7 and 10 days, the ratio of $[M]/([M] + [M-f])$ tends to decrease as DP increases in the range DP 4 to 7 and then levels off, which confirms that more than 70% of the molecules flying in the spectrometer have lost their focal points. This loss of focal unit may be an indication of the low percentage of cyclised molecules in the analysed sample. However, the plot for the 1 day sample shows an opposite trend, which is easily explained in terms of experimental error since, after one day, the amounts of oligomers with DP > 6 are very small (see *Figures 5.7* and *5.9*). An alternative way of presenting this data is to plot the evolution of the ratio *versus* time for the products from the polymerisation experiment defined as case 3 in Chapter 4. This is shown in *Figure 5.12*. In summary, the data shows that about 70% of the oligomers are flying without focal points, which can be interpreted as the fact that at least 70% of the material is not cyclised.

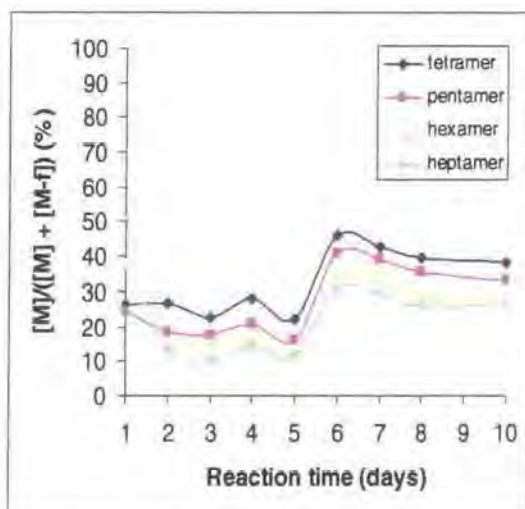


Figure 5.12. Evolution of the ratio $[M]/([M] + [M-f])$ with time for the case 3

A comparison of those graphs with those obtained for the same polymerisation performed in Carius tubes (Chapter 4, case 4) will confirm the differences already observed during the kinetic study, namely that lower DP values were obtained due to the lack of free radical polymerisation. Indeed, the plot of the distribution of the ions associated with complete oligomers after 1, 4, and 7 days, for case 4 shows a much less polydisperse distribution, hence lower DP values, compare *Figures 5.13* and *5.7*.

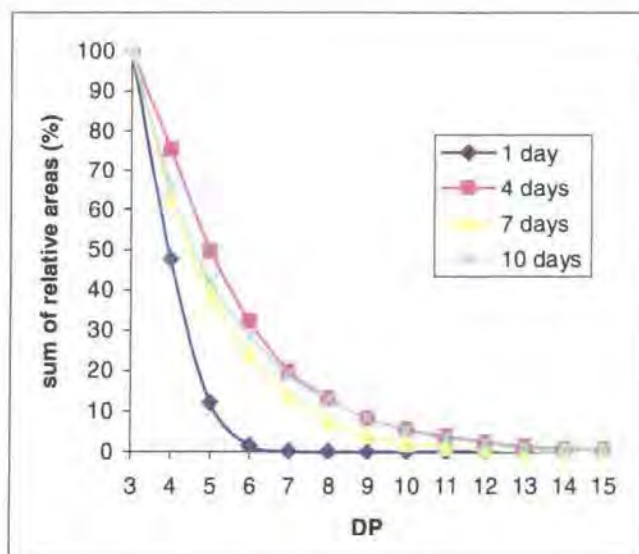


Figure 5.13. Distribution of the complete oligomers for the case 4, Chapter 4

As a consequence, the evolution of the relative proportions of oligomers with time does not happen as rapidly as was observed in case 3, compare Figures 5.14 and 5.8.

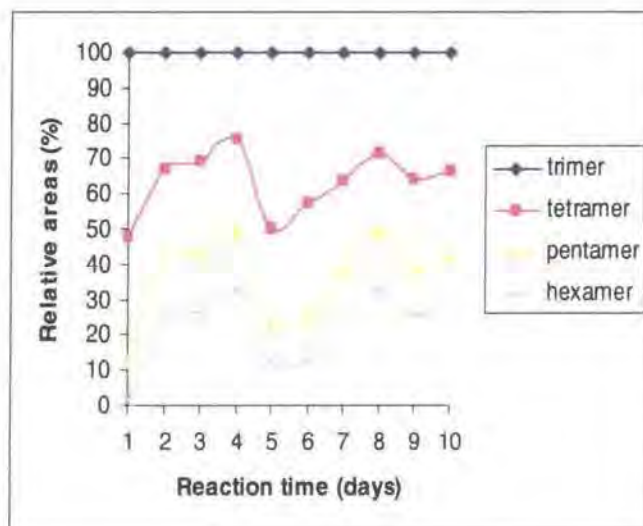


Figure 5.14. Evolution of the complete oligomers with time for the case 4

As observed for case 3, the ions associated with oligomers without focal units follow a much faster evolution of their distribution, polydispersity and DP than observed for the intact molecules, compare Figures 5.15 and 5.13. This observation once again suggests that a vast majority of the molecules fly without their focal point, which means that very little or no cyclisation occur within these systems.

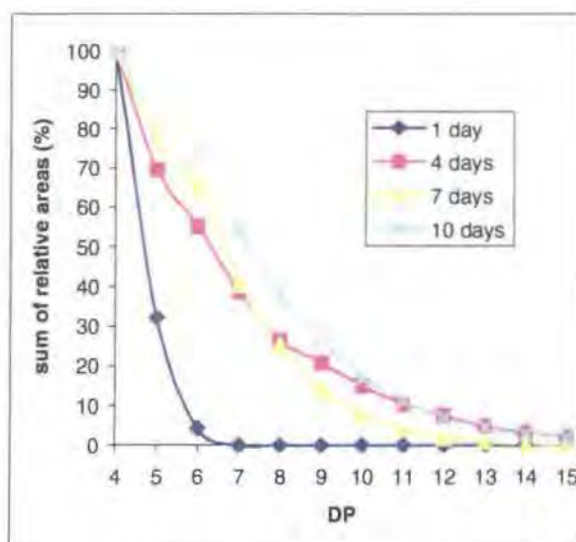


Figure 5.15. Distribution of the oligomers minus focal unit for the case 4

As established for case 3, Figure 5.16 shows a steady increase, in the abundance of the higher molecular weight oligomers with time, as expected.

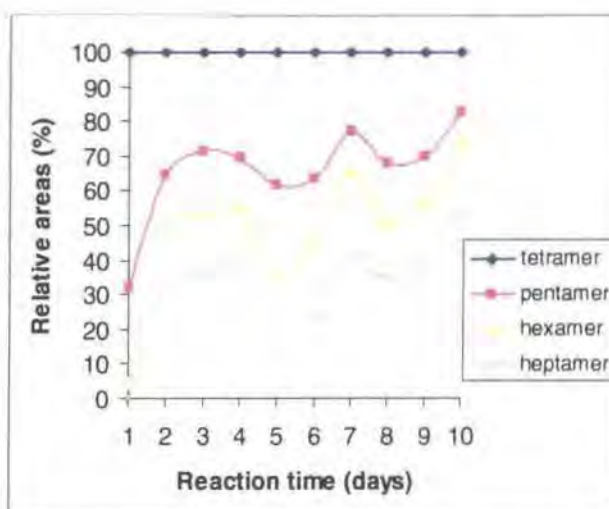


Figure 5.16. Evolution of the oligomers minus focal unit with time for the case 4

The relative abundance of oligomers minus focal unit *versus* the complete oligomers is shown in Figure 5.17, which shows that the ratio $[M]/([M] + [M-f])$ reaches a plateau value of about 30 to 50% with increasing DP, suggesting that the higher molecular weight oligomers tend to lose their focal points easily. More than 50% of the oligomers fly without focal points. The data points corresponding to the day 1 experiment have to be ignored because the abundance of ions corresponding to DP > 6 species is very low.

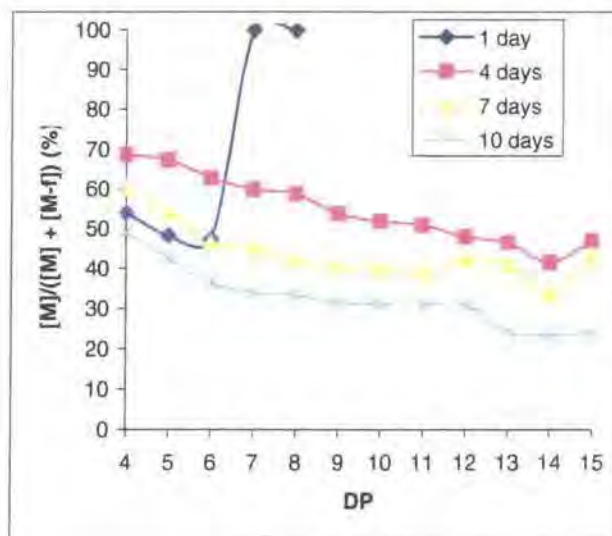


Figure 5.17. Distribution of the ratio $[M]/([M] + [M-f])$ for the case 4

The value for this ratio remains, within the experimental error, relatively constant (ca 50 ± 10 %) over time for each oligomer, see Figure 5.18.

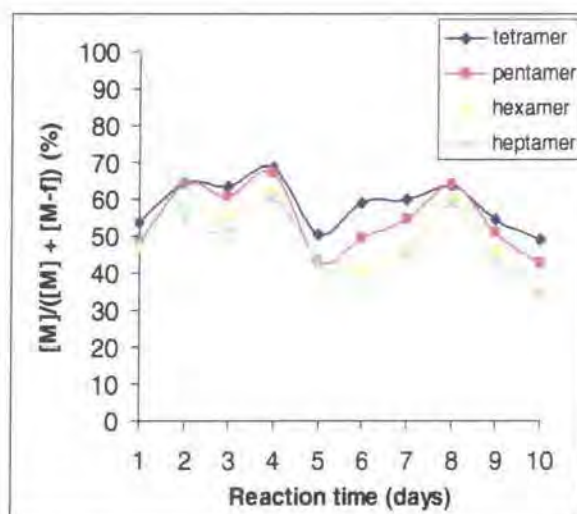


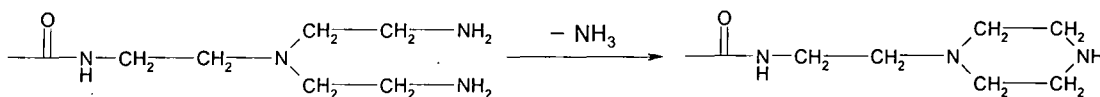
Figure 5.18. Evolution of the ratio $[M]/([M] + [M-f])$ with time for the case 4

As a conclusion for the study of the analysis of the MALDI-TOF spectra of the samples obtained by the aqueous solution polymerisation of N-acryloyl-1,2-diaminoethane hydrochloride, in ampoules closed with Teflon taps or in sealed Carius tubes, the author observed the anticipated steady growth of the DP and polydispersity of the samples with reaction time. This growth was in some cases enhanced by the formation of higher molecular weight samples by free radical polymerisation (case 3), which occurred as an unwanted side-reaction. In both cases, it was observed that more

DP	[M+H]	[M+Na]	[M+K]	[M-17]
3	343.25	365.25	381.25	325.25
4	457.33	479.33	495.33	439.33
5	571.4	593.4	609.4	553.4
6	685.48	707.48	723.48	667.48
7	799.56	821.56	837.56	781.56
8	913.64	935.64	951.64	895.64
9	1027.72	1049.72	1065.72	1009.72
10	1141.8	1163.8	1179.8	1123.8
11	1255.88	1277.88	1293.88	1237.88
12	1369.96	1391.96	1407.96	1351.96
13	1484.04	1506.04	1522.04	1466.04
14	1598.12	1620.12	1636.12	1580.12
15	1712.2	1734.2	1750.2	1694.2
16	1826.28	1848.28	1864.28	1808.28
17	1940.36	1962.36	1978.36	1922.36
18	2054.43	2076.43	2092.43	2036.43
19	2168.52	2190.52	2206.52	2150.52
20	2282.59	2304.59	2320.59	2264.59
21	2396.67	2418.67	2434.67	2378.67
22	2510.75	2532.75	2548.75	2492.75

Figure 5.20. List of peaks observed in MALDI-TOF spectra of samples synthesised by the aqueous polymerisation of *N*-acryloyl-1,2-diaminoethane

This sequence implies a loss of ammonia from a standard hyperbranched poly(amidoamine) and since these polymers have primary amine terminal groups, the formation of structural imperfections can be postulated as shown below.



Such defects could occur during the synthesis and it might reasonably be expected that the defects would be statistically distributed. A close examination of the spectra revealed that some very weak peaks corresponding to m/z values of $[114n - 34]$, that is two such defects in one oligomer, could be detected, which adds further support to this hypothesis. Similar defects have been identified in the PAMAM dendrimers produced by Tomalia¹¹, which are the “perfect” analogues of the hyperbranched polymers under consideration here.

The absence of the series of ions at m/z of $[114n - 54]$, that is loss of the focal acryloyl unit, also merits comment. The discussion in section 5.2 established that this

is a major fragmentation route and the absence of ions associated with this process implies that there is a vanishingly small concentration of focal units in these oligomers. The only explanation for this is that cyclisation occurs in the polymerisation of the free base monomer, whereas there is no evidence for cyclisation in the case of the hydrochloride salt analogues. This can be attributed to conformational effects; thus the polyelectrolyte will prefer a relatively rigid extended conformation, which will inhibit cyclisation, whereas the free base analogue is likely to have a high degree of conformational mobility, allowing cyclisation to occur, as in other conformationally mobile systems such as hyperbranched polyesters.^{45, 46}

Using the method described in section 5.2, the distribution of oligomer molecular weights could be determined for the cases 1' and 2' as described in Chapter 4. Identical oligomers molecular weight distributions (Figure 5.21) and evolutions of oligomers with time (Figure 5.22) were obtained using both experimental procedures. There is no noticeable evolution of the distribution of oligomers with time for the samples obtained after 0, 30, 60 and 90 minutes. This observation confirms the high reactivity of the free base monomer, which allows the growing oligomers to reach high DP values even at room temperature. Furthermore, cyclisation inhibits the growth of the oligomers once a certain DP value is reached and the consumption of the unreacted vinyl focal units contributes to the high DP values calculated using the ¹H NMR data and to the impossibility to determine the exact rate constant associated with the polymer growth, as described in Chapter 4.

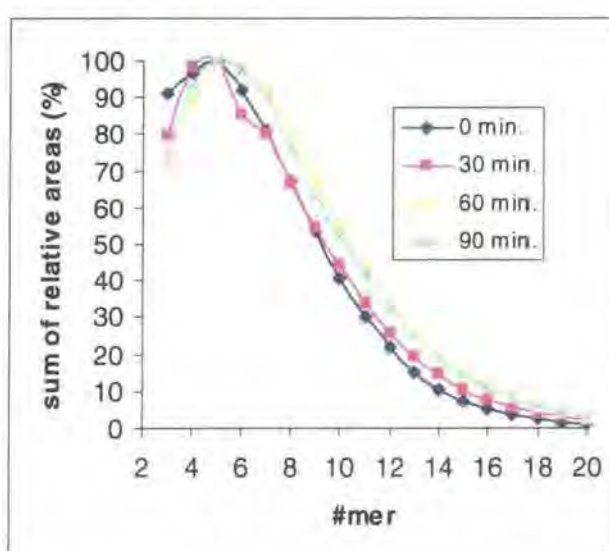


Figure 5.21. Distribution of oligomers for cases 1' and 2' (Chapter 4)

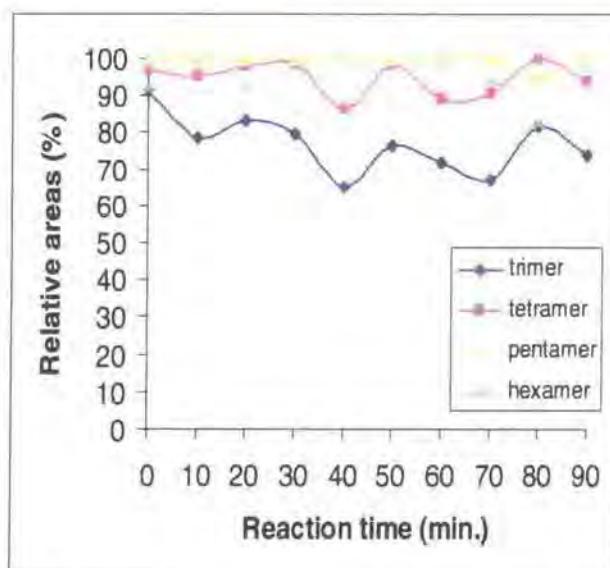


Figure 5.22. Evolution of oligomers with time for cases 1' and 2' (Chapter 4)

The analysis of the MALDI data collected for the hydrochloride polymers confirmed that the polydispersity and the value of DP increase with regard to the reaction time, as predicted by the theory. Using this technique, it was possible to establish that most oligomers still possess a focal unit, thus allowing the author to confirm that no cyclisation could be observed for these polyelectrolytes due to their relatively rigid extended conformation inhibiting cyclisation. The same study applied to the polymers synthesised using the free base monomer showed that high values of DP were achieved at the early stages of the reaction, thus confirming the high reactivity of free amino groups towards the vinyl moiety. The relative simplicity of the recorded spectra confirmed that most of these new polymers were cyclised, thus preventing further growth of the oligomers.

Chapter Six

Conclusions and suggested future work

6.1. Conclusions

Following Hobson's work³⁴, the synthesis of hyperbranched poly(amidoamine)s from the melt polymerisation of N-acryloyl-1,2-diaminoethane hydrochloride was successfully reproduced and gave materials exhibiting a degree of branching equal to 1 and high DP values after only 4 hours at 210°C. However, the purity of the monomer was responsible for the synthesis of a new product that was postulated to be a linear polymer generated by the solid state polymerisation of the crystalline monomer. The difficulty in reproducing the melt experiment as often as desired lead to the investigation of the polymerisation of the monomer in aqueous solution at 100°C, which provided a very reproducible method for obtaining hyperbranched materials, provided that the formation of side-products by free radical polymerisation was prevented by using Carius tubes sealed under vacuum as polymerisation reactors. However, only modest degrees of conversion were reached after relatively long reaction times (10 days). The study of the kinetics of polymer growth for this experiment allowed the precise determination of the rate constant associated with the growth of the oligomers. The characterisation of the samples using MALDI-TOF mass spectrometry confirmed the theoretically predicted increase of polydispersity and DP with time and proved that no cyclisation could be observed for these polymers.

In order to decrease the reaction times required for the production of high molecular weight samples, the free base monomer, N-acryloyl-1,2-diaminoethane was synthesised but could only be analysed in dilute solution and not as a pure dry compound because of the high reactivity of the free amino groups, which, as concentration increases, leads to high degrees of conversion in less than two hours. The analysis of the samples by MALDI-TOF mass spectrometry showed strong signs of cyclisation, which made the kinetic analysis and the rate constant determination irrelevant.

6.2. Suggested future work

In order to achieve GPC analysis in chloroform or THF of the various water-soluble oligomers and polymers, the modification of the hydrophilic surface groups

could be achieved by suitable reactions with long hydrophobic aliphatic molecules that would modify the overall solubility of the macromolecules, making the GPC analysis easier to perform on these compounds.

Another potential work would consist in the slow dropwise addition of an aqueous solution of the free base monomer to a dilute solution of multifunctional core (triamine, for example). This has been proved to allow better control over the polydispersity and the molecular weight, providing a cheap route to pseudo-dendrimers.

Finally, new topologies could be synthesised, using controlled processes involving the unreacted vinyl focal point, such as controlled radical polymerisation. It would then be possible to build new supramolecular architectures.

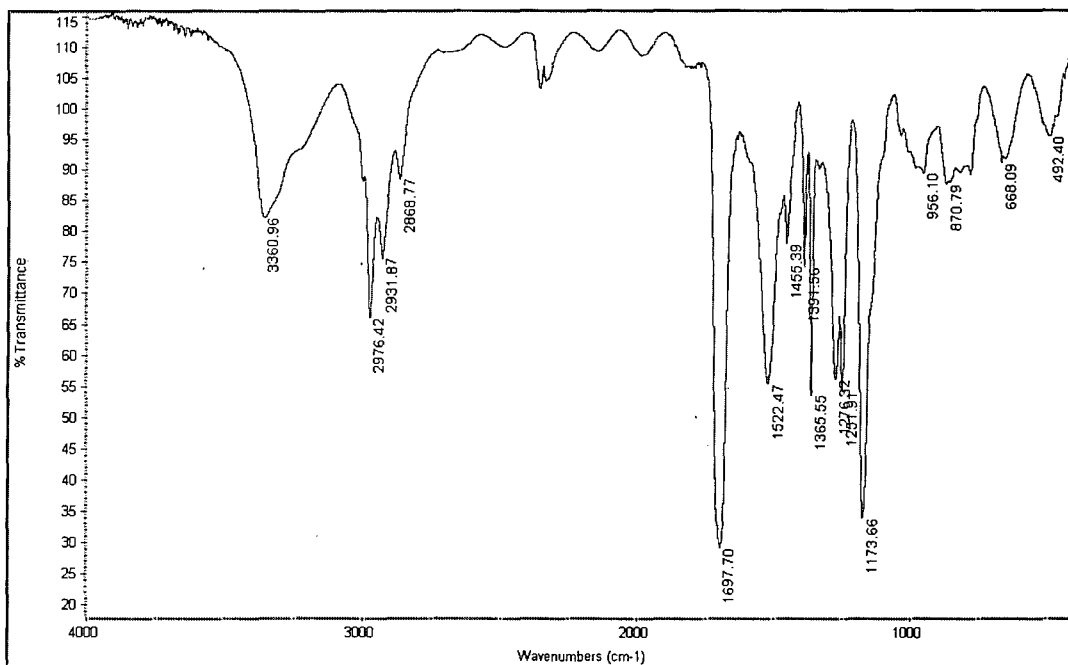
References

- (1). Tomalia, D.A., *Macromol. Symp.*, 1996, **101**, 243
- (2). Tomalia, D.A., Baker, H., Dewald, J., Hall, M., Kallos, G., Martin, S., Roeck, J., Ryder, J., Smith, P., *Polymer Journal*, 1985, **17(1)**, 117
- (3). Farin, D., Avnir, D., *Angew. Chem. Int. Ed. Engl.*, 1991, **30(10)**, 1379
- (4). De Gennes, P.G., Hervert, H., *J. Phys. Lett.*, 1982, **44**, L-351
- (5). Lescanec, R.L., Muthukumar, M., *Macromolecules*, 1990, **23**, 2280
- (6). Naylor, A.M., Goddard, W.A., *J. Am Chem. Soc.*, 1989, **111**, 2339
- (7). Fréchet, J.M.J., Hawker, C.J., *Comprehensive Polymer Science*, 2nd Suppl., Pergamon Press, Oxford, 1996, 71
- (8). Denkewalter, R.G., Kolc, J., Lukasavage, W.J., *U. S. Patent*, 1981, 4 289 872
- (9). Tomalia, D.A., Hall, M., Hedstrand, D.M., *J. Am Chem. Soc.*, 1987, **109**, 1601
- (10). Tomalia, D.A., Durst, H.D., *Topics in Current Chemistry*, 1993, **165**, 197
- (11). Hummelen, J.C., Van Dogen, J.L.J., Meijer, E.W., *Chem. Eur. J.*, 1997, **3(9)**, 1489
- (12). Wooley, K.L., Hawker, C.J., Fréchet, J.M.J., *J. Chem. Soc. Perkin Trans. 1*, 1991, 1059
- (13). Hawker, C.J., Wooley, K.L., Fréchet, J.M.J., *Polymer Preprints*, 1991, **32(3)**, 623
- (14). Wooley, K.L., Hawker, C.J., Fréchet, J.M.J., *J. Am Chem. Soc.*, 1993, **115(24)**, 11496
- (15). Hawker, C.J., Fréchet, J.M.J., *J. Chem. Soc. Chem. Commun.*, 1990, 1010
- (16). Miller, T.M., Neenan, T.X., Zayas, R., Bair, H.E., *J. Am Chem. Soc.*, 1992, **114**, 1018
- (17). Mekelburger, H.B., Jaworek, W., Vögtle, F., *Angew. Chem. Int. Ed. Engl.*, 1992, **31(12)**, 1571
- (18). Jansen, J.F.G.A., De Brabander Van Den Berg, E.M.M., Meijer, E.W., *Science*, 1994, **266**, 1226
- (19). Hawker, C.J., Wooley, K.L., Fréchet, J.M.J., *J. Am Chem. Soc.*, 1993, **115**, 4375
- (20). Jin, R., Aida, T., Inoue, S., *J. Chem. Soc. Chem. Commun.*, 1993, 1260
- (21). Dykes, G.M., Brierley, L.J., Smith, D.K., McGrail, P.T., Seeley, G.J., *Chem. Eur. J.*, 2001, **7(21)**, 4730
- (22). Flory, P.J., *Principles of Polymer Chemistry*, Cornell University Press, 1953, Chapter 9

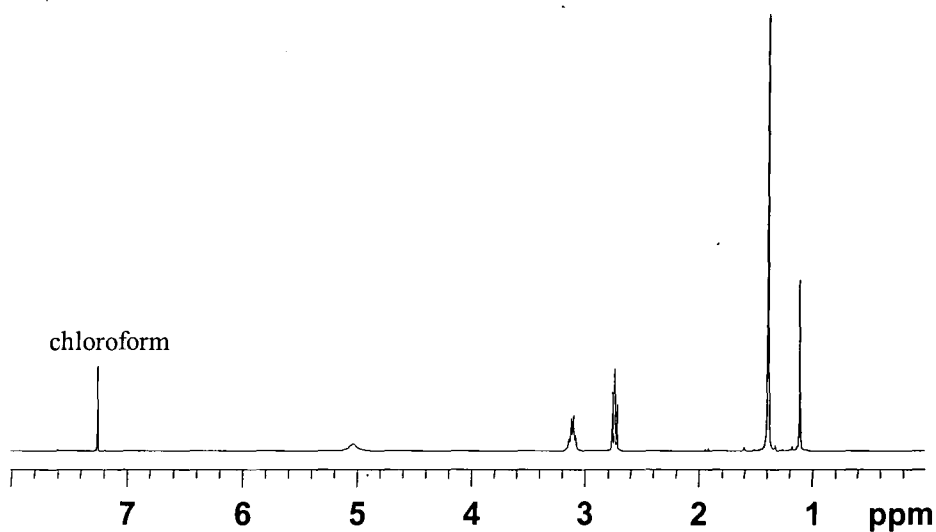
- (23). Hult, A., Johansson, M., Malmström, E., *Advances in Polymer Science*, 1999, **143**, 3
- (24). Kim, Y.H., Webster, O.W., *J. Am Chem. Soc.*, 1990, **112**, 4592
- (25). Kim, Y.H., Webster, O.W., *Macromolecules*, 1992, **25**, 5561
- (26). Kim, Y.H., Beckerbauer, R., *Macromolecules*, 1994, **27**, 1968
- (27). Kim, Y.H., *J. Polym. Sci.: A: Polym. Chem.*, 1998, **36**, 1685
- (28). Hawker, C.J., Lee, R., Fréchet, J.M.J., *J. Am Chem. Soc.*, 1991, **113**, 4583
- (29). Holter, D., Frey, H., *Acta Polymerica*, 1997, **48**, 295
- (30). Hult, A., Johansson, M., Malmström, E., *Macromol. Symp.*, 1995, **98**, 1159
- (31). Malmström, E., Johansson, M., Hult, A., *Macromolecules*, 1995, **28**, 1698
- (32). Malmström, E., Hawker, C.J., Johansson, M., Hult, A., *Polym. Mat. Sci. Eng.*, 1997, **77**, 151
- (33). Feast, W.J., Stainton, N.M., *J. Mater. Chem.*, 1995, **5**, 405
- (34). Hobson, L.J., Feast, W.J., *Polymer*, 1999, **40**, 1279
- (35). Hawker, C.J., Fréchet, J.M.J., Grubbs, R.B., Dao, J., *J. Am Chem. Soc.*, 1995, **117**, 10763
- (36). Gaynor, S.G., Matyjaszewski, S.Z., *Macromolecules*, 1996, **29**, 1079
- (37). Suzuki, M., Li, A., Saegusa, T., *Macromolecules*, 1992, **25**, 7071
- (38). Hawker, C.J., Chu, F., *Macromolecules*, 1996, **29**, 4370
- (39). Hobson, L.J., Kenwright, A.M., Feast, W.J., *Proc. American Chemical Society, Polymeric Materials Science and Engineering Meeting, Las Vegas, NV*, 1997, **77**, 220
- (40). Hobson, L.J., Kenwright, A.M., Feast, W.J., *J. Chem. Soc. Chem. Commun.*, 1997, 1877
- (41). Personal communication, W. J. Feast.
- (42). Cotter, R.J., *Time of Flight Mass Spectrometry*, American Chemical Society, Washington D.C., 1997
- (43). Montaudo, G., Garozzo, D., Puglisi, C., Samperi, F., *Macromolecules*, 1995, **28**, 7983
- (44). Budzikiewicz, H., Djerassi, C., Williams, D.H., *Mass spectrometry of organic compounds*, Holden-Day, INC, 1967, Chapter 4, page 210
- (45). Parker, D., Feast, W.J., *Macromolecules*, 2001, **34**, 2048
- (46). Parker, D., Feast, W.J., *Macromolecules*, 2001, **34**, 5792



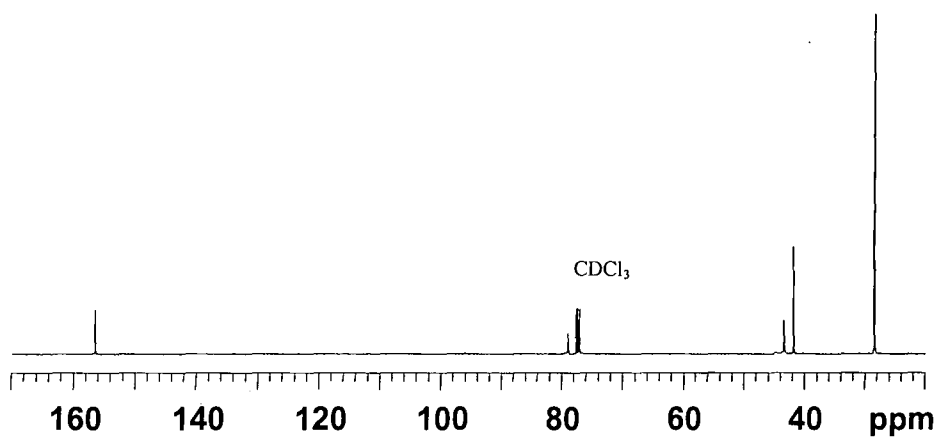
Appendix



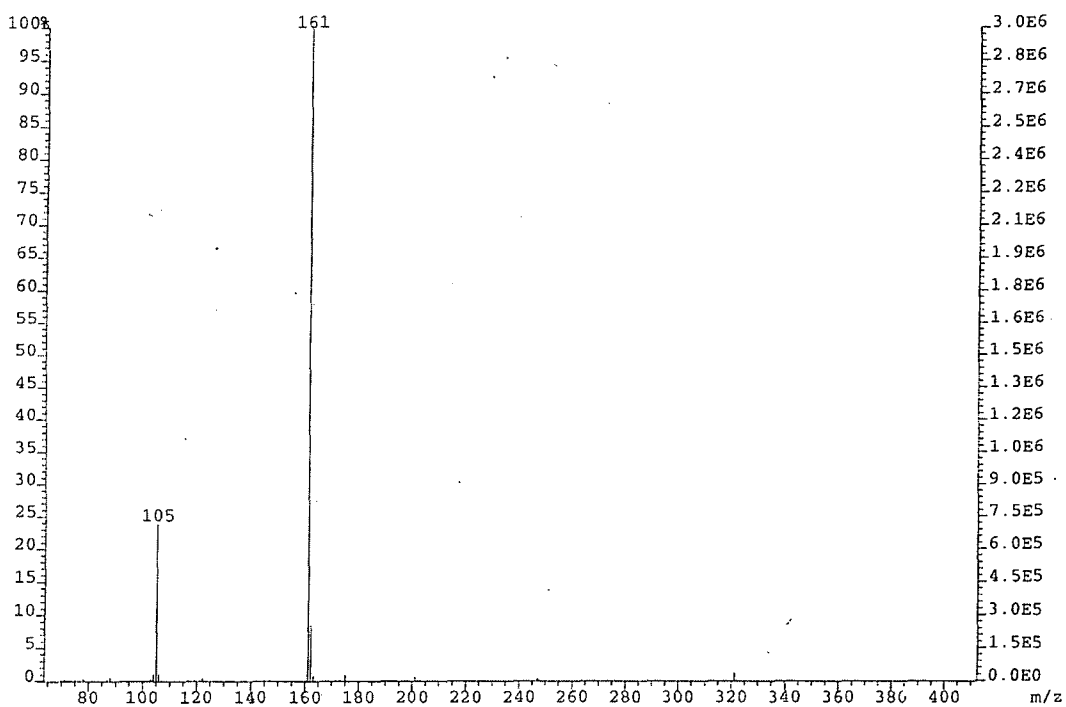
Appendix 1.1. FTIR spectrum (liquid film on KBr) of *N*-*tert*-butoxycarbonyl-1,2-diaminoethane



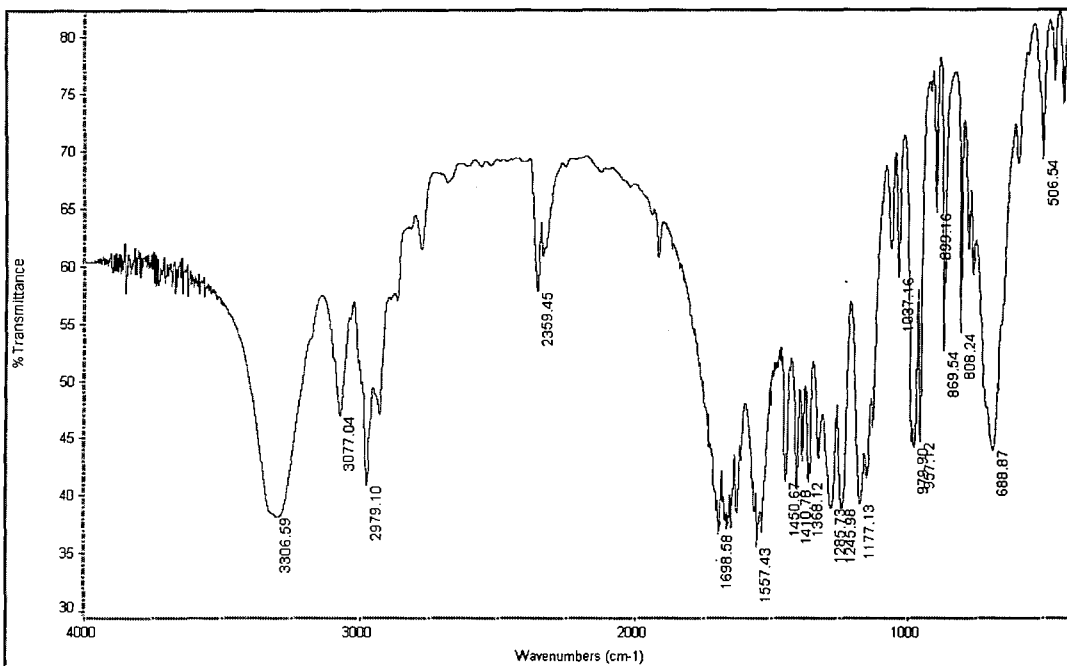
Appendix 1.2. ¹H NMR spectrum (300 MHz) in CDCl₃ of *N*-*tert*-butoxycarbonyl-1,2-diaminoethane



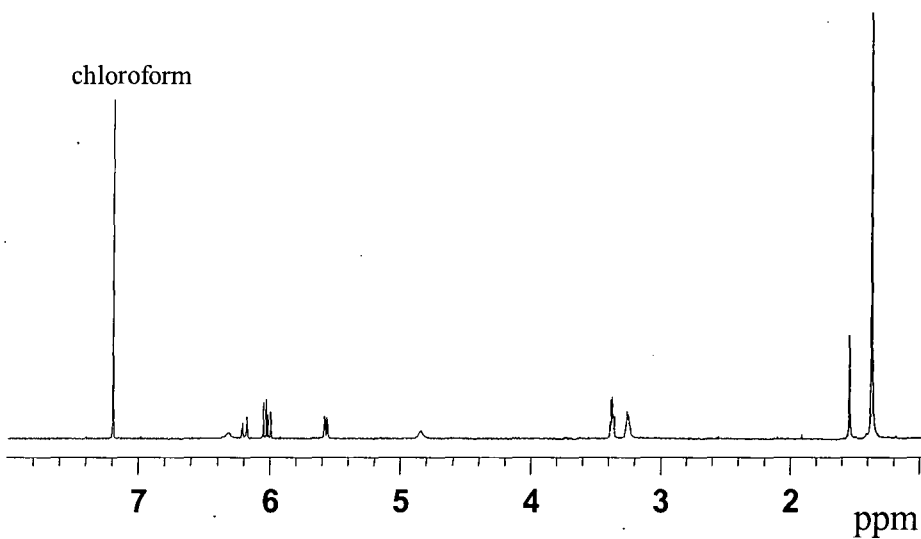
Appendix 1.3. ^{13}C NMR spectrum (125 MHz) in CDCl_3 of *N*-*tert*-butoxycarbonyl-1,2-diaminoethane



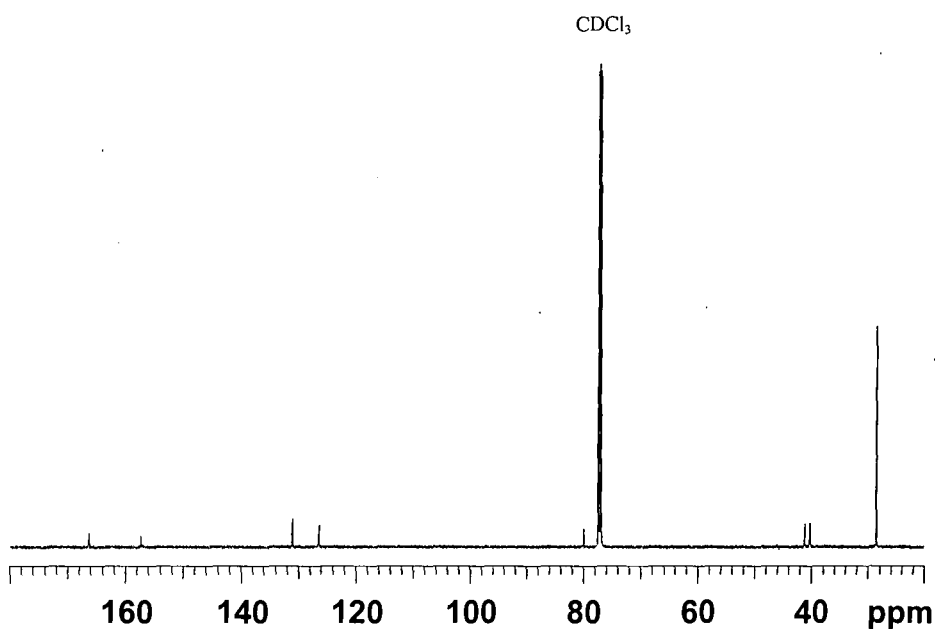
Appendix 1.4. Mass spectrum (CI^+) of *N*-*tert*-butoxycarbonyl-1,2-diaminoethane



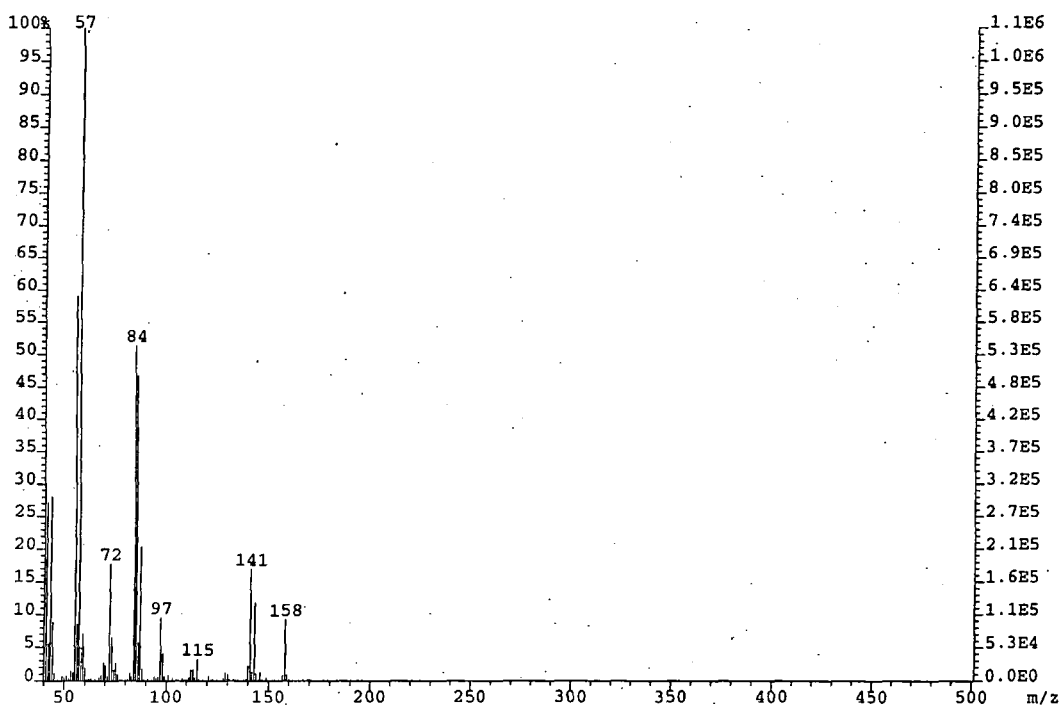
Appendix 1.5. FTIR spectrum (KBr disc) of *N*-*tert*-butoxycarbonyl-*N'*-acryloyl-1,2-diaminoethane



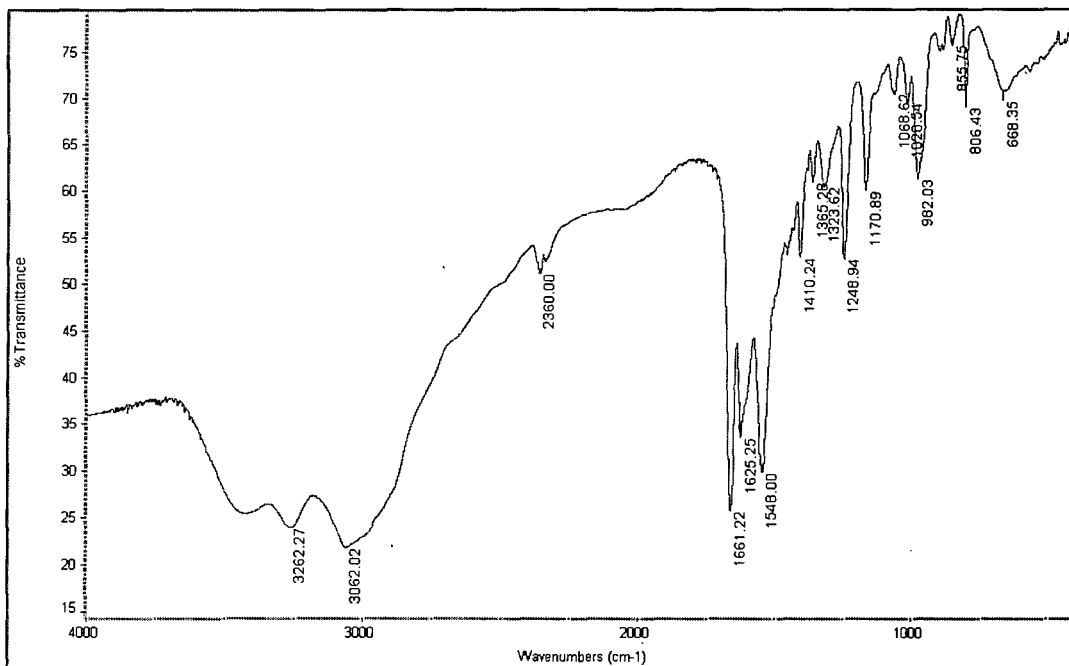
Appendix 1.6. ¹H NMR spectrum (500 MHz) in CDCl₃ of *N*-*tert*-butoxycarbonyl-*N'*-acryloyl-1,2-diaminoethane



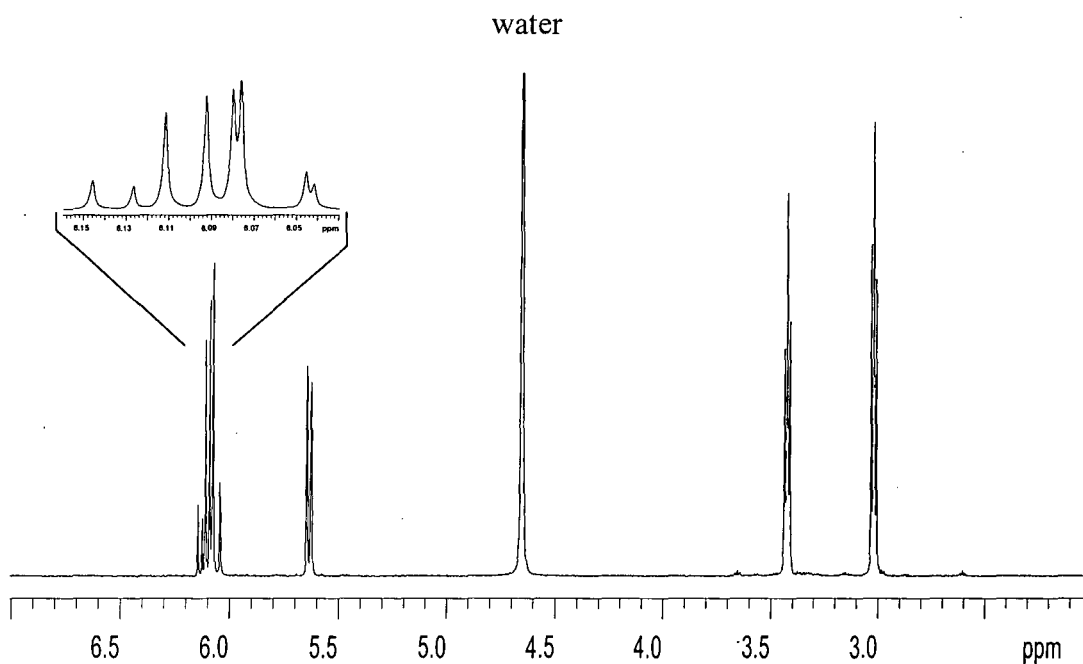
Appendix 1.7. ¹³C NMR spectrum (125 MHz) in CDCl₃ of *N*-*tert*-butoxycarbonyl-*N*'-acryloyl-1,2-diaminoethane



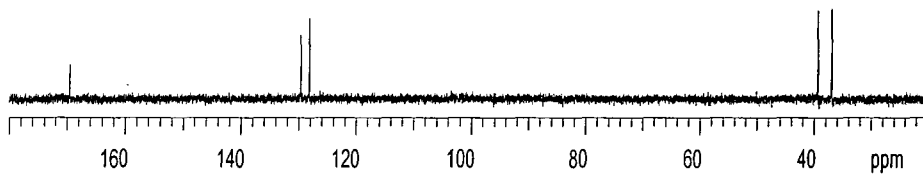
Appendix 1.8. Mass spectrum (EI+) of *N*-*tert*-butoxycarbonyl-*N*'-acryloyl-1,2-diaminoethane



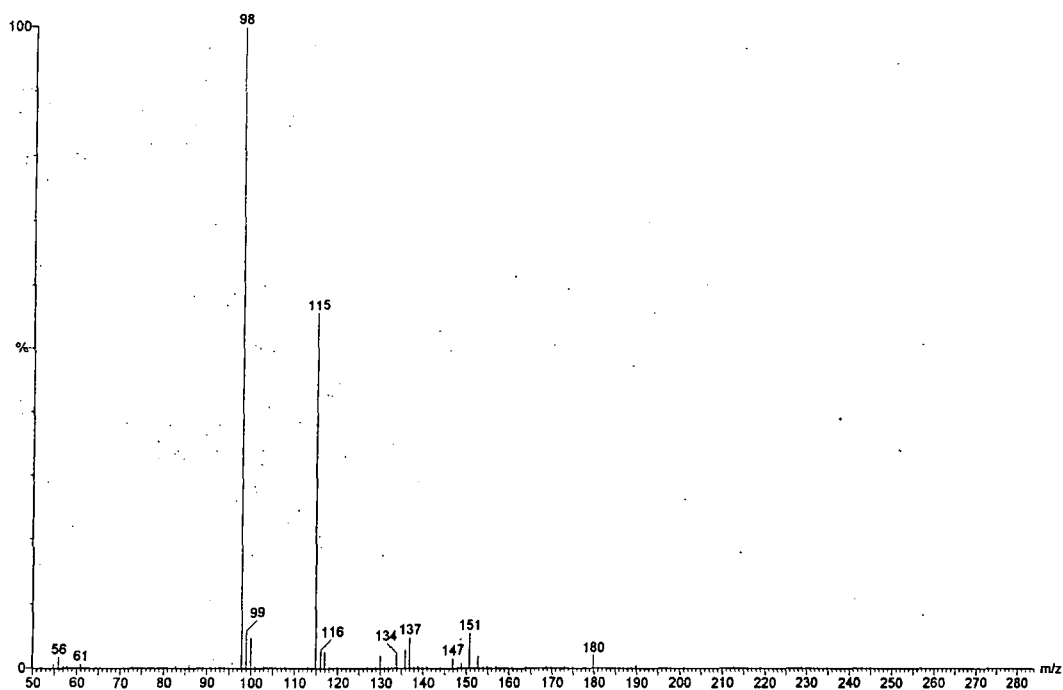
Appendix 1.9. FTIR spectrum (KBr disc) of N-acryloyl-1,2-diaminoethane hydrochloride



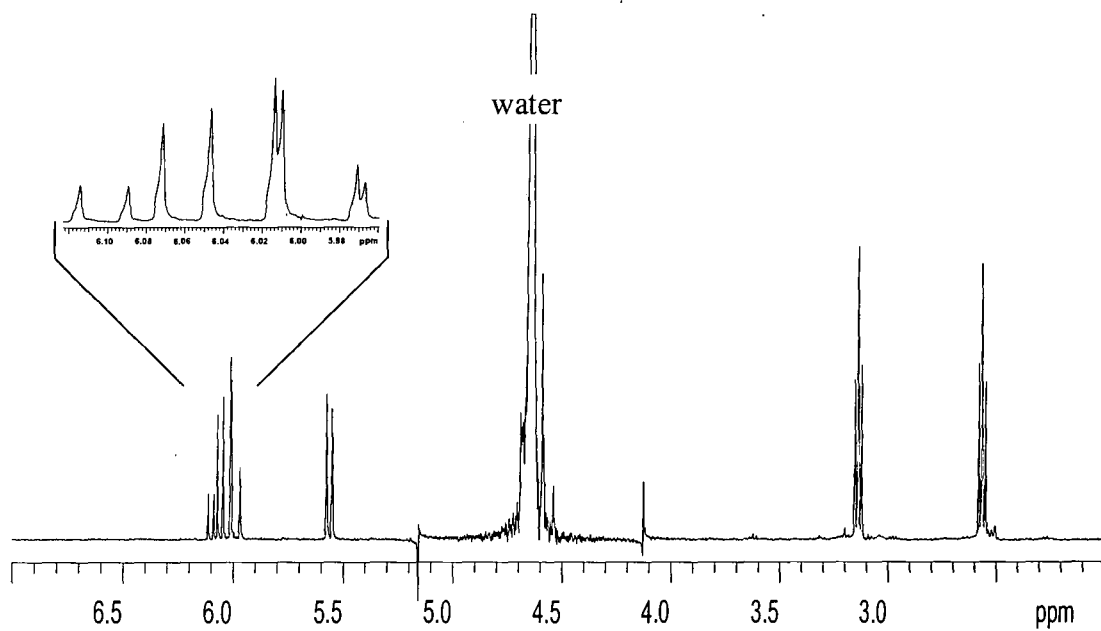
Appendix 1.10. ^1H NMR spectrum (500 MHz) in D_2O of N-acryloyl-1,2-diaminoethane hydrochloride



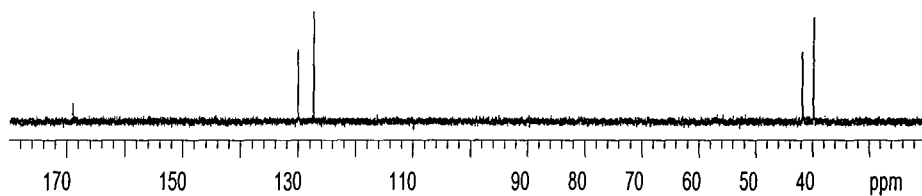
Appendix 1.11. ^{13}C NMR spectrum (125 MHz) in D_2O of N-acryloyl-1,2-diaminoethane hydrochloride



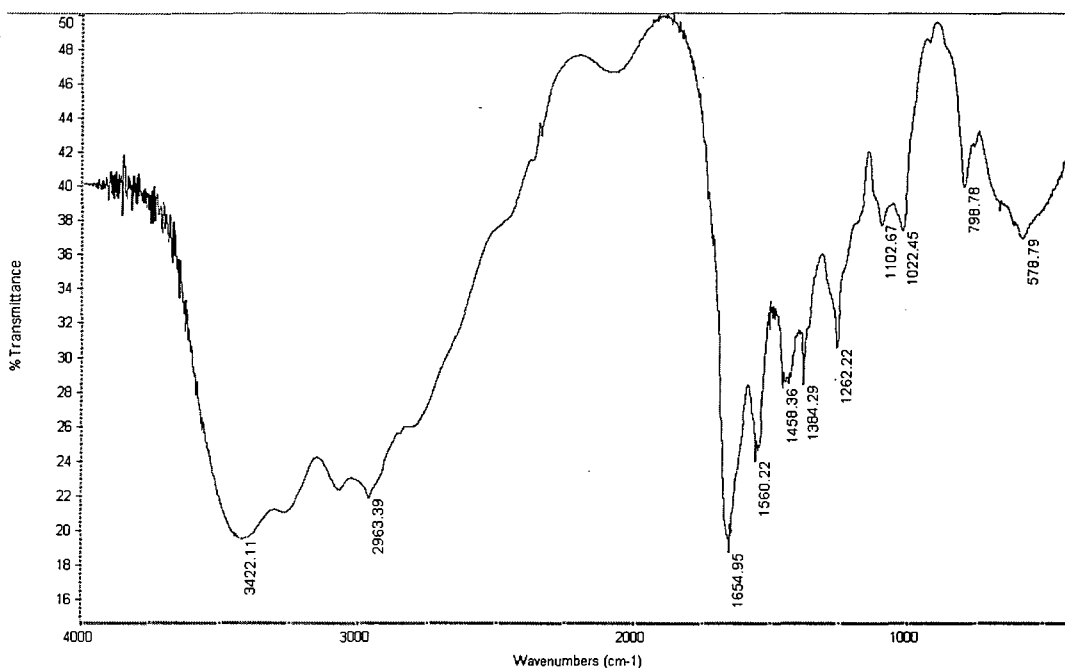
Appendix 1.12. Mass spectrum (ES+) of N-acryloyl-1,2-diaminoethane hydrochloride



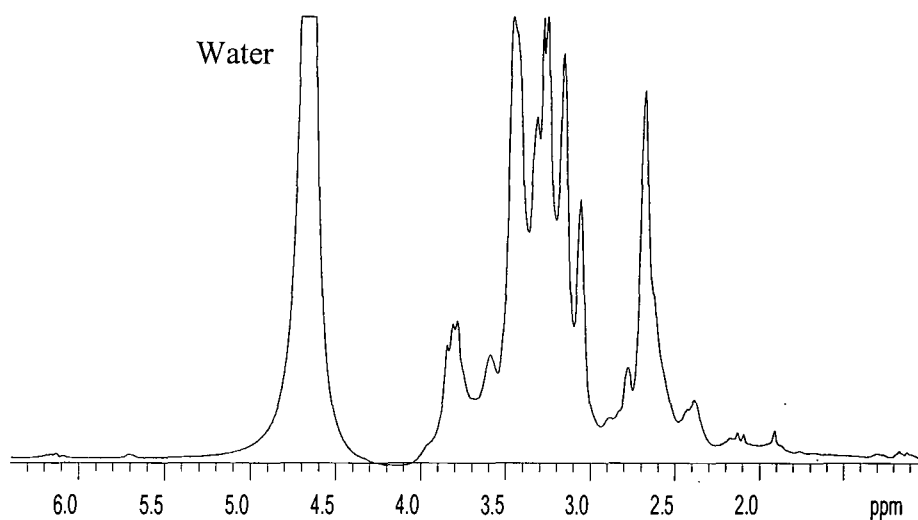
Appendix 1.13. ^1H NMR spectrum (400 MHz) in D_2O of N-acryloyl-1,2-diaminoethane



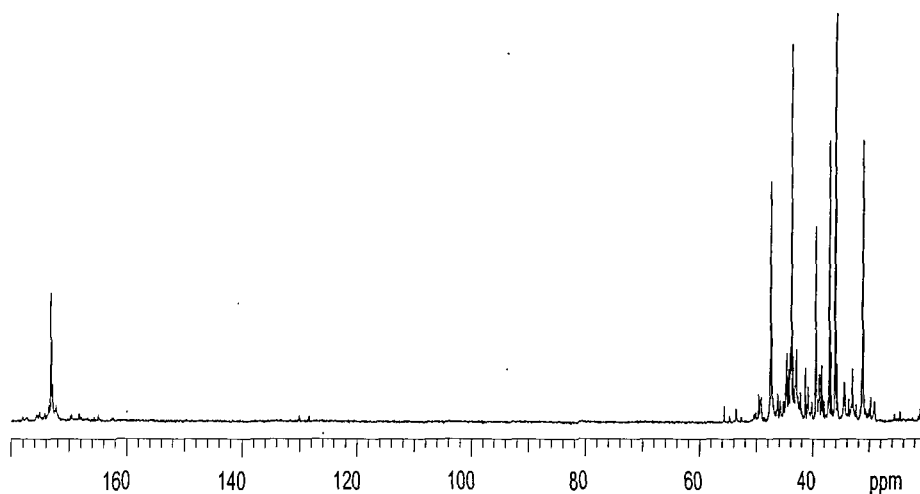
Appendix 1.14. ^{13}C NMR spectrum (100 MHz) in D_2O of N-acryloyl-1,2-diaminoethane



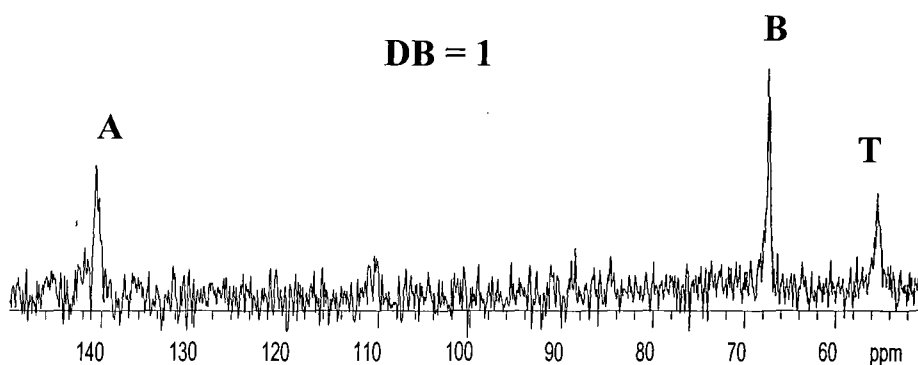
Appendix 2.1. FTIR spectrum (KBr disc) of a hyperbranched polymer (DP = 188) obtained by melt polymerisation of N-acryloyl-1,2-diaminoethane hydrochloride



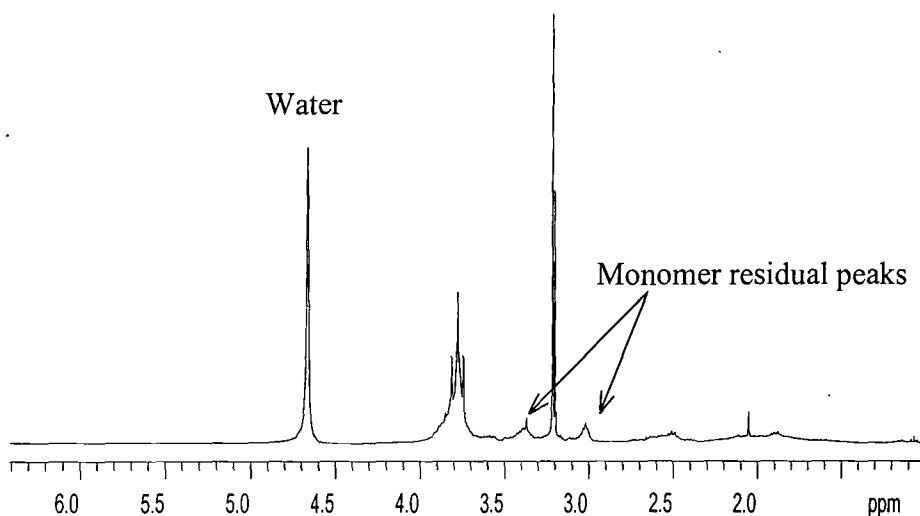
Appendix 2.2. ¹H NMR spectrum (400 MHz) in D₂O of a hyperbranched polymer (DP = 188) obtained by melt polymerisation of N-acryloyl-1,2-diaminoethane hydrochloride



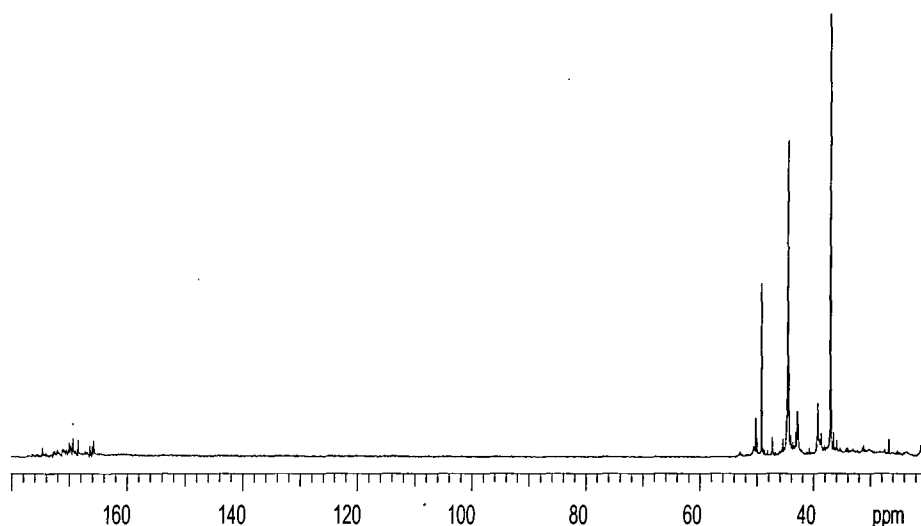
Appendix 2.3. ^{13}C NMR spectrum (100 MHz) in D_2O of a hyperbranched polymer (DP = 188) obtained by melt polymerisation of N-acryloyl-1,2-diaminoethane hydrochloride



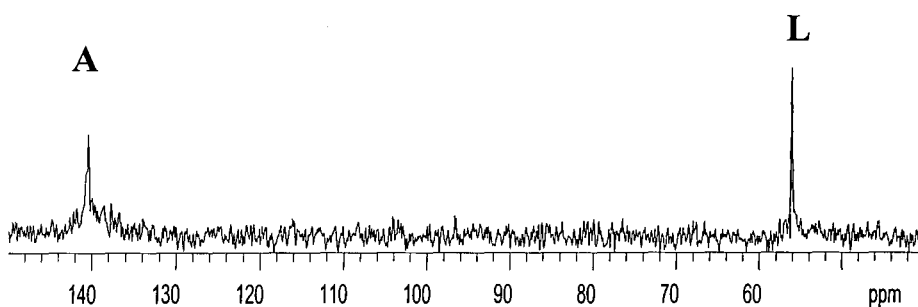
Appendix 2.4. ^{15}N NMR spectrum (40 MHz) in D_2O of a hyperbranched polymer (DP = 188) obtained by melt polymerisation of N-acryloyl-1,2-diaminoethane hydrochloride



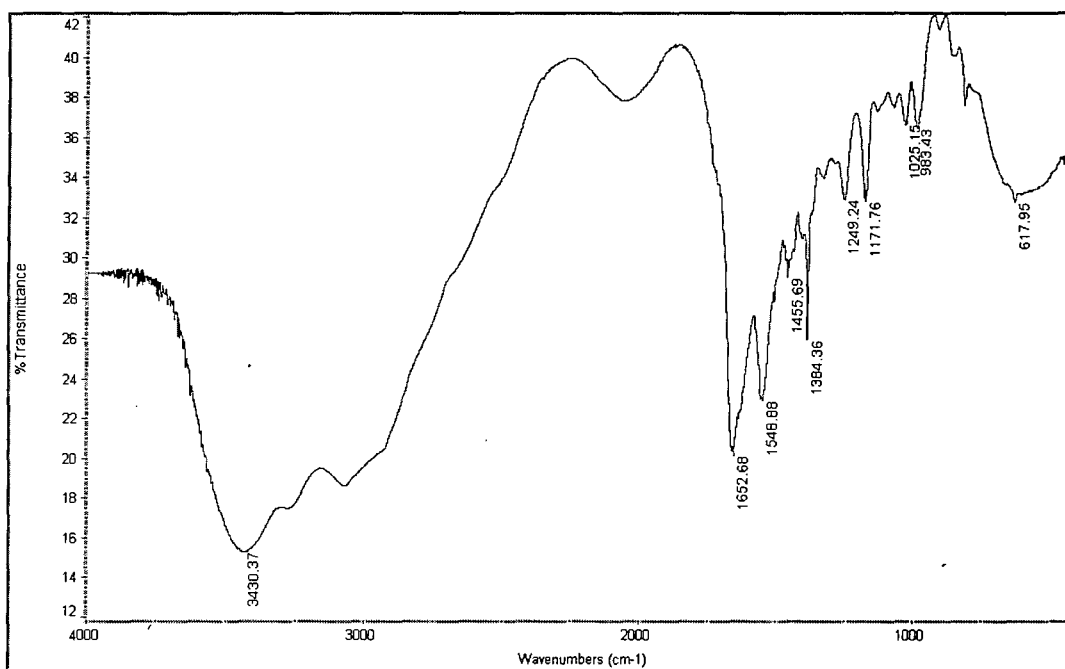
Appendix 2.5. ^1H NMR spectrum (400 MHz) in D_2O of the product of the thermal solid state conversion of N-acryloyl-1,2-diaminoethane hydrochloride into a new product of unknown structure (see discussion 3.3.1, page 48)



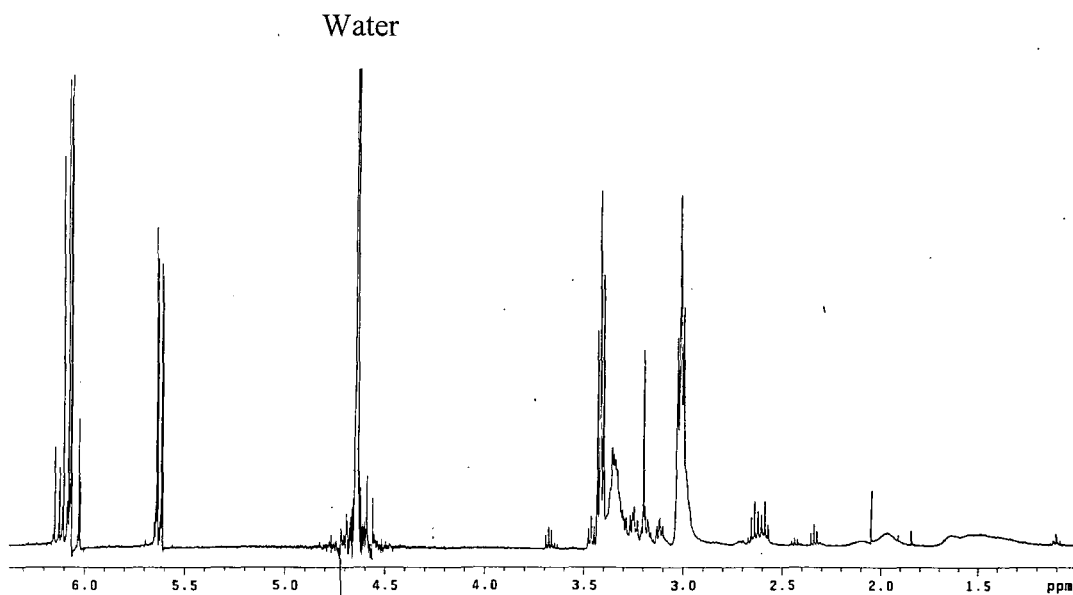
Appendix 2.6. ^{13}C NMR spectrum (100 MHz) in D_2O of the product of the thermal solid state conversion of N-acryloyl-1,2-diaminoethane hydrochloride into a new product of unknown structure



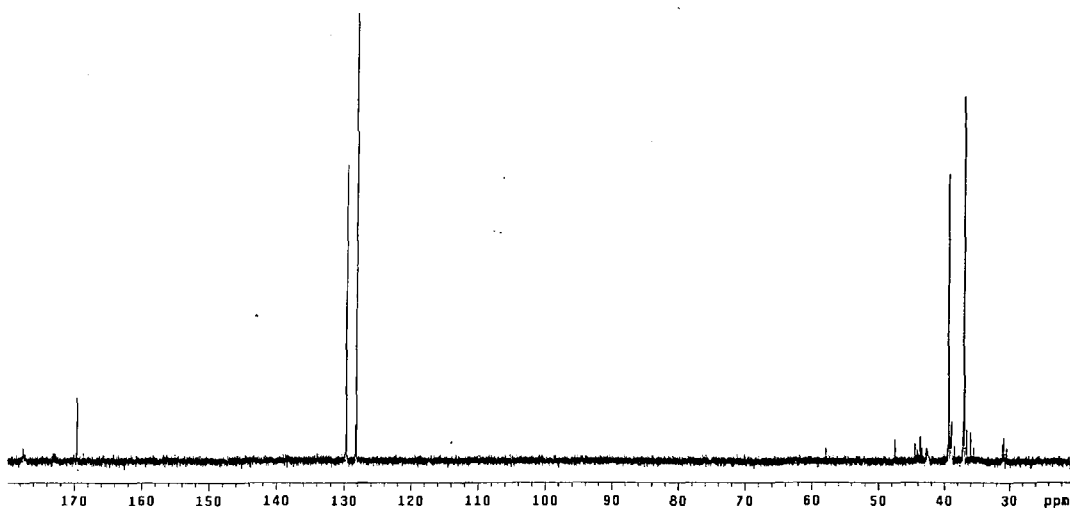
Appendix 2.7. ^{15}N NMR spectrum (40 MHz) in D_2O of the product of the thermal solid state conversion of N-acryloyl-1,2-diaminoethane hydrochloride into a new product of unknown structure



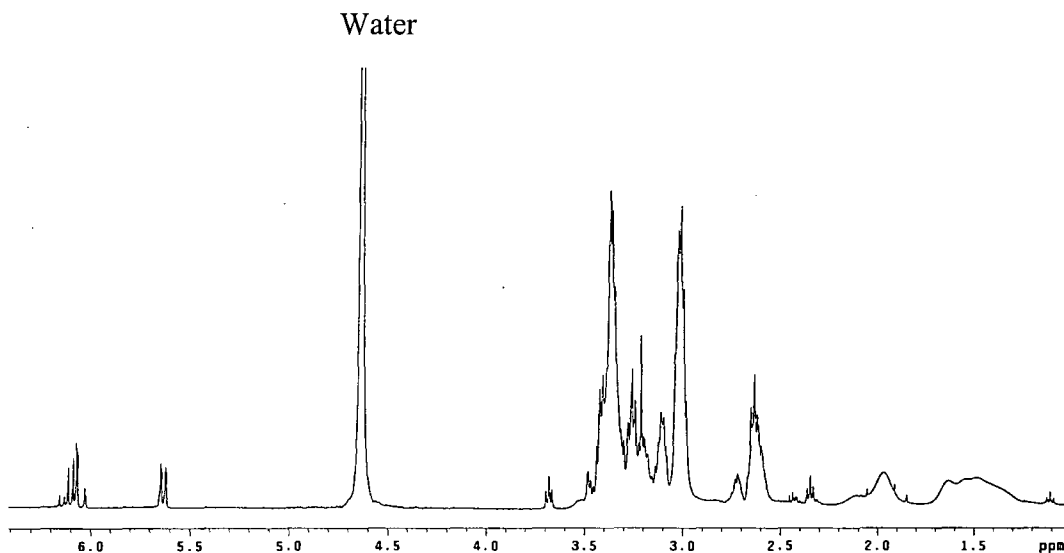
Appendix 2.8. FTIR spectrum (KBr disc) of a dimer (DP = 2) obtained by aqueous solution polymerisation of N-acryloyl-1,2-diaminoethane hydrochloride in an ampoule after 1 day



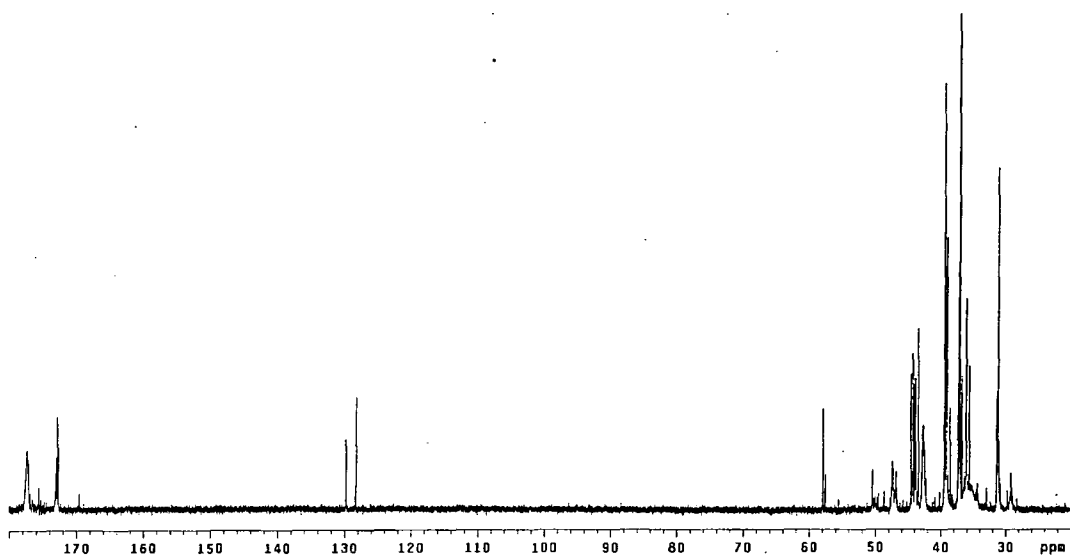
Appendix 2.9. ¹H NMR spectrum (400 MHz) in D₂O of a dimer (DP = 2) obtained by polymerisation in aqueous solution of N-acryloyl-1,2-diaminoethane hydrochloride in an ampoule after 1 day



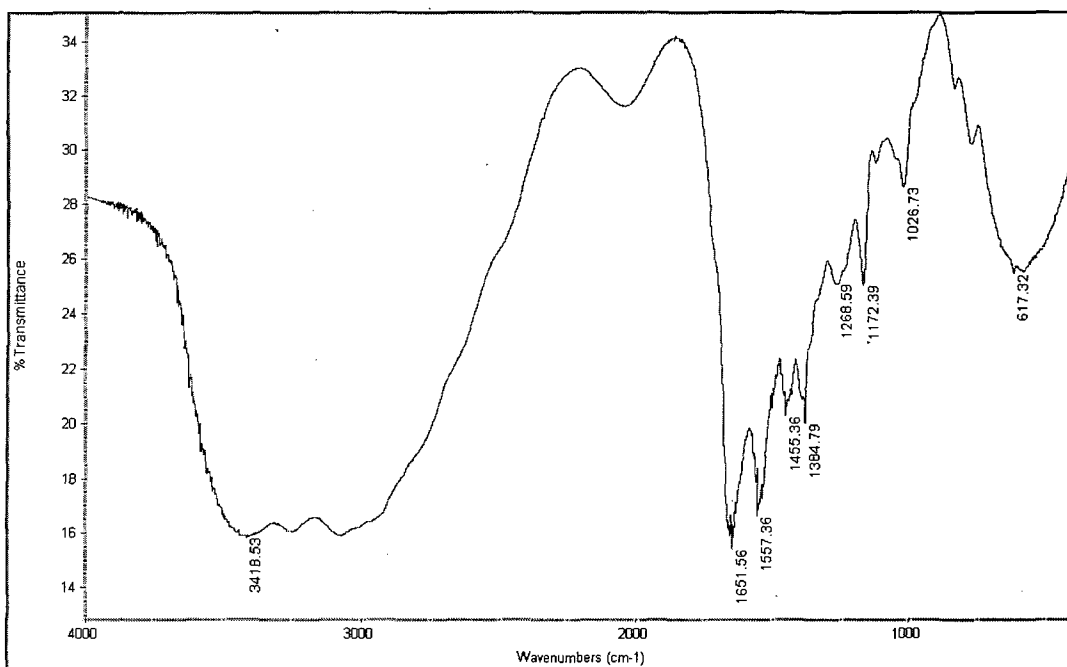
Appendix 2.10. ¹³C NMR spectrum (100 MHz) in D₂O of a dimer (DP = 2) obtained by polymerisation in aqueous solution of N-acryloyl-1,2-diaminoethane hydrochloride in an ampoule after 1 day



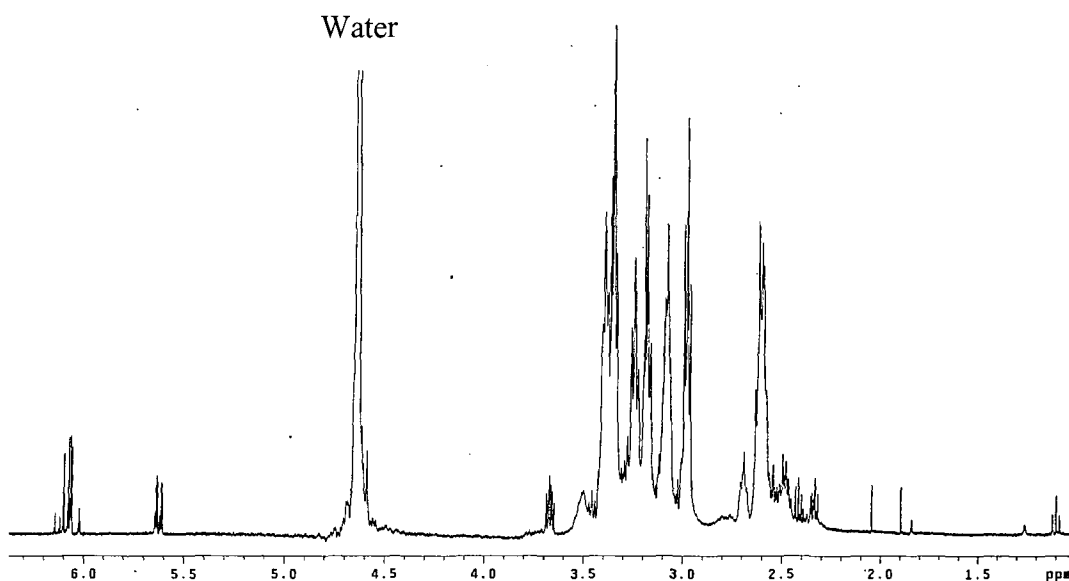
Appendix 2.11. ^1H NMR spectrum (400 MHz) in D_2O of a hyperbranched polymer (DP = 15) obtained by polymerisation in aqueous solution of N-acryloyl-1,2-diaminoethane hydrochloride in an ampoule after 5 days



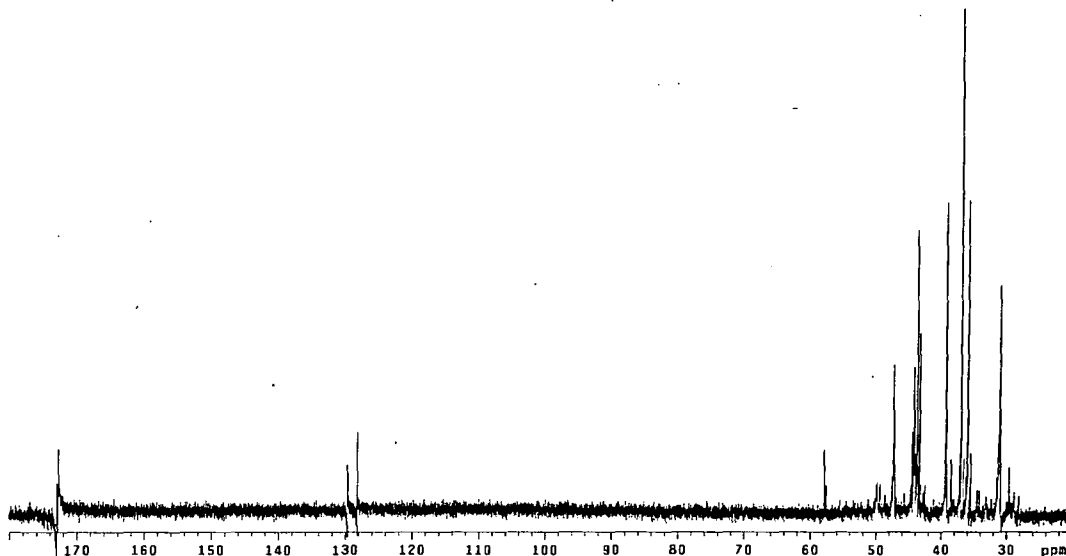
Appendix 2.12. ^{13}C NMR spectrum (100 MHz) in D_2O of a hyperbranched polymer (DP = 15) obtained by polymerisation in aqueous solution of N-acryloyl-1,2-diaminoethane hydrochloride in an ampoule after 5 days



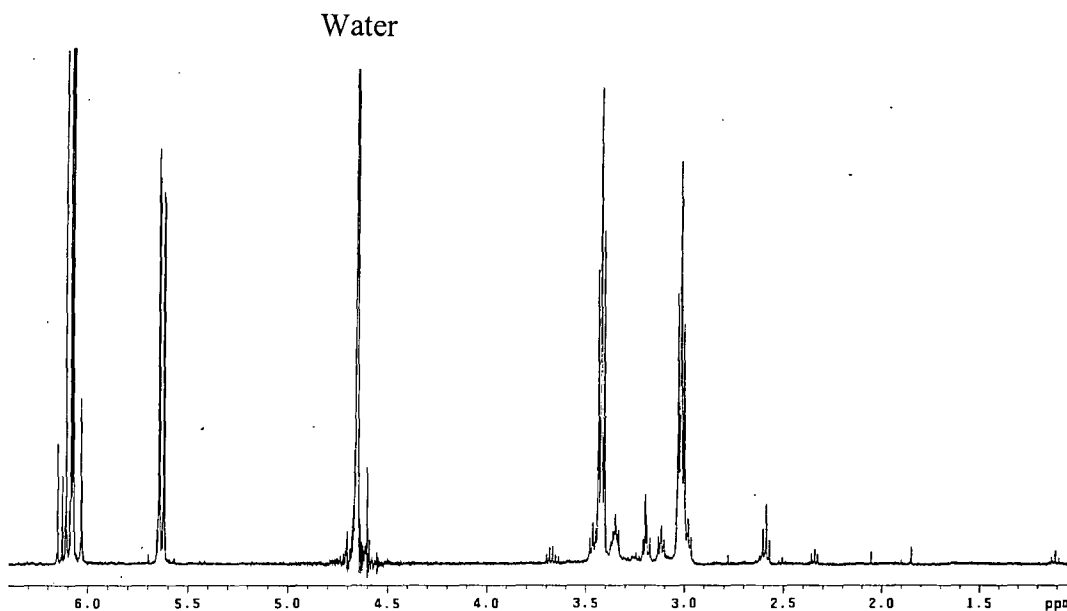
Appendix 2.13. FTIR spectrum (KBr disc) of a hyperbranched polymer (DP = 23) obtained by aqueous solution polymerisation of N-acryloyl-1,2-diaminoethane hydrochloride in an ampoule after 10 days



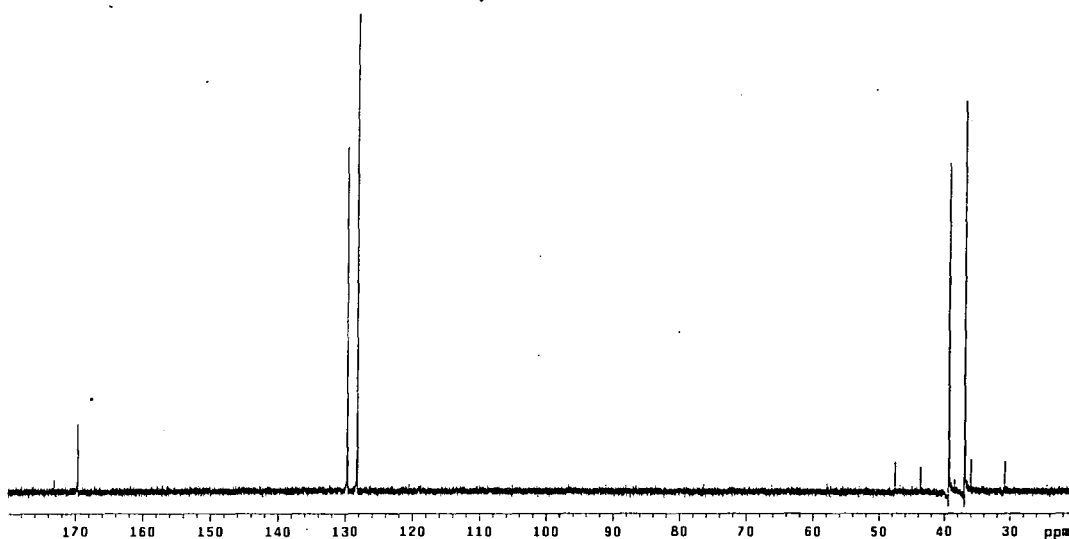
Appendix 2.14. ¹H NMR spectrum (400 MHz) in D₂O of a hyperbranched polymer (DP = 23) obtained by polymerisation in aqueous solution of N-acryloyl-1,2-diaminoethane hydrochloride in an ampoule after 10 days



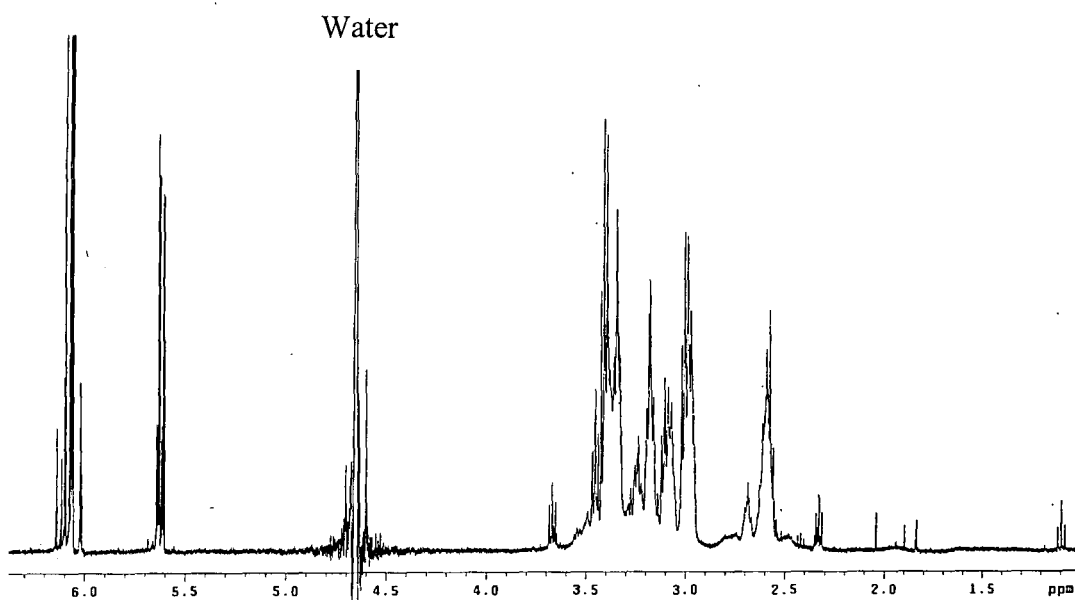
Appendix 2.15. ^{13}C NMR spectrum (100 MHz) in D_2O of a hyperbranched polymer (DP = 23) obtained by polymerisation in aqueous solution of N-acryloyl-1,2-diaminoethane hydrochloride in an ampoule after 10 days



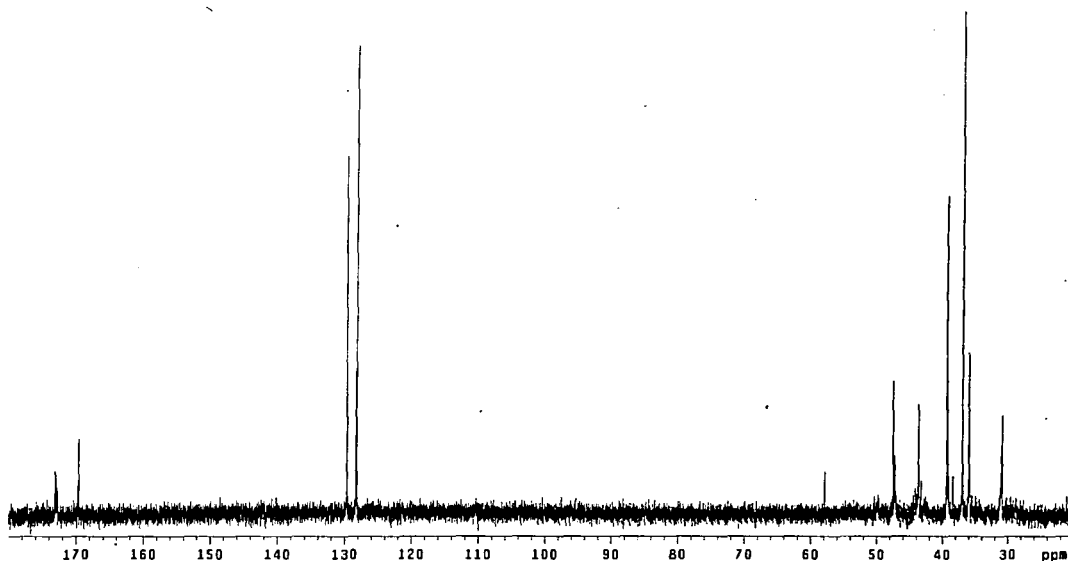
Appendix 2.16. ^1H NMR spectrum (400 MHz) in D_2O of an oligomer (DP = 1.3) obtained by polymerisation in aqueous solution of N-acryloyl-1,2-diaminoethane hydrochloride in a Carius tube after 1 day



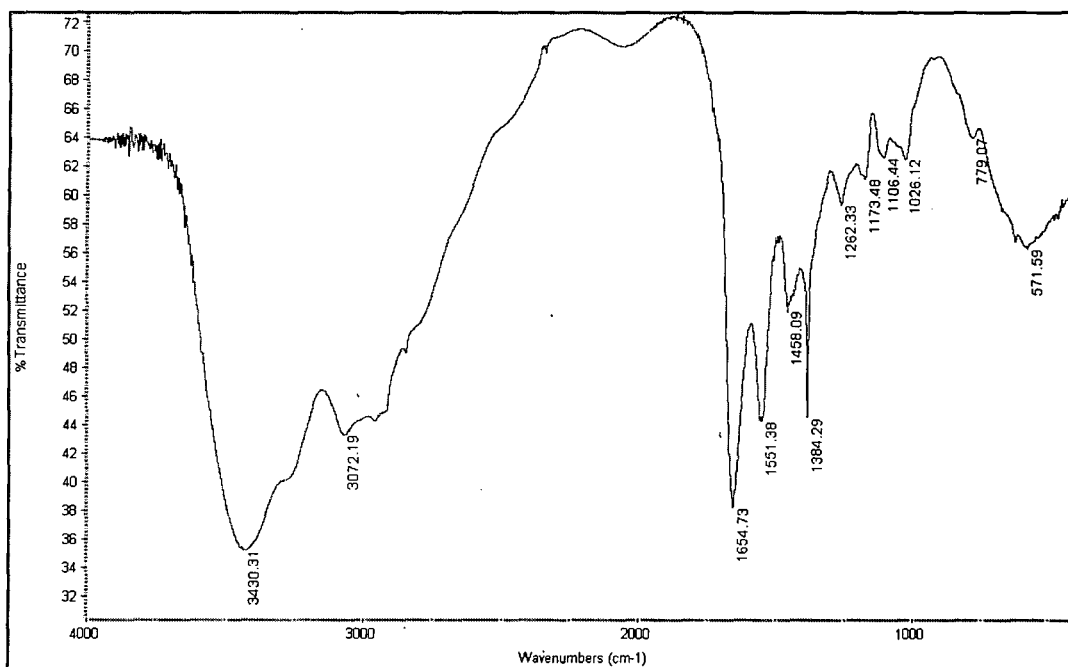
Appendix 2.17. ^{13}C NMR spectrum (100 MHz) in D_2O of an oligomer (DP = 1.3) obtained by polymerisation in aqueous solution of N-acryloyl-1,2-diaminoethane hydrochloride in a Carius tube after 1 day



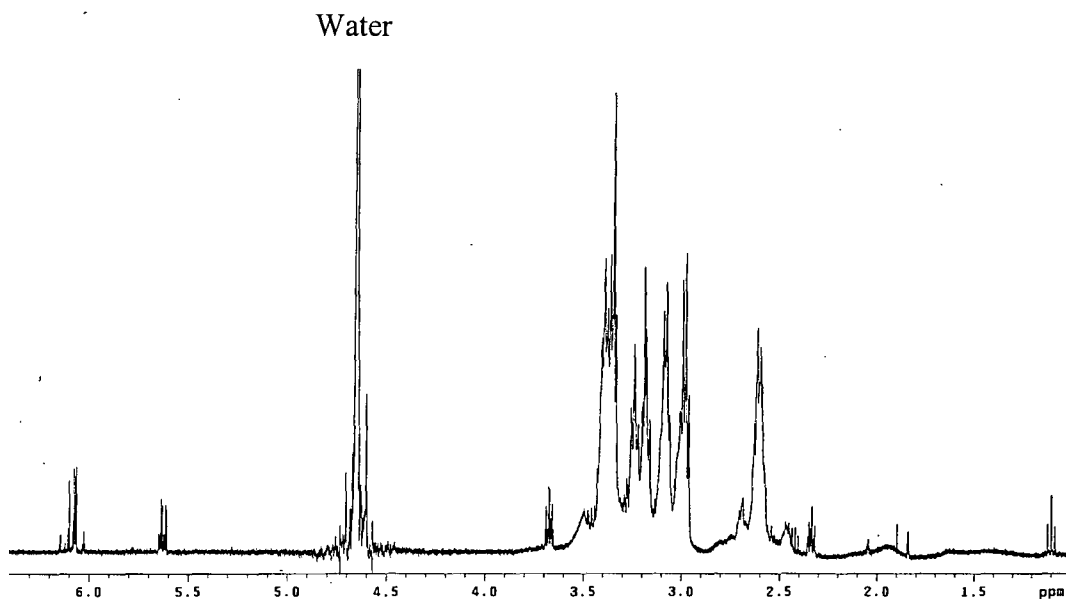
Appendix 2.18. ^1H NMR spectrum (400 MHz) in D_2O of an oligomer (DP = 3.3) obtained by polymerisation in aqueous solution of N-acryloyl-1,2-diaminoethane hydrochloride in a Carius tube after 5 days



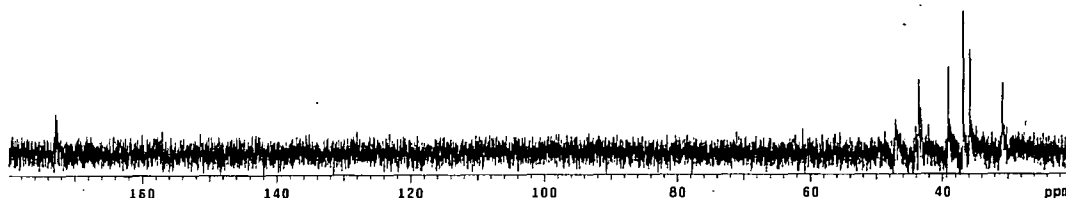
Appendix 2.19. ^{13}C NMR spectrum (100 MHz) in D_2O of an oligomer (DP = 3.3) obtained by polymerisation in aqueous solution of N-acryloyl-1,2-diaminoethane hydrochloride in a Carius tube after 5 days



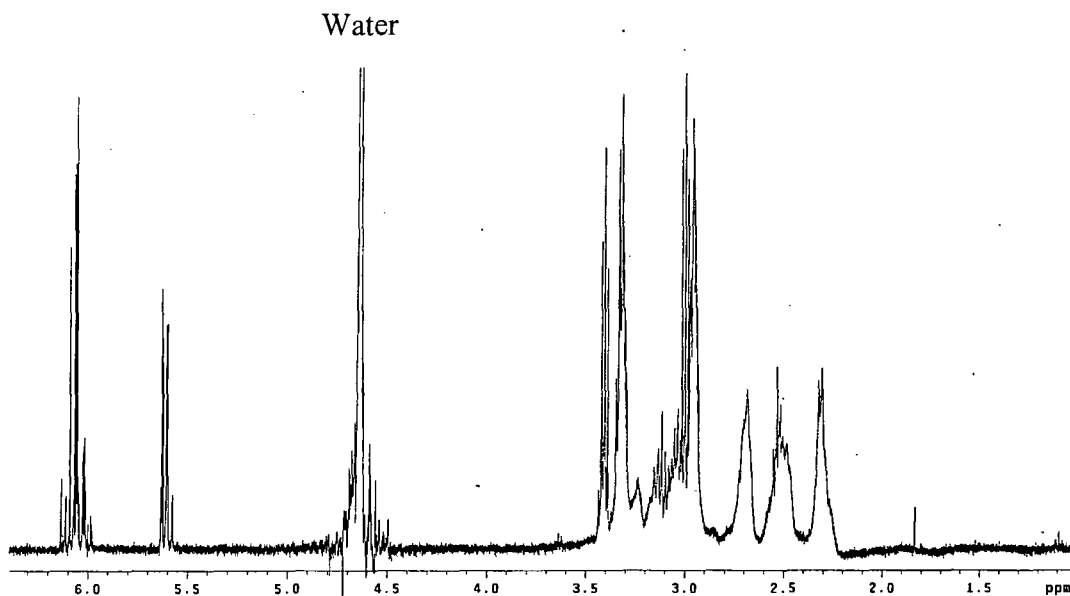
Appendix 2.20. FTIR spectrum (KBr disc) of a hyperbranched polymer (DP = 22) obtained by aqueous solution polymerisation of N-acryloyl-1,2-diaminoethane hydrochloride in a Carius tube after 10 days



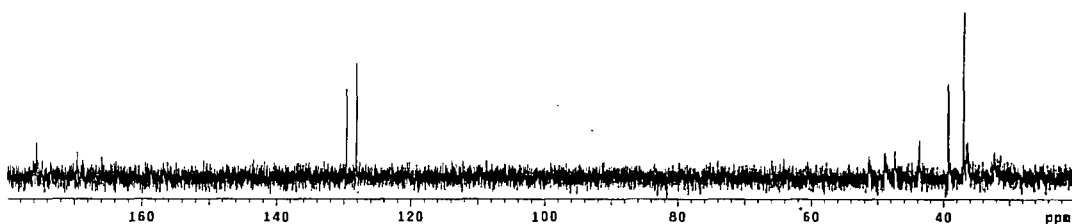
Appendix 2.21. ^1H NMR spectrum (400 MHz) in D_2O of a hyperbranched polymer (DP = 22) obtained by aqueous solution polymerisation of N-acryloyl-1,2-diaminoethane hydrochloride in a Carius tube after 10 days



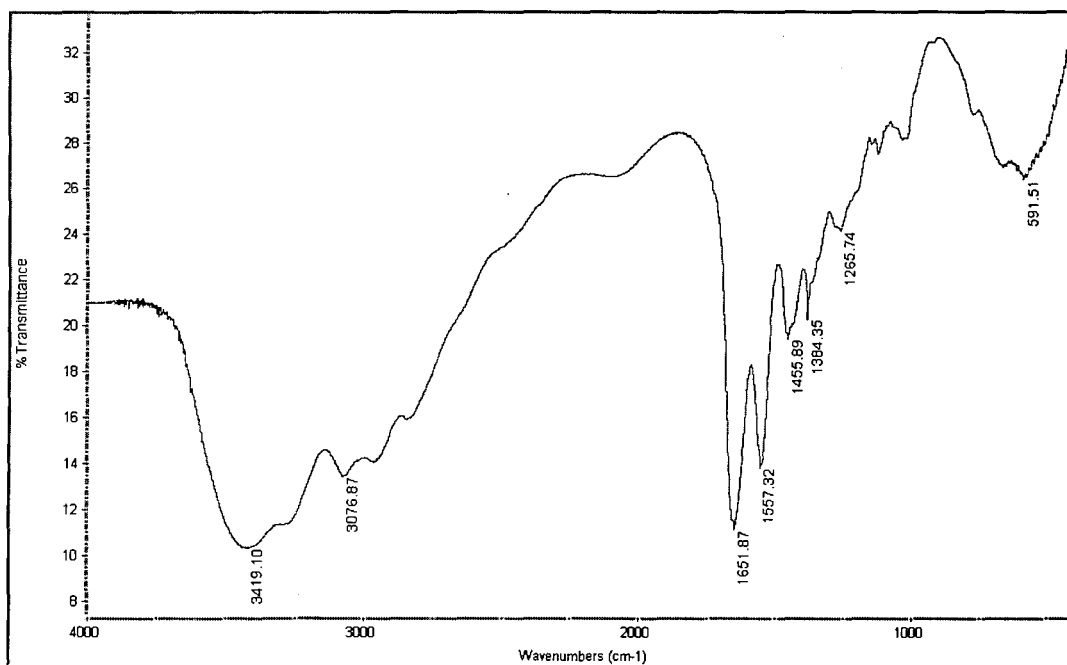
Appendix 2.22. ^{13}C NMR spectrum (100 MHz) in D_2O of a hyperbranched polymer (DP = 22) obtained by aqueous solution polymerisation of N-acryloyl-1,2-diaminoethane hydrochloride in a Carius tube after 10 days



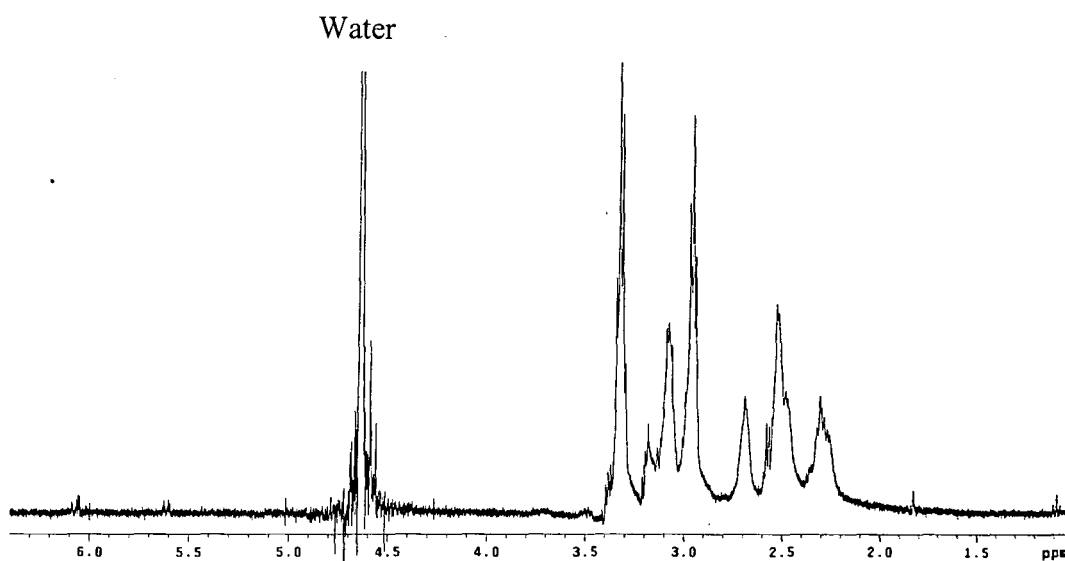
Appendix 2.23. ^1H NMR spectrum (400 MHz) in D_2O of a hyperbranched polymer (DP = 4) obtained by the freeze-drying of a high concentration aqueous solution of N-acryloyl-1,2-diaminoethane



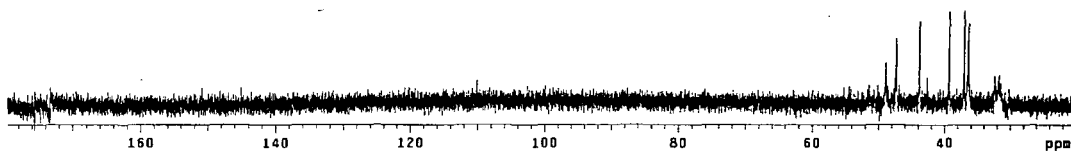
Appendix 2.24. ^{13}C NMR spectrum (100 MHz) in D_2O of a hyperbranched polymer (DP = 4) obtained by the freeze-drying of a high concentration aqueous solution of N-acryloyl-1,2-diaminoethane



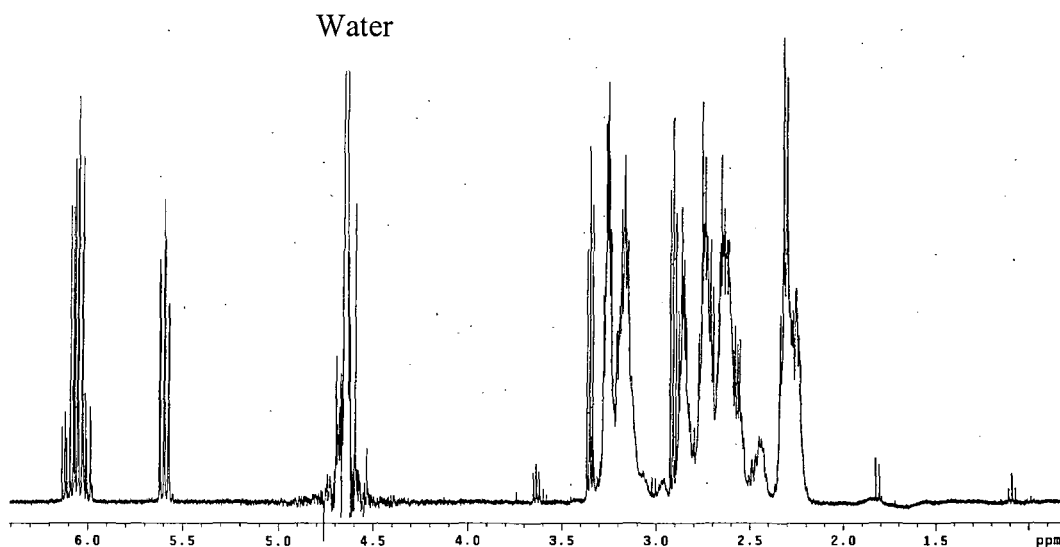
Appendix 2.25. FTIR spectrum (KBr disc) of a hyperbranched polymer (DP = 62) obtained by polymerisation in a Carius tube of a high concentration aqueous solution of N-acryloyl-1,2-diaminoethane after 90 minutes



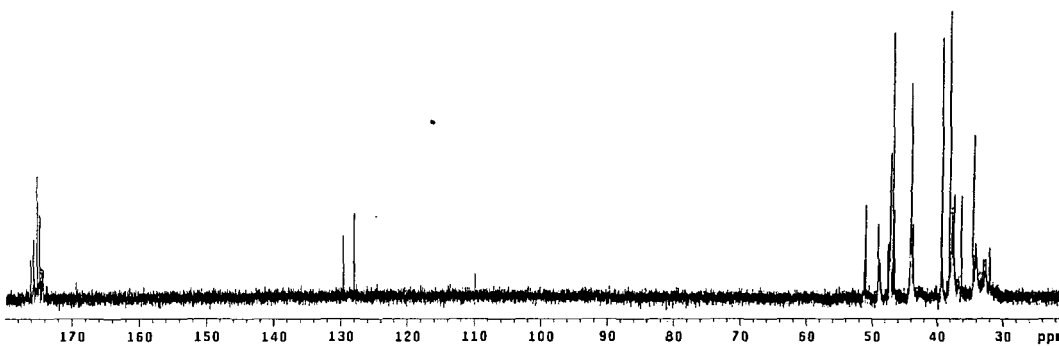
Appendix 2.26. ¹H NMR spectrum (400 MHz) in D₂O of a hyperbranched polymer (DP = 62) obtained by polymerisation in a Carius tube of a high concentration aqueous solution of N-acryloyl-1,2-diaminoethane after 90 minutes



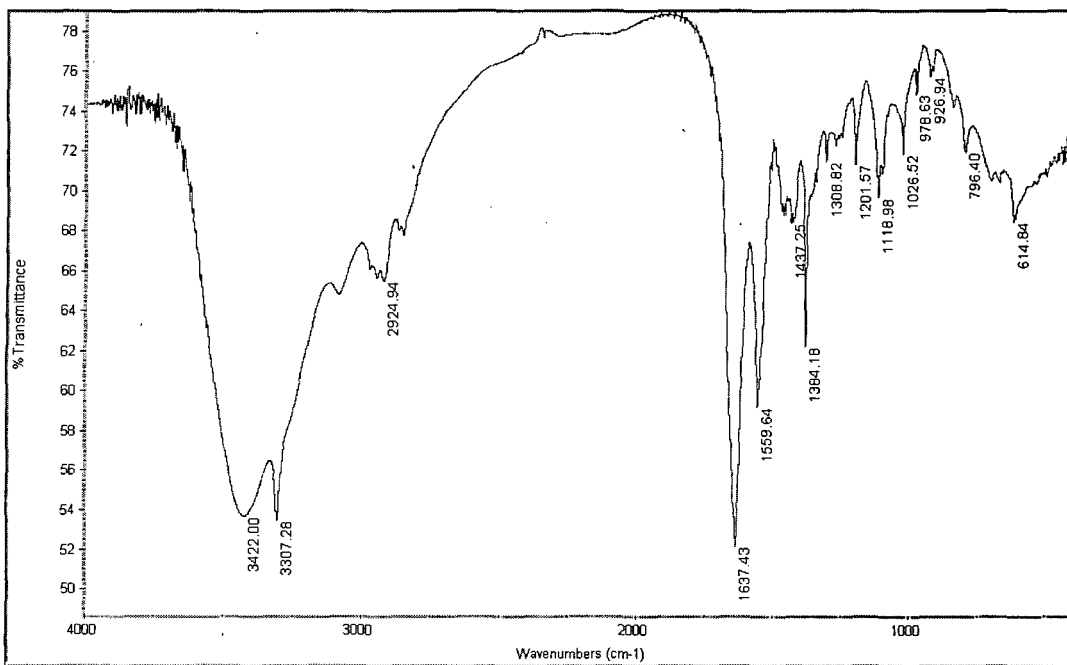
Appendix 2.27. ^{13}C NMR spectrum (100 MHz) in D_2O of a hyperbranched polymer (DP = 62) obtained by polymerisation in a Carius tube of a high concentration aqueous solution of N-acryloyl-1,2-diaminoethane after 90 minutes



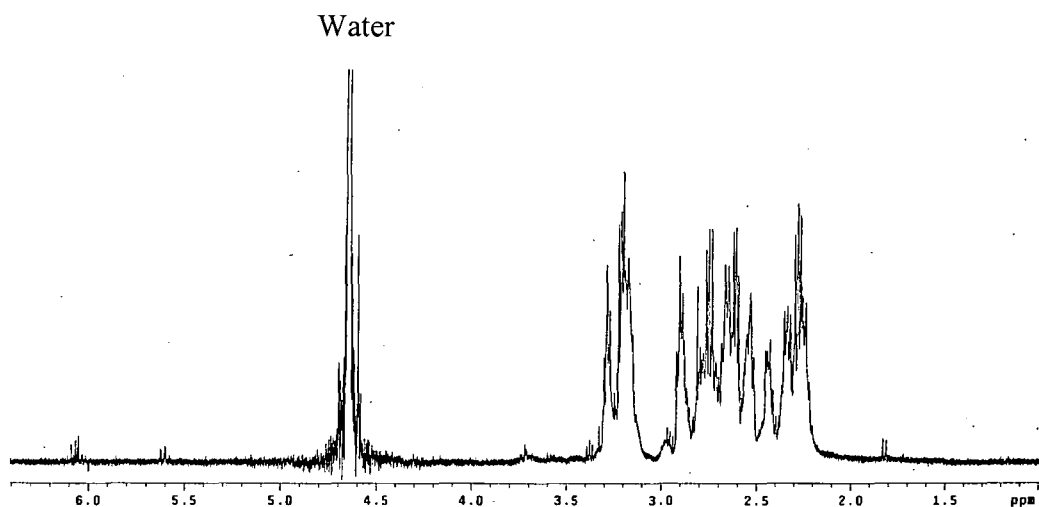
Appendix 2.28. ^1H NMR spectrum (400 MHz) in D_2O of an oligomer (DP = 5) obtained by the freeze-drying of a low concentration aqueous solution of N-acryloyl-1,2-diaminoethane



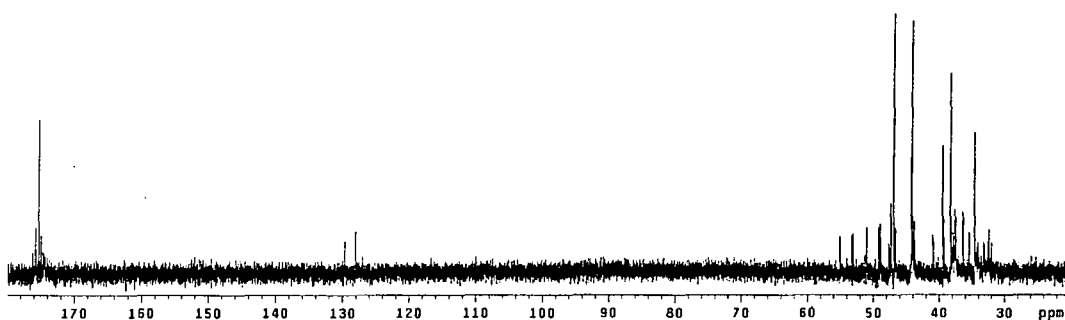
Appendix 2.29. ^{13}C NMR spectrum (100 MHz) in D_2O of an oligomer (DP = 5) obtained by the freeze-drying of a low concentration aqueous solution of N-acryloyl-1,2-diaminoethane



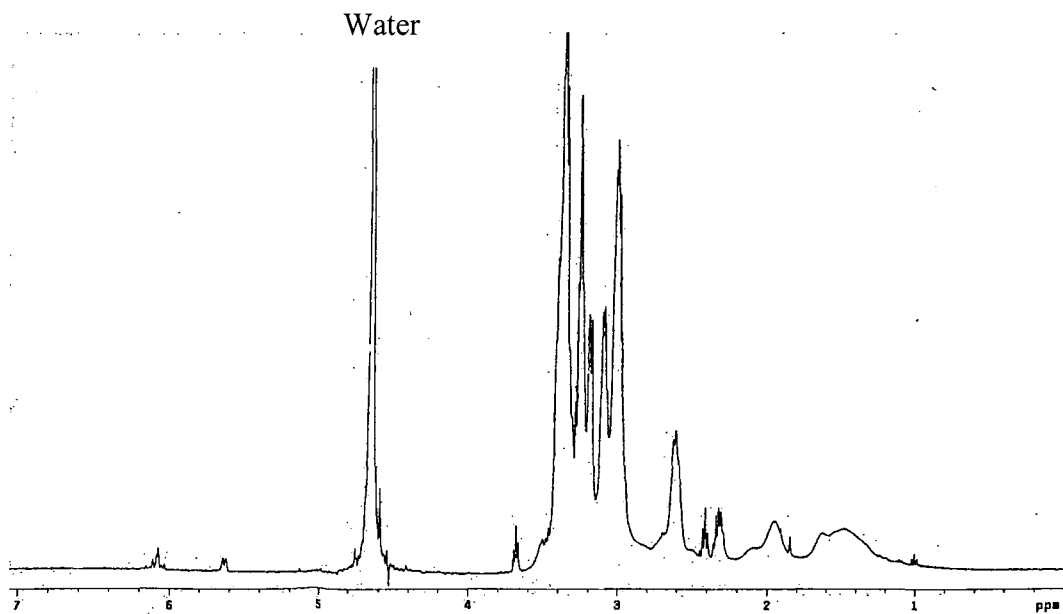
Appendix 2.30. FTIR spectrum (KBr disc) of a hyperbranched polymer (DP = 80) obtained by polymerisation in a Carius tube of a low concentration aqueous solution of N-acryloyl-1,2-diaminoethane after 90 minutes



Appendix 2.31. ^1H NMR spectrum (400 MHz) in D_2O of a hyperbranched polymer (DP = 80) obtained by polymerisation in a Carius tube of a low concentration aqueous solution of N-acryloyl-1,2-diaminoethane after 90 minutes



Appendix 2.32. ^{13}C NMR spectrum (100 MHz) in D_2O of a hyperbranched polymer (DP = 80) obtained by polymerisation in a Carius tube of a low concentration aqueous solution of N-acryloyl-1,2-diaminoethane after 90 minutes



Appendix 2.33. ¹H NMR spectrum (400 MHz) in D₂O of a hyperbranched polymer (DP = 95) obtained by polymerisation in an ampoule of a high concentration aqueous solution of N-acryloyl-1,2-diaminoethane hydrochloride after 4 days at 100°C

